STRUCTURAL SYSTEMS
RESEARCH PROJECT

Report No.
SSRP - 93/03

NASTRAN MODELING OF FLIGHT TEST COMPONENTS FOR UH-60A AIRLOADS PROGRAM TEST CONFIGURATION

by

Florentino R. Idosor
Frieder Seible

Final report on a research project funded through
NASA Research Grant Number NCC2-712

February 1993

Department of Applied Mechanics
and Engineering Sciences
University of California, San Diego
La Jolla, California

University of California, San Diego
Structural Systems Research Project

Report No. SSRP-93/03

NASTRAN MODELING OF FLIGHT TEST COMPONENTS FOR UH-60A AIRLOADS PROGRAM TEST CONFIGURATION

by

FLORENTINO R. IDOSOR
Staff Research Associate

and

FRIEDER SEIBLE
Professor of Structural Engineering

Final report on a research project funded through
NASA Research Grant Number NCC2-712

February 1993

Department of Applied Mechanics and Engineering Sciences
University of California, San Diego
9500 Gilman Drive
La Jolla, California 92093-0411

Abstract

Based upon the recommendations of the UH-60A Airloads Program Review Committee, work towards a NASTRAN remodeling effort has been conducted. This effort modeled and added the necessary structural/mass components to the existing UH-60A baseline NASTRAN model to reflect the addition of flight test components currently in place on the UH-60A Airloads Program Test Configuration used in NASA-Ames Research Center's Modern Technology Rotor Airloads Program. These components include necessary flight hardware such as instrument booms, movable ballast cart, equipment mounting racks, etc. Recent modeling revisions have also been included in the analyses to the reflect the inclusion of new and updated primary and secondary structural components (ie. tail rotor shaft service cover, tail rotor pylon) and improvements to the existing finite element mesh (ie. revisions of material property estimates). Mode frequency and shape results have shown that components such as the Trimmable Ballast System baseplate and its respective payload ballast have caused a significant frequency change in a limited number of modes while only small percent changes in mode frequency are brought about with the addition of the other MTRAP flight components. With the addition of the MTRAP flight components, update of the primary and secondary structural model, and imposition of the final MTRAP weight distribution, modal results are computed representative of the 'best' model presently available.

Table of Contents

List of Figures

List of Tables

List of Appendices

I. INTRODUCTION

1. UH-60A Airloads Program Review Committee Recommendations

Based upon the recommendations of the UH-60A Airloads Program Review Committee, which met with members of the various rotorcraft and flight test groups of NASA Ames Research Center in May 1990, work for a NASTRAN remodeling effort is conducted. The committee, including engineers and faculty from both industry and academia, suggested that a vibration survey of the UH-60A flight test airframe should be included as a complementary component of the continuing UH-60A flight test program. It was shown that in-flight vibration test data would be of minimal use unless a parallel commitment was made to a complete ground vibration test and modal analysis with accompanying finite element analysis of the flight test airframe configuration.

2. Additional Modeling of Flight Components

Previous UH-60A finite element modeling and ground vibration test efforts through Sikorsky Aircraft and NASA Ames Research Center have studied the changes in correlative results due to reconfigured mass distributions, secondary structure additions, and optimization tests. However, no direct study has been conducted to evaluate the current UH-60A Airloads Program Flight Test Configuration which includes additional structural or mass components and is unique and different in overall layout when compared to a baseline production vehicle. Analytical remodeling work for the addition/validation of structural and mass components is presented to support the Modern Technology Rotor Airloads Program and UH-60A test plan. This programming and work task was required to discretize the necessary structural/mass components to the existing UH-60A NASTRAN model in order to reflect the addition of flight test components and ballast currently in place on the UH-60A Airloads Program Test Configuration.

A study by the authors conducted previously using the a baseline UH-60 NASTRAN model [1] had included several secondary structural components, modeling revisions, and a mass distribution similar to that of the UH-60A Airloads Program Test Configuration (designated "NASA/AEFA"). The study consisted of a modal comparison using data found through ground

vibration tests (GVT) and subsequent modal test analyses that were conducted by Sikorsky Aircraft using a *flight weight configuration henceforth denoted as "NASA/AEFA"* (preceding Phase I program flight tests at the U.S. Army's **A**viation **E**ngineering **F**light **A**ctivity, **AEFA** at Edwards Air Force Base, California). The NASA/AEFA GVT aircraft was tested for modal frequencies and shapes and compared with its NASTRAN finite element model counterpart. Previous undamped results showed significant differences in modal response data. These differences could be attributed, in part, to modeling assumptions made concerning the influence of secondary structural components. Secondary components such as firewalls, transmission bridge, cockpit doors, etc. were not part of the analytical model of primary structure. The authors denoted this primary and secondary structure model as **F**inite **E**lement **M**odel **I** or simply **FEM I.** An improved modal shape and frequency correlation was achieved with the addition of secondary components and several modeling revisions. (An example of this improved correlation using FEM I is presented in Table I.).

The current MTRAP test configuration of the UH-60A flight test aircraft is shown in Figure 1. This unique vehicle is dissimilar to the previously described NASA/AEFA configuration used in GVTs and its corresponding NASTRAN finite element model (FEM I) documented in previous reports. In addition to ***extra weight and ballast,*** this flight test aircraft carries the corresponding ***structural flight test components*** such as instrumentation racks, ballast rack, ballast cart, etc. For this aircraft, a mass distribution different from previous GVT and NASTRAN model configurations is utilized. We also note that changes in stiffness due to these flight components have not been previously considered since they were not included in NASA/AEFA shake tests or analyses. Additional flight instrument components such as instrumentation systems and mounts have also been added since the previous NASA/AEFA GVT. A list of flight members contributing mass *and/or* structural stiffness to the UH-60A MTRAP flight configuration is presented in Table II.

A few of these components were deemed insignificant in contributing stiffness or mass to the model (ie. laser cube mount). However, many of these items have contributed a notable difference in dynamic response in conjunction with other components such as various instrument baseplates. This is particularly true of those items located on the cabin floor where a full ballast rack, ballast cart, and several instrument mounts add local stiffness thus affecting vibratory response. The role of other members in changing global dynamic response, such as the instrument boom and bar, needed to be ascertained. Both these members are mounted directly to frames and longitudinal beams in the forward cabin and cockpit. A majority of these members were added to the existing finite element model through the use of partial

discretization approximations or fully discretized substructures that reflect their appropriate stiffness and mass effects.

Using a UH-60A NASTRAN model with secondary components, MTRAP flight components, and updates/revisions developed by the Sikorsky Aircraft Dynamics Group, the implemented modeling changes provide structural/mass agreement with the UH-60A Airloads Program Flight Test Configuration for future analyses and correlations with planned flight and modal tests. This accumulation of flight components and updates/revisions was called **FEM III.** This FEM III is the end result upon the completion of the three steps that will be described in a later discussion of basic model configurations.

In this report, the remodeling task and comparative analysis of an updated NASTRAN model discretizing the UH-60A Airloads Program Flight Test Configuration including various flight components is described. The most recent GVTs and updated NASTRAN models are also described in the following.

II. BACKGROUND

1. Design Analysis Methods for VIBrationS (DAMVIBS)

To understand the development of the UH-60A large scale finite element model, sufficient program background should be presented. With the U.S. rotorcraft industry's capability to accurately calculate static characteristics of helicopter fuselage structures, the even greater dynamic design problem of vibration prediction and control still remained in the late 1970's. One can restate the importance of significant and problematic vibration levels as they decrease overall vehicle performance and flight safety, increase maintenance efforts, and cause great concern in terms of human factors. On numerous occasions, inaccurate analytical predictions have led to costly "quick fixes" and unwelcome design compromises.

Several programs have contributed to the development of rotorcraft finite element models and their predictive capabilities. One recent advance in assessing the requirements for definitive vibration prediction and control came from Phase I of the completed DAMVIBS program. To achieve a superior capability in utilizing finite element models to support the Country's industrial design of helicopter airframe structures, NASA Langley Research Center sponsored the DAMVIBS program (Design/Analysis Methods for VIBrationS) with industry and academia in between 1984 and 1991 [2]. As a result of this program, major technological contributions were given and received by the four industrial participants: Boeing Vertol, McDonnell Douglas Helicopters, Bell Helicopter Textron, and Sikorsky Aircraft. Each participant discussed, planned, and modeled a large scale finite element model of its own chosen production helicopter. Shake tests and modal test analyses were subsequently performed and correlated with the analytical model.

The results from this program indicate that significant deficiencies exist in the development of rotorcraft finite element models and their subsequent correlations with experimental results. It had also demonstrated the need for improved basic finite element modeling guidelines, efficient computational procedures, and commonly accepted methodologies in treating this unique structural dynamics problem. For specific experimental tasks such as the UH-60A Airloads Program, which has the experimental and theoretical characterization of

rotor-fuselage coupling as one of the principal objectives, the DAMVIBS Program has given NASA engineers a baseline finite element model which can be improved and modified for special flight configuration studies and applications. We note that finite element model data from both the author's previous NASA/AEFA study and this current MTRAP study have been used by NASA and Army engineers for specific UH-60A analyses with rotorcraft predictive codes such as CAMRAD.

2. United Technologies Sikorsky Aircraft Contributions

Work with the UH-60A NASTRAN model is continued by the Dynamics Group at Sikorsky Aircraft in support of the existing production and also the design of advanced mission configurations. Sikorsky Aircraft's contribution to the DAMVIBS, NASA/AEFA, and MTRAP programs have come through its development and continued refinement of the UH-60A Black Hawk finite element model. Sikorsky's NASTRAN model of the UH-60A DAMVIBS baseline weight and primary structural configuration is the foundation and fundamental starting point for the current model. The Dynamics Group at Sikorsky Aircraft continues to maintain the development of the UH-60A finite element model through the inclusion of secondary structural components, the re-evaluation of mass, material, and geometric member properties, and the continued performance evaluation of the existing mesh discretization in support of its own engineering programs.

3. Modern Technology Rotor Airloads Program (MTRAP)

The UH-60A finite element model will serve an important role in the **M**odern Technology **R**otor **A**irloads **P**rogram (**MTRAP**) in future ground vibration tests and flight test analyses. NASA and the U.S. ARMY are currently sponsoring this program with the participation of industry and academia to experimentally define vibratory airloads for the:

Validation of Computational Fluid Dynamics and Comprehensive Rotorcraft Codes
Investigation of Unique Flow Phenomena
Modernization of Industry Empirical Design Methods

Hence, a comprehensive database is being formed through the MTRAP alone to validate the techniques and methodologies required to improve the performance, dynamics, acoustics, and

handling qualities of civil and military rotorcraft. A justification for this research consists of past acoustic, aerodynamic, aeroelastic, and interdisciplinary studies identifying rotor system vibratory airloads as the main source of rotorcraft noise and vibration.

The key element of the MTRA Program is the **UH-60A Black Hawk test plan** [1] (also known as the UH-60A Airloads Program) which will further contribute to the database through numerous flight tests, model scale, and full scale wind tunnel tests for rotor airload definitions in conjunction with the development of specific code applications for analytical predictions and correlations (ie. NASTRAN modal prediction/correlation). This remodeling effort of the NASTRAN model presented here serves as a complementary contribution to the UH-60A test plan. The completed NASTRAN model (FEM III) includes additional secondary structural components, an improved primary/secondary structure, flight test structural components, and a modified flight weight distribution as prescribed by the NASA/ARMY Modern Technology Rotor Airloads Program. Through the validation and continuing improvement of a predictive analytic model, a generic understanding of inherent fuselage characteristics may be achieved. Ultimately, their role within rotor-fuselage coupling behavior may be characterized and resulting overall vibration may be controlled in design.

4. Test Configurations

The principal objective of this applied research study is to address the need for an accompanying finite element model for both the current flight and ground vibration tests configurations. The planned shake test will be a NASA Ames in-house effort and is scheduled tentatively for late 1995 or early 1996. The planned shake test configuration will reflect the unique structural layout and weight distribution of the MTRAP flight aircraft currently involved in flight programs. This MTRAP configuration will be only one in a series of previously built-up ground vibration articles that have been analyzed including the first baseline DAMVIBS (**D**esign/**A**nalysis **M**ethods for **VIB**ration**S**) configuration and the NASA/AEFA weight distribution. A description and summary of their subsequent analyses of these articles is provided:

4.1 DAMVIBS

Ground vibration tests were performed in the DAMVIBS program using weight distributions resembling the UH-60A Airloads Program Flight Test Configuration. The baseline configuration of the UH-60A production aircraft or DAMVIBS configuration weighed 10,000 lbs and was among the first helicopters to undergo full-scale shake testing under the NASA Langley sponsored DAMVIBS program. UH-60A ground vibration testing for the NASA Langley DAMVIBS was conducted by Sikorsky Aircraft in Stratford, Connecticut. NASA/AEFA shake testing for the Modern Technology Rotor Airloads Program was performed in conjunction with similar tests for the DAMVIBS Program. We note that a finite element model of this baseline UH-60A had been developed for GVT correlation and comparison at this time.

4.2 NASA/AEFA

Soon after the baseline DAMVIBS UH-60A was tested for various modal response functions and parameters, equivalent masses of flight components were added at specific locations to duplicate the NASA/AEFA flight weight distribution and a retest was performed. We note that no adequate model describing the NASA/AEFA GVT or flight test configuration had been developed at this time. The NASA/AEFA GVT was conducted using this weight and baseline structural configuration. The NASA/AEFA GVT article is described as a flight worthy, government owned UH-60A helicopter (S/N 86-24507) with the following parts and equipment removed for GVT purposes [3]:

Main rotor blades	Tail rotor blades
Main rotor hub	Tail rotor hub
Spindles	Cabin troop seats
Bearings	Tail gearbox cover
Dampers	Intermediate gearbox cover
Bifilars	Nose absorber access cover
Lower pylon fairing	*Various aerodynamic fairings/covers
Fuel	

*Various aerodynamic fairings and covers were removed to allow access to measurement locations.

The presence of most secondary structural components intact in both DAMVIBS and NASA/AEFA GVT articles is noted. Also, the nose, forward cabin, and aft cabin vibration absorbers were rendered inactive. The following are installed in the NASA/AEFA GVT article:

Modified Black Hawk main rotor hub**
Main rotor head ballast
Main & tail rotor excitation hardware
Main & tail rotor suspension hardware
Dummy tail rotor hub

**640 pounds were added to the main rotor hub, in the form of shaker hardware and dummy steel plates, to simulate 50 percent of the flapping mass of the main rotor blades and bifilar mass. This additional mass *approximately* simulated the 4/rev rotor impedance of the UH-60A and consequently yielded test modes near 4/rev. The dynamic properties were therefore similar to the modes of an inflight aircraft which has frequencies in the 4/rev region.

To satisfy the NASA/AEFA flight test weight distribution requirement as defined by the NASA/AEFA flight test aircraft, a specific flight mass distribution was defined for the GVT article. The *equivalent masses* of the following flight components were added to the aircraft for modal testing as seen in Figure 2:

Pilot
Copilot
Ballast
Full Fuel
Instrumentation Racks (3)

One notes that these additions to the GVT article effectively change mass distribution only (ie. the stiffness contributions from the addition of true flight test components such as instrument racks, ballast rack, etc. is not reflected in GVT data). Due to this fact, subsequent NASTRAN modeling and analyses emphasized modeling these masses to achieve

better correlations with GVT data. Thus, one sees a need for a ground vibration test using all flight test components. The sole difference between the NASA/AEFA and DAMVIBS GVT configurations is the addition of the component masses mentioned above. The NASA/AEFA shake test configuration weighs approximately 17,800 lbs with the addition of the seven components, while the base DAMVIBS shake test article weighs 10,140 lbs. It is not expected that the DAMVIBS or NASA/AEFA NASTRAN models will achieve accurate correlations with the planned shake test of the UH-60A Airloads Program Flight Test Configuration because that test has yet a third configuration.

4.3 MTRA Program

The MTRAP or UH-60A Airloads Program Flight Test Configuration expands on both these previous weight distributions of the baseline UH-60A particularly that of the NASA/AEFA weight configuration. The MTRAP configuration has a unique weight distribution and structural layout corresponding to the maintenance of a constant center of gravity under flight conditions, telemetry and data gathering equipment, and other objectives such as are mentioned in a preliminary Longitudinal Centroidal Gravity Expansion Program. The 1995 shake test configuration will include relevant flight test structural components, equipment, and those additional ballast weights related to the flight aircraft and its previous flight test objectives.

III. MODELING APPROACH

1. Basic Model Configurations for Study

Three basic model configurations have been considered throughout this study. Each of these models reflects a separate stage of improvement between the previous study by the authors and the most current or 'best' model available that is of greater interest. Throughout this study, the completion of the unique UH-60A Modern Technology Rotor Airloads Program (ie. MTRAP) Configuration is of primary importance. The three basic Finite Element Model (**FEM**) configurations are described and denoted as follows:

FEM I. A Primary/Secondary Structural Model

FEM II. The Primary/Secondary Structural Model with MTRAP Flight Components

FEM III. A final Updated and Revised Primary/Secondary Structural Model with MTRAP Flight Components

First using **FEM I**, the primary and secondary structural model previously used by the authors in the September '90 study of the NASA/AEFA Configuration and secondary structural additions is modified down to two pre-defined starting reference configurations that vary with respect to mass distribution. In the second step, these two starting reference configurations are used respectively in the **B**uild-**U**p of **C**omponent **S**tructure and **B**uild-**U**p of **C**omponent **M**ass **S**tudies (henceforth denoted as **BUCSS** and **BUCMS** respectively) giving **FEM II** upon completion to determine the influence of components on an individual basis. With this step, a check-out of the MTRAP flight components is completed. Finally, updates and revisions that have been made to the full primary/secondary structural model by the Dynamics Group at Sikorsky Aircraft as of November '92 are brought together with the MTRAP flight components and their unique flight mass distribution to constitute **FEM III** or the 'best' model available. A list of items that are accumulated as a result of each of these three steps is presented in Table III.

2. Modeling Approaches

A basic guiding philosophy is followed in this study with respect to the modeling of these flight components. The modeling guidelines define the minimum model that will accurately discretize each flight component. In the end, a modified and equivalent stiffness matrix is required that is characteristic of the additional component stiffnesses. A modified and equivalent mass distribution is also required.

3. Rigorous Geometric Model vs. Equivalent Stiffness Approach

One should differentiate between the two finite element approaches that can be used to simulate the behavior of an additional dynamic component. The finite element method is viewed as successful in that a *rigorous geometric model* with accurate cross sectional, material property data, and an appropriate grid point and element mesh can define the physical component being modeled and generate the associated mass and stiffness matrices. To simplify the modeling effort, one may also consider the significant dynamic and static stiffness influences of additional components when added to a global physical model and include them such that an *equivalent stiffness* and mass matrix is modeled and the dynamic and static responses are equivalently simulated. In this case, those parts of the flight components that are considered to be the main structural and mass features are modeled by modifications to the existing mesh. Such modifications may include the re-computation of a 'composite' cross section and material which represents the overlap of the added component on the primary structure.

In considering the UH-60A finite element model, three general approaches are used to include the additional stiffnesses of the more complex flight components:

1) Full discretization of each flight component.
2) Equivalent and partial discretization of the flight component
3) Modification of existing mesh to account for additional stiffness

These are described as follows:

3.1 Full Discretization of Each Component

In this method, the flight component to be modeled is discretized by a mesh that accurately depicts the geometric domain of the component. The mesh is made with a similar order or fineness as the existing global mesh of the UH-60A. An appropriate grid point and element numbering system that is non-coincident with any systems in the global model is assigned. Cross sectional properties such as neutral axis locations, and area are determined through design or manufacturing blueprints or computed. Material properties and other complementary data are similarly gathered or computed.

We note that the existing mesh of the UH-60A is not highly refined but is sufficiently advanced to allow an estimation of low frequency modes below 20 Hz. Any mesh order developed for flight components that is significantly higher than that of the global model would not contribute in a positive way because the global response of interest will perform only as accurately as its weaker formulation (namely, the lower order mesh of the existing model). The modeling of the Trimmable Ballast System (TBS) Ballast Rack is an example of this approach.

3.2 Equivalent and Partial Discretization of Flight Structures

An equivalent or partial discretization of a flight component structure may also be performed to account for the projected types of modes and basic flexural action of the components. In this case, the modeler is asked to determine the principal structural members and mass features of the components that contribute most significantly in terms of stiffness and mass effects. These main structural and mass features are modeled exclusively as well as the tie-down points of the components to the primary structure. The less important structural features of the components are combined together with significant mass items as they are not considered to contribute significantly to the dynamics of the component relative to main structures.

The modeling of the Flight Engineer's Instrumentation Rack in the forward right-hand section of the cabin is one such component that requires this modeling approach. The instrumentation rack shelves and cover are composed of very thin sections. The rack itself, however, is supported by two T-section beams that are attached to the top and bottom half of an aircraft frame. The attachment of the T-section beams is made

with two L-beams that fasten the top and lower ends of the two T-beams to the frame. These T-section and L-beams are the main structural features while the instrumentation rack's thin cover sections and light equipment loads are considered to be the important mass item. Using an approach where an *equivalent or partial discretization* is required, structural beams and angles are modeled while the instrumentation rack cover and thin walled structural cover and shelves are distributed as mass.

3.3 Modification of Existing Mesh

Another approach is the local modification of the existing global mesh by accounting for changes in the area moment of inertia, modulis of rigidity, and structural configuration that are due to an additional component. While *convenient in terms of geometry and program modification*, this is the *least flexible or stiffest* estimate of the three methods for enacting model modifications. In this method, the modeler modifies the existing mesh of the global model to allow for the superposition of a component model. New area moments of inertia and material properties are then calculated to include the superposition of the component (as in the computation of a cross section consisting of one or more different sectional areas and isotropic materials). Such an approach is elaborated upon in the following example and compared with a full discretization approach.

4. Case Example: Ballast Rack

To incorporate the structural and mass contribution of an additional component to a global finite element model, several approaches can be used. One approach requires the tuning of existing finite elements (modification of existing mesh) in the global model in order to simulate the additional stiffness and weight associated with an added component. Another approach requires the full finite element discretization of the component in a scale appropriately fitted to the global model and a reasonable estimate of the displacement boundary conditions (such as those representative of cabin tie-down points). Clearly, both approaches have their limitations as will be shown. One will find that although a modification of the existing mesh is an easier approach, limitations encountered in terms of geometry of the existing mesh warrant the full discretization of the added component.

In a method requiring the modification of the existing mesh, we consider the example of the addition of the Trimmable Ballast System ballast rack to the UH-60A cabin floor to illustrate the approach. The following steps are carried out. First, the geometry, node points, and material properties of the cabin floor elements are found using model data. Second, the geometry and material properties of the ballast rack are defined. A graphical overlay of the ballast rack over the cabin floor is created at this point to determine which cabin floor finite elements require tuning. If the overall shape and geometric details of the ballast rack are not coincident with elements in the cabin floor mesh, modifications to the mesh is made. Element properties are then recalculated to account for the new combined geometric and material cross sections which result in an equivalent stiffness model representative of the ballast rack. These elements are fixed to the cabin floor.

In a method utilizing a complete finite element discretization, we again consider the working example of the ballast rack to the cabin floor to illustrate the approach. The following step are carried out. As in the previous method, the geometry and node points of the cabin floor elements are found using the model data. Second, the geometric, material, and cross sectional properties of the ballast rack are defined as are any required tie-down point or displacement boundary conditions. A graphical overlay of the ballast rack over the cabin floor is created again but is instead used to determine where tie-down points of the fully discretized ballast rack would require companion tie-down points on the cabin floor mesh. If such node points on the cabin floor mesh are not geometrically coincident with the corresponding tie-down points of the ballast rack, the existing floor mesh is modified. Lastly, a discretization of the ballast rack of mesh order similar to that of the cabin floor is developed with appropriate tie-down node points. Displacement boundary conditions at these node points are specified to connect the added component to the global model. In this approach, proper displacement conditions are required to bring about an equivalent stiffness model representative of the ballast rack which is fixed to the cabin floor only at the tie-down locations.

Clearly, each approach has its advantages and disadvantages. If one requires the tuning of existing finite elements which is easier to implement, the shape of the global element mesh coincident with that of the component mesh is required. This is often not the case when the component mesh consists of elements that are angled and have shapes characteristic of complex cut-outs (as in the case of the ballast rack). This approach also assumes that the component acts as a one-piece composite with the component mesh. We note that displacement boundary conditions as exhibited by characteristics such as tie-down points of the ballast rack to the

cabin floor are not considered in this easier approach. Equivalent boundary conditions in this respect assume that all component mesh nodal points will share the same kinematic history as those of the coincident global mesh.

Similar disadvantages can be seen in the approach where a full discretization of the component is required. The complete component model with nodal points defining tie-down locations requires coincident nodal points on the attaching global mesh surface. However, modifications to achieve this can be performed on the global mesh without effecting changes that are unrepresentative of the mesh stiffness such as a local mesh refinement. Through this approach, a correct component stiffness model and proper displacement conditions can be defined. Thus in viewing a 'composite' action versus direct stiffness approach, one sees that due to the geometry of the existing global mesh, that the full discretization of additional components and appropriate boundary conditions is warranted in the practical component modeling effort and build-up study that is presented here for a majority of the components. In the case of the ballast rack and a majority of the structural flight components, a full discretization was used.

5. Additional Modeling Considerations

There are other aspects of this component modeling that require consideration. The order of the grid point and element mesh should be considered. A poor selection may produce an overstiff mesh and modal behavior uncharacteristic of the physical interaction between global and local component meshes (ie. interaction between cabin floor and ballast rack.). We also note that mesh refinement must be gradual as one moves from a low number of elements in a given region to a much higher number of elements in an adjacent region while maintaining necessary tie-down grid point definitions and the accurate discretization of the component. A non-gradual refinement may lead to excessively large stiffness terms compared to surrounding terms in the stiffness matrix. This leads to the possibility of an ill-conditioned matrix, a poor problem formulation, and subsequent incorrect eigensystem solution. Attention has also been paid to ensuring the best and most proper element sizes and tapers, definition of tie-down points, and acceptable component discretization in each flight component case for the global model.

We also note that an effort in generating a high order mesh for the global or local component model is driven by an interest in a large number of response locations in the component or in very accurate modal frequency or shape results regarding the component mesh itself. Fortunately, we are interested in global response to a larger degree rather than specific

local response. Thus, details regarding the generation of component grid point and element mesh, within correct physical modeling principles, may be guided by the overall interest in the global helicopter fuselage response.

We note that in this limited study many experimental verifications of the individual flight components were not conducted. For example, the accurate discretization of each component was not verified with experimental strain or modal tests. Such a validation is recommended in any future GVT study.

Other modeling aspects were considered as one moves the component from blueprints or manufacturing plans to its respective element discretization. The determination of coordinates specifying the neutral axis is important as it determines the respective area moments of inertia. This evaluation of the neutral axis is unique for each structural bar, beam, or tube member and depends on their connection to the global fuselage model and primary flexural action of the component. The determination of important element properties is also required including cross sectional areas, moments of inertia, material properties, Young's modulus, mass density, and the accurate definition of tie-down points.

6. Summary

Clearly, several approaches were considered in the modeling of each additional flight component. The approaches involved in the finite element modeling of these components are summarized by three methods: 1) A *full discretization* that equivalently brings about a stiffness matrix representative of the component, 2) A *partial discretization* of the component that equivalently brings about a stiffness matrix characteristic only of the significant flexural parts of the local component, and 3) The *modification of the existing mesh* to model the 'composite' flexural action of the component plus the global structure mesh.

It will be seen in the following sections that a full discretization (method 1) was warranted in most component cases, although a partial discretization (method 2) is sufficient in at least one case (ie. flight engineer's instrumentation rack). *Alternatively*, although method 3 was not used in this study, a modification of the existing mesh was deemed as a fair and flexible approximation that was easier to implement when the similar component and global mesh geometries were similar. While a modification of the existing mesh to form an equivalent stiffness is simpler to implement for any single component, it may not be convenient due to

limitations set by the pre-existing or even nonexistent global mesh geometry that shares locality with the component. In all three approaches, a correct definition of displacement boundary conditions between components and the global mesh are an area of concern.

IV. PRIMARY/SECONDARY STRUCTURAL SYSTEMS

1. Objective

The final results of this study encompass the incorporation of three important finite element model parts in terms of structural contribution and weight distribution. Each of these three have been included in the FEM III or the 'best' model currently available. These include:

1) Primary Structural System
2) Secondary Structural System
3) Flight Components

These systems are reviewed in the following:

2. Primary Structure

The first structural system describes the **primary structure** of the rotorcraft fuselage exclusively. Generically defined, primary structures are components that are designed to be load carrying members. The primary structure consists of aluminum semi-monocoque structures including frames, stringers, skins or panels, beams, and bulkheads. In areas of high temperature or concentrated load, titanium and machined parts are used. The finite element model for this primary structural system is composed of 8,803 elements, specified geometrically by 4,669 grid points, and utilizes 25,509 degrees of freedom (DOF) as presented in Figure 3. The primary structure represents a baseline UH-60A aircraft at 10,000 lbs. By using dynamic reduction methods, the number of global DOF's are decreased to 77 modal coordinates. This primary structure is included in FEM I, II, and III.

3. Secondary Structure

The secondary structural system combines both the **primary structure and specific secondary structural components (FEM I).** Generally, glass, plexiglass,

fiberglass, and kevlar coverings or skins fall into the secondary structure category. They are generally formed in a composite sandwich construction made up of aluminum honeycomb cores with laminated fiberglass or kevlar skins. In some areas, the aluminum core is not used with the fiberglass and kevlar skins. The windows in the mid-cabin and side cockpit are stretch plexiglass. The windshields, which have wipers, are laminated glass inside with an outside layer of PVB plastic. In addition to the selected secondary structural components, several modeling revisions were included to correct physical and material properties of the former primary structure model by Sikorsky.

Many of these modifications were motivated by Sikorsky studies using a nonlinear programming code called PAREDYM (PArameter REfinement of DYnamic Models), which identified changes required in a finite element model to yield improved correlations with GVT results. To satisfy the flight weight distribution as was done in the NASA/AEFA GVT, the following *equivalent masses* of several flight components were incorporated by the authors into the mass discretization of the UH-60A NASTRAN finite element model:

Pilot
Copilot
Ballast
Full Fuel
Instrumentation Racks (3)

We note that not all flight test instrumentation components are modeled in terms of mass and structural contribution (such as are found in the current MTRAP configuration and study). Depending upon the flight test objectives, some components are included as ballast payload in a number of locations throughout the longitudinal length of the helicopter. Possible ballast payloads and their respective locations are presented in Table IV under the general arrangement for the longitudinal center of gravity expansion program which has set aside a series of pre-determined mounting surfaces in the UH-60A aircraft where additional ballast can be placed for various flight test purposes.

The primary and secondary structural system is discretized by 9,185 elements, geometrically described by 4,842 grid points, and requires 26,547 DOF's as presented in Figure 4. One can compare these model attributes to those of the primary structural system alone which had 8,803 elements and 25,509 DOFs. Thus, the addition of secondary structure brought about an additional 382 elements and 1,038 DOFs. By reduction methods, the number

of DOF's are decreased to a smaller modal subset. This NASTRAN model has an equivalent weight of 17,660 lbs (including lumped masses of pilot, copilot, fuel, ballast, and instrumentation racks).

4. Flight Components

Flight components unique to the MTRAP Flight Test Configuration were added to two versions of the primary/secondary structural model. The first version is a model used by the authors to study the NASA/AEFA GVT configuration in September of 1990 and was used currently to study the BUCSS and BUCMS. The second version is a recently updated version of the UH-60A including material property revisions and updated primary and secondary structural components and will constitute FEM III or the 'best' model (Figure 5). Flight components have been included in FEM II and III only. The evaluation and modeling of flight components are discussed in the sections to follow.

V. FLIGHT COMPONENTS

1. Evaluation

The first step of this modeling effort began with the determination of those significant structural and mass components on the flight test aircraft that required modeling based on physical modeling principles. A list of those flight test components that are unique to the MTRAP configuration, not found on previous baseline configurations of the UH-60A, has been generated with a complete description of the individual components and their test purpose. Reference materials including blueprints and physical measurements were gathered to aid in the evaluation of the listed components [4]. Best estimates of material and physical dimensional properties were made regarding those components fabricated at the Army Engineering Flight Activity, Edwards Air Force Base during 1986 flight tests as no formal design and manufacturing plans were made. Assumptions were then made as to the significance of the contribution of these components in terms of structural stiffness and mass. Those components that significantly contribute stiffness to the overall structure and its resulting structural dynamics were individually modeled. Smaller structural mountings were considered negligible in this respect, although the weight of all flight components were incorporated.

It should be noted at this point that no effort was made to estimate or incorporate damping contributions of these components. Critical damping ratios of the individual global modes may be measured in future modal testing planned and used to revise those modal frequency estimates that are to be presented here.

2. Description of Flight Components

For this finite element model, flight components were categorized into different groups based on their location within the UH-60A or their structural or weight contribution to the fuselage response. For purposes of clarity in such a categorization, each flight component were defined in only one of the following categories:

External Structural Components
Internal Structural Components
Mass Items

External Structural Components are those structures that are mounted to the exterior frames or shells of the aircraft and contribute in some manner to the overall stiffness characteristics and weight distribution. Physical test equipment items which fall in this category are for example, the instrumented test boom and LASSIE bar. These external structural components are seen in Figures 6 and 7. Analogously, *Internal Structural Components* are those items found inside the UH-60A fuselage (ie. cabin, cockpit, etc.) that contribute structural stiffness and mass to the fuselage response. The physical test items that are categorized as Internal Structural Components are presented in Figures 8 through 16. *Mass Items* are those components that have been deemed as contributing to the weight distribution exclusively and negligible stiffness. They are henceforth modeled as a single or series of concentrated point masses in the finite element analyses regardless of their internal or external location. Physical items that fall into the category of mass items are seen in Figures 17 through 20. Each component is described in the following section. Please note that item locations are described in a standard aircraft coordinate system (units in inches) with fuselage station, butt, and water line notation. The origin is denoted forward of the nose of the aircraft (beginning with the main rotor blade forward tip), level with the cabin floor, and symmetric about both halves of the rotorcraft.

2.1 External Structural Components

A. Instrumented Test Boom

An instrumented test boom is attached to the forward right side of the UH-60A underneath the cockpit door and forward cabin (Figure 6). The test boom length is 152.4 inches. The test boom includes a swiveling pitot-static tube and angle of attack-sideslip vanes at the front of the boom. The long boom consists of a series of welded and/or threaded structural tubes of various diameters and thicknesses. Two separate multi-bolted connection webs attach the complete boom assembly to aircraft frames at fuselage stations 247.0 and 188.0. This assembly was fabricated at AEFA for 1988 flight tests. The weight of the instrumented test boom is calculated to be 22 lbs

including forward instrumentation and the two mounting assemblies that attach the boom to the airframe. This item was modeled with a full discretization.

B. Instrumented LASSIE Bar

Additional external instruments are required in MTRAP flight tests. An instrumented bar has replaced the pre-existing FM antenna at the cockpit door opening on the starboard side (Figure 7). An Elliot Low SenSing and Indicating Equipment (**LASSIE**) assembly is placed at the top of this bar. The LASSIE bar is considered to contribute very minor structural stiffness and mass to the global model. This assembly was previously fabricated at AEFA for 1988 flight tests. The self-weight of the LASSIE Bar is calculated to be 10 lbs including the accompanying LASSIE instrumentation. This item was modeled with a full discretization.

2.2 Internal Structural Components

A. Trimmable Ballast System: Baseplate ("Ballast Rack")

To offset the effects of a changing center of gravity due to fuel mass loss during flight operation and equivalently maintain a constant longitudinal center of gravity, a trimmable moving ballast system has been developed and manufactured through Ames in-house efforts. The trimmable ballast system (Figure 8), situated across the length of the cabin floor of the MTRAP configuration, consists of two principal components: a baseplate (commonly referred to as the 'ballast rack') and a movable ballast box (Figure 9). In the trimmable ballast system, only the baseplate is considered to be a structural component within the internal structure of the craft. This item was modeled with a full discretization.

The 0.5" thick aluminum baseplate of the ballast system, connected redundantly at fifteen separate cabin floor tie-down points, runs longitudinally across the the center length of the UH-60A cabin floor between stations 265.5 through 398.0. It consists of

large cabin floor mount with a slightly smaller track/rail overlay which serves as a track system upon which a movable ballast cart sits. The baseplate also serves as a mounting surface for the flight engineer's seat installation. The ballast cart is allowed to move longitudinally across the track as directed by a computerized control unit to compensate for the changing center of gravity due to the loss of fuel mass. The ballast rack is modeled structurally in the NASTRAN model as it is considered to contribute significant structural and mass effects to the cabin floor in concert with the baseplates/mounts of other flight related equipment. The baseplate weighs 376 lbs according to pre- and post-manufacture specifications by Sikorsky Aircraft. As a side note, we note that in the effort to maintain a predetermined center of gravity and gross weight configuration for the helicopter, a general arrangement for the longitudinal center of gravity of expansion program has defined the baseplate as a ballast item at station 333.20 .

B. Instrumentation Racks:

Flight Engineer Instrumentation Rack (Fwd Rt Cabin)
Center of Gravity (C.G.) Rack (Aft Central Cabin)
Instrumentation Panel (Aft Right Cabin)
Pallet Rack (Aft Left Cabin)

Due to the nature of comprehensive flight testing, a significant amount of on-board and user accessible instrumentation and computational equipment is required. Three instrumentation racks and one instrument panel have been installed inside the UH-60A cabin with attachments to their respective frames and bulkheads.

B.1 Flight Engineer Instrumentation Rack (Forward-Right Hand Side)

The first rack to be considered is the flight engineer's instrumentation rack located behind the starboard cockpit seat in the forward cabin area (Figure 10). The instrumentation rack is mounted through support beams situated at the station 247.0 frame which separates the cockpit and cabin sections. This assembly was fabricated by the Army Engineering Flight Activity (AEFA) for 1988 flight tests. The flight engineer's instrumentation rack has a self and equipment load weight of 75 lbs by

previous AEFA estimates. This item was modeled with a partial but equivalent finite element discretization.

B.2 Center of Gravity (C.G.) Rack (Aft Central Instrumentation Rack)

One instrumentation rack (48.1 inches high) is centrally located against the transition section in the aft cabin (Figure 11). The C.G. Rack is intended to carry Rotating Data Acquisition System (RDAS) and C.G. installation equipment including TM signal conditioners, power supply and converter boxes, yaw and roll accelerometers, gyroscopes, and the other related electronics packages. The rack is an aluminum sheet assembly that resembles a three-shelf structure which sits above the aft end of the trimmable ballast baseplate at station 391.5, buttline 0.0. This component is composed of an upper and lower frame with adjustable shelf trays and is mounted at both the ballast rack aft end and the transition section wall. This instrumentation rack is considered to contribute minor structural stiffness and mass to the aft cabin section and is modeled through the full discretization method. The C.G. Rack was also recently designed and manufactured through Ames in-house efforts. Previous flight test efforts have used an AEFA built instrumentation rack which was similar to the one presently installed. The C.G. Rack serves to replace the AEFA instrumentation rack. By calculated estimates, the self-weight of the C.G. Rack is 35 lbs. The maximum equipment load of 125 lbs is specified in the design of the rack. By conservative estimate, 75% of this maximum load is taken as the actual equipment load during flight (ie. 93.75 lbs). Thus, the weight of the total component is 128.75 lbs. This type of approximation regarding percentage of the maximum equipment load is acceptable given that slight differences such as these in the overall mass of the rotorcraft model has been shown in previous studies to cause miniscule differences in the overall global modal response. This item was modeled with a full finite element discretization.

B.3 Instrumentation Panel (Aft-Right Hand Side)

Additional instrumentation is required for flight data acquisition and was stored on one instrumentation panel situated in the aft cabin (Figure 12). The instrumentation panel on the starboard side, next to the multiplexer and formatter, is composed of two

separate steel panels between the station 370.0 and 398.0 frames. This assembly was fabricated by the AEFA for 1988 flight tests and is currently in place for MTRAP tests. The instrumentation panel with equipment load weighs 175 lbs by AEFA estimate. This item was modeled with a full discretization.

B.4 Pallet Rack (Aft-Left Hand Side)

A fourth instrumentation rack has been recently installed inside the aft cabin on the left side cabin wall between station 370.0 and 398.0 frames at baselines 28.75" through 36.0" (Figure 13). The three-shelved pallet rack is intended to store calibration boxes, power supply units, synchronization boxes, and all related hardware. It measures 40" in height with shelf area dimensions approximately 19.88" by 7.25". The pallet rack is mounted to the cabin floor with an aluminum baseplate of an area measuring approximately 292 square inches. Both the baseplate and pallet rack assembly is modeled in the finite element model as the entire component is expected to contribute minor structural stiffness and mass influencing frequency response results. The pallet rack is unique in comparison to the previously installed AEFA instrumentation rack in that it is mounted through a cabin floor baseplate unlike the AEFA rack which was mechanically fastened to the cabin wall frames and bulkheads. This item was modeled with a full discretization.

The component was designed and manufactured by NASA Ames to replace recently returned AEFA instrumentation racks. Previous flight test efforts have used the AEFA built instrumentation rack. The pallet rack has a calculated self-weight of 66 lbs. As with the C.G. rack, the manufacturing designs accounting for stress and failure criteria allow a maximum equipment load of 25 lbs. The total equipment load is used as the actual flight test load as the 25 lbs is a low estimate for the built-up structure. Thus, 90 lbs constitute the total weight of the component.

C. Static Frequency Converter Baseplate

The frequency converter is another flight component that requires a mounting surface (Figure 14). The tape recorder baseplate is a one-piece 0.125" aluminum

sheet covering approximately 13.0" by 20.0 " in area. The frequency converter plate assembly is located on the right front side of the cabin floor behind the flight test engineer's instrumentation rack. It is fastened to the cabin floor at station 283.0 and centered about baseline 23.58. Four shock mounts on top of the baseplate support the static frequency converter. Based on UTTAS flight designs, this installation was redesigned and manufactured at NASA Ames. With shock mounts, the simple baseplate is estimated to weight 7.5 lbs. The static frequency converter has a self-weight of 80 lbs. This item was modeled with a full finite element discretization.

D. Adapter Plate Assembly

Many baseplates and mounts for self-enclosed instrumentation boxes are included in the MTRAP flight configuration and attached at a series of cabin floor tie-down points. These include mounts for power sources, multiplexers, etc. Although these component mounts will not contribute significantly to the structural stiffness, the sum of all these mounts in concert may "fine tune" the vibratory response of the cabin floor through their minor additive stiffness and mass contributions. These baseplates and mounts include the Adapter Plate Assembly (Figure 15). This item was modeled with a full discretization.

A single adapter plate assembly was designed and manufactured at NASA Ames to replace individual NASA/AEFA baseplates for the mounting of the following components:

Formatter/Multiplexer
Tape Recorder I
Tape Recorder II

The single 0.50" thick aluminum baseplate has several main cutouts due to weight considerations and is located on the right aft cabin floor in the right cabin door way. The plate assembly covers an area 110.75" by 27". between stations 329.0 and 397.0. Three component trays for the formatter, multiplexer, and tape recorders, are attached to the adapter plate through a series of shock mounts. The formatter, multiplexer, and tape recorders have significant weights and are considered to be important mass items as opposed to equipment load weights which are modeled differently. These differences will be elaborated upon in a later discussion regarding mass modeling. The self-weight of the

adapter plate and assembly is 44.10 lbs by NASA Ames stress and failure design specifications.

We also note that a limited analysis of the formatter/multiplexer rack has been completed by NASA Ames Systems Engineering Division to determine safety and failure criteria for installation. For our purposes, this rack and its distributed self-weight was considered to be separate from the lumped masses of the formatter and multiplexer.

E. Over Fuel Cell Ballast Assemblies

To maintain a predetermined longitudinal center of gravity of the helicopter during flight test studies, several locations along the length of the UH-60A have been set aside for ballast support structures. Such locations for the support structures include the nose bay, the cabin floor, the aft cabin area, and tail section. The over fuel cell ballast assemblies are examples of such support structures located behind the aft cabin above the right and left hand side fuel tanks (Figure 16). Located at spaces between baselines +/-10.0 and +/- 30.0 on both the right and left sides of the aircraft center line, the over fuel cell ballast structure is composed of two identical tri-beam support/baseplate assemblies that may carry up to fifteen lead sheets (19.31" by 36.75" area baseplate each). Each assembly is capable of supporting 750 lbs of lead sheets to be treated equivalently as simulated equipment loads. The over fuel cell assemblies have a self-weight of 130 lbs each to ensure a gross ballast load of 1,760 lbs for both sides with the weight of the assemblies included. Because of the rigid design of this installation, the over fuel cell ballast assemblies are modeled with respect to stiffness in addition to mass. These installations were designed and manufactured at Sikorsky Aircraft. We note that under the general arrangement for a longitudinal center of gravity expansion program, the Over Fuel Cell ballast had been defined as a ballast item that may range between the full 1,760 lbs to as low as 274 lbs at station 421.0 It had often been the case, that no ballast was added to the assemblies. This item was modeled with a full discretization.

2.3 Mass Items

A. RDAS II Instrumentation System

The RDAS II Instrumentation System replacing the previous RDAS I system or 'MUX bucket' consists of various types of telemetry/computer hardware stored inside a cylindrical enclosure (Figure 17). The system is located at station, butt, and waterline (341.215, 0.0, 315.0). The RDAS enclosure is mounted to the top of the main rotor head. Although the RDAS II System may undergo slight mass modifications to suit future flight test needs, the system has been weighed at 133 lbs. RDAS II is not considered to make a structural contribution to the global or local fuselage structure. As with the previous RDAS I, the RDAS II instrumentation system was designed and manufactured through NASA Ames in-house efforts.

B. Pilot, Co-Pilot, Flight Test Engineer

Passenger weights are clearly defined as mass items contributing weight to the flight configuration solely. A individual weight of 200 lbs for the pilot, co-pilot, and flight test engineer or observer has been designated as an acceptable standard passenger weight. Both the pilot and co-pilot are located at station, butt, and water line coordinates (F.S. 227.10, B.L. 24.0, W.L. 234.70) and (F.S. 227.10, B.L. -24.0, W.L. 234.70) at right and left hand sides in the cockpit section respectively. Seated in the forward cabin, the flight test engineer is located at (F.S. 277.0, B.L. 0.0, W.L. 218.781) on the observer seat mounted on top of the forward section of the ballast rack. We note that under a general arrangement for the LCGEP, both the pilot and copilot would have been defined as ballast items at station 229.00 .

C. Full Fuel

Full fuel for the MTRAP configuration weighs 2,448 lbs by UH-60A Project Office estimates. This standard full fuel weight for most production UH-60A craft is divided into two equal weights corresponding the right and left hand sides of the fuel tank in the aft cabin. These locations correspond to global coordinates (F.S. 420.80, B.L. -

19.0, W.L. 221.90) and (F.S. 420.80, B.L. 19.0, W.L. 221.90). Fuel weight has not been generally accepted as a pre-determined number for past configuration studies. Previous configurations such as DAMVIBS have used a lower total fuel weight of 2,300 lbs as the configuration was considered for ground vibration tests only. As a side note, empty right and left hand side fuel tanks weigh 160 lbs each.

D. Laser Cube Assembly (2)

Several devices have been dedicated for purposes of telemetry. Among them are two laser cube assemblies mounted externally on both stub wings on the right and left hand sides (Figure 18). The right and left stub wing cube assemblies have been estimated to weigh 8 lbs each at locations (F.S. 256.25, B.L. 49.0, W.L. 205.2583) and (F.S. 256.25, B.L. 49.0, W.L. 205.2583) respectively. Both laser cube assemblies have been design and manufacture through NASA Ames in-house efforts.

E. Trimmable Ballast System: Movable/Adjustable Ballast Box Assembly

Although the baseplate/ballast rack is considered to contribute significant structural stiffness to the cabin floor, two subcomponents of the trimmable ballast system warrant modeling in terms of mass contribution only. These subcomponents include the observer seat with flight test engineer/observer weight and the ballast box assembly with added lead ballast. Developed and manufactured by NASA Ames, the movable/adjustable ballast box (Figure 9) serves as a welded enclosure for the addition of lead sheet ballast plates (each with 9.62" by 21.62" area and .62" thickness dimensions) up to a maximum of 2900 lbs (2,500 lbs for the MTRAP configuration) As fuel is used during a flight operation causing changes in the center of gravity, the controlled movement of this box allows the maintenance of a constant longitudinal center of gravity. It is operated by a self-attached gear motor along the track and guide rails on the baseplate. The assembly centrally occupies the track length between stations 290.0 to 398.0, between baselines -10.0 and 10.0 on the right left sides of the aircraft centerline. Although a structurally rigid component in itself, the ballast box is modeled with respect to mass only because it does not contribute structural stiffness to the cabin floor or to the global fuselage response. A single lumped weight of 3,163 lbs is used to represent the box assembly and the other equipment components mounted on the box assembly. This lumped weight includes the following:

Item	Weight (lbs)
Ballast Box Assembly	238.0
Guide Shaft	15.0
Screw Jack Assembly	5.0
Gear Motor Assembly	5.0
Lead Sheet Ballast	2,900.0
TOTAL	3,163.0 lbs

This lumped weight representation is located at global coordinates (F.S. 313.75, B.L. 0.0, W.L. 218.781). The ballast box assembly was designed and manufactured originally by Sikorsky Aircraft for UTTAS flight tests. Also, we note as in the case of the ballast rack previously described in section 2.2, that a general arrangement for the longitudinal center of gravity of expansion program has defined the ballast box assembly as a ballast item moving between stations 303.4 and 350.8 in the effort to maintain a predetermined center of gravity and gross weight configuration for the helicopter,

F. Observer Station Seat

Three seats are present on the MTRAP flight test configuration. Two of these seats belong to the pilot and co-pilot and are already included in the gross weight configuration while the third extra seat is used for the seating of an observer or flight test engineer. This third seat (Figure 19) is situated in the forward cabin and is mounted on top of the forward track end of the trimmable ballast rack. This member is considered to be a mass item since only its respective mounting surface, the ballast baseplate, is considered to contribute significant structural stiffness to the cabin floor. The observer station seat weighs 63.4 lbs denoted and is located at coordinates (F.S. 277.0, B.L. 0.0, W.L. 218.781) with the flight engineer/observer location. The seat was purchased from Simula, Inc.

G. Tape Recorder I, Tape Recorder II, Formatter, & HALPS Multiplexer

The adapter plate assembly previously described serves as a mounting surface for three individual equipment trays. Each tray is mounted to the adapter plate through a series of shock mounts. Two flight data tape recorders, a formatter, and multiplexer (Figure 20) are placed on these trays. The two recorders with their respective trays weigh 52.5 lbs each (the recorder at 50 lbs, equipment tray at 2.5 lbs) and occupy the first two forward trays. The locations of tape recorder I and II are (F.S. 337.875, B.L. 29.375, W.L. 212.156) and (F.S. 358.125, B.L. 29.375, W.L. 212.281) respectively. The formatter occupies the last aft cabin equipment tray with the HALPS multiplexer placed on top towards the forward portion of the formatter enclosure deck. The formatter and multiplexer together with its equipment tray weigh 226.9 lbs (the formatter at 143.0 lbs, the multiplexer at 78.9 lbs, and the larger equipment tray at 5.0 lbs). The HALPS enclosure was designed and manufactured at NASA Ames while the other internal equipment components were purchased or on loan. These subcomponents were treated as lumped masses and placed with the adapter plate assembly. The tape recorders each have their respective lumped masses while the formatter and multiplexer centers of gravity were computed and averaged commensurate to their mass contribution and separation distance such that a single lumped mass could be specified for the two sub-components. The centroid location of the formatter and multiplexer lumped mass has its global coordinate at (F.S. 379.149, B.L. 25.3167, W.L. 224.4573).

H. Over Fuel Cell Ballast

The over fuel cell ballast also requires a companion description to the external structural component, the over fuel cell ballast assembly. Ballast over the net self-weight of the ballast assembly could be modified depending upon the flight requirements for maintaining a predetermined longitudinal centroid of the helicopter. As previously described in the section dealing with internal structural components, each assembly on either the right or left hand side on top of the full cell has a self-weight of 130 lbs to which a maximum of 750 lbs of additional ballast may be supported. The additional ballast is placed approximately between locations (F.S. 400.5803, B.L. 21.2029, W.L. 242.542) and (F.S. 439.8803, B.L. 21.2029, W.L. 242.542) on the right side and

(F.S. 400.5803, B.L. -21.2029, W.L. 242.542) and (F.S. 439.8803, B.L. -21.2029, W.L. 242.542) on the left side. The assembly and lead ballast plates were designed and manufactured by NASA Ames.

I. MTRAP Instrumented Main Rotor Blades

Although rotor blades have not been considered as structural components in past DAMVIBS finite element analyses, the mass of the four rotor blades were included. A single blade weighs 211 lbs. The rotor head mass in the NASTRAN model is equal to the static non-flapping mass of the aircraft rotor head plus 50% of the instrumented main rotor blade flapping mass. Two of the four rotor blades are uniquely instrumented and were designed and manufactured by Sikorsky Aircraft.

An itemized summary of the flight components and their respective weights is presented in Table V. A description of optional flight components that have been used within the MTRA Program but that are not onboard the current configuration are presented in Appendix A-1 for reference. A practical worksheet detailing the sub components and weights layout may also be seen in Appendix A-2.

3. SUMMARY

In this section and evaluation and description of most important flight components have been summarized. Also, a list of flight components unique to the MTRAP Flight Configuration (over a baseline production configuration) has been generated. These components fall into one of three categories that specify their location and contribution in terms of stiffness and/or mass: 1) External Structural Components, 2) Internal Structural Components, and 3) Mass Items. Each component has been described with respect to its location in the global model, assessed in terms of its structural and/or weight importance, and considered with appropriate estimations of any ballast or flight payloads if applicable. The modeling method used to discretize the respective structural flight component was described.

VI. MODELING OF COMPONENTS

1. Objective

The effort to model the relevant flight components was conducted in three parts:

1) Evaluation of Current Flight Components
2) Gathering of Component Modeling Data
3) Finite Element Discretization of Component Data

A general description of these steps is described:

2. Evaluation of Current Flight Components

After the total list of flight components was made and each component categorized, the components were evaluated in terms of their individual contribution in significantly changing the structural and mass properties of the global response model. The modeling effort must ensure the correct discretization of additional finite element structures. Hence, a rigorous definition of the articles was necessary in order to address the following characteristics and determine their importance in the global model:

1) Complex structural cut-outs (fillets, minor curved surfaces)
2) Definition of tie-down points
3) Selection of finite element mesh size
4) Displacement boundary conditions at tie-down interfaces
5) Lumped mass modeling of small and large flight components (ie. ballast racks, and laser cubes mounts)
6) Lack of physical tests to validate FE model accuracy

3. Gathering of Component Modeling Data

With a list of those flight components that required structural modeling, a significant part of the modeling effort could be dedicated to the gathering of manufacturing blueprints and/or physical measurements and estimations. This was required to obtain necessary modeling data including the following: 1) component dimension data, 2) material property data, 3) connection or tie-down information, and 4) general weight and ballast layout information. Component dimension data includes sheet thicknesses, details regarding beam cross sections, overall component dimensions, and other information relevant to modeling the geometry of the given flight component. Material property data includes elastic moduli, Poisson's ratio, and other data regarding the mechanical behavior of the component material(s) also used in the finite element formulation. With regards to connection or tie-down information, data is required to determine how the component is fixed to the test vehicle so that displacement boundary conditions may be specified between respective nodes of the discretized flight test component and the existing finite element mesh of the UH-60A model. Information regarding the general weight and ballast layout on the test vehicle was gathered to determine the locations on the UH-60A model or on the individual flight components at which concentrated masses could be placed. All modeling data was obtained from design blueprints or found through direct physical measurements of the components on board the UH-60A test vehicle. Generally, cross referencing between these two main sources of data provided the best modeling estimates of a limited number of components where no formal information was listed. Other related references such as material property tables were additionally utilized. We also note that previous data from sources such as DAMVIBS and NASA/AEFA ground vibration testing and modeling have been useful (for example, in the determination of spatial locations of mass items).

4. Finite Element Discretization of Component Data

The UH-60 components were modeled using MSC NASTRAN [5]. The following is a description of the NASTRAN elements used to model these components. Based on the modeling data gathered for each respective flight component, a finite element mesh was defined with grid points (GRIDs) in terms of the basic coordinate system (COORD) of the UH-60A NASTRAN model:

The connectivity, material properties, and dimensional characteristics of structural members of the MTRAP flight components are discretized analytically through the formulation and selective combination of several basic finite elements. Elements, such as quadrilateral plates (CQUAD4s) used to model thin shell structures, are characterized by the coupling of bending and membrane stiffnesses. CQUAD4s are selected and implemented based on the respective flight component and its specific structural composition. Likewise, triangular CTRIA3 thin plate/shell elements can used in place of CQUAD4s to describe highly curved, warped, or swept surfaces or to represent nonrectangular sections in modeling difficult or complex geometries. CTRIA3 elements, like CQUAD4s, are also characterized by the coupling of bending and membrance stiffnesses and are thus subject to bending and twisting moments in addition to shear and normal forces.

Beam-type element are also required in the discretization of MTRAP flight components. CBAR or CTUBE elements may be used where needed to model items such as angled or hollowed cylindrical beams of uniform cross section. CBARs are uniaxial bar elements that may exhibit extension, torsion, and bending behavior and thus may be subjected to torque and bending moments in addition to shear and axial forces. CTUBEs are tubular elements describing beams of circular cross section that may undergo tension, compression, and torsion behavior.

For both thin-shell and beam-type elements, isotropic material properties, cross-sectional data, and other related element parameters are specified on MAT1 material property cards in association with PSHELL, PBAR, and PTUBE element property cards.

Multiple point constraint or MPC cards are used to define displacement relations between appropriate degrees of freedom. Other constraints such as those describing tie-down points between flight component and UH-60A mesh are also defined similarly. Concentrated masses (CONM2) reflecting flight component mass, cargo, or other ballast are defined and distributed at appropriate grid points (GRID) and may be connected respectively with rigid elements such as RBE3 if appropriate.

A graphical summation of the finite element components representing the structural flight items are presented in Figure 21. A detailed description of the modeling of each component is given below.

4.1 External Structural Components

A. Instrumented Test Boom

The finite element mesh modeling the instrumented test boom is described by 33 grid points and a total of 32 CTUBE elements. The test boom geometrically consists of a series of cylindrical tubes of various diameters and wall thicknesses and is modeled with CTUBE elements. Constraint relations describe the two rigid supports between the test boom and appropriate fuselage station frames This basic grid mesh for the component is presented in Figure 22. The number of each grid point is identified in the figure.

B. Instrumented LASSIE Bar

The finite element mesh modeling the LASSIE bar is described by 24 grid points and a total of 23 elements. Of these 23 elements, 21 are CTUBE elements and 2 are CBAR elements. The LASSIE bar grid point mesh is presented in Figure 23.

4.2 Internal Structural Components

A. Trimmable Ballast System: Baseplate ("Ballast Rack")

The finite element mesh modeling the Trimmable Ballast System (TBS) ballast rack is described by 479 grid points and a total of 350 elements. Of these 350 elements, there are 192 CQUAD4 quadrilateral elements, 100 CTRIA3 triangular plate elements, and 58 CBARs. The ballast rack is modeled in detail with CQUAD4 triangular plate elements to represent the extruded baseplate with its respective cutouts. The various guide angles and rails for the moving ballast box are also modeled with the observer seat tracks. These angle and rail elements are modeled with CBAR bar elements and connected to the baseplate through displacement relations that may be defined through MPC cards. The ballast rack in itself is 'tied down' at eleven points to the cabin

floor through MPC relations at appropriate points consistent with the tie-down points defined on the ballast rack mesh. This mesh is presented in Figure 24.

B. INSTRUMENTATION RACKS:

Flight Engineer Instrumentation Rack (Fwd Rt Cabin)
C.G. Rack (Aft Central Cabin)
Instrumentation Panel (Aft Right Cabin)
Pallet Rack (Aft Left Cabin)

B.1 Flight Engineer Instrumentation Rack (Forward-Right Hand Side)

The finite element mesh modeling the flight test engineer's instrumentation rack is described by 20 grid points and a total of 16 elements. All 16 of these elements are CBARs. The major cross beams that run from the bottom to the top of the station frame and the two mounting beam surfaces in the forward right hand side section are modeled as they are the main structural feature with significant cross section and material stiffness relative to the instrumentation box which is supported by the cross beams. This item is modeled with an equivalent but partial discretization since the equipment box mounted is relatively much less stiffer than the major cross beams which may be modeled correctly with a small number of finite elements. The instrumentation rack is tied to the station frame ribs through the two mounting beam surfaces. This mesh is presented in Figure 25.

B.2 Center of Gravity (C.G.) Rack (Aft Central Instrumentation Rack)

The finite element mesh modeling the C.G. rack is described by 129 grid points and a total of 180 elements. Of these 180 elements, 96 are CQUAD4s and 84 are CBARs. The shelf angles, trays, and side panels are modeled with CBAR bar and CQUAD quadrilateral elements respectively. The C.G. rack is mounted to the top of the TBS ballast rack in the aft central cabin through a series of MPC displacement relations describing the appropriate six tie-down points. The C.G. rack component model is presented in Figure 26.

B.3 Instrumentation Panel (Aft-Right Hand Side)

The finite element mesh modeling the instrumentation panel in the aft right hand side of the cabin is described by 55 grid points and a total of 40 elements. Of these 40 elements, 36 are CQUAD4s and 4 are CBARs. The two separate upper and lower sections of instrumentation panel are modeled with CQUAD4 quadrilaterals as they are essentially single piece thin plates with miniscule cut outs mounted to the side cabin at various tie-down points (seven) on station frame ribs. An adjoining mounting beam angle separating the upper and lower sections is described by CBAR bar elements and is of significant area cross section, inertia, and material stiffness. The component model is presented in Figure 27.

B.4 Pallet Rack (Aft-Left Hand Side)

The finite element mesh modeling the pallet rack in the aft left hand side section of the cabin is described by 74 grid points and a total of 97 elements. Of these 97 elements, 38 are CQUAD4 quadrilateral elements, 3 are CTRIA3 triangular elements, and 56 are CBAR bar elements. The shelf angles, trays, and side panels of the pallet rack are modeled with CBAR bar and CQUAD4 quadrilateral elements respectively. The baseplate that serves as a mounting surface for the pallet rack is also modeled through CQUAD4 elements. MPC displacement relations describe the eight tie-downconnections between the rack and the mounting baseplate and also the those between the baseplate and the cabin floor skin. This component model is seen in Figure 28.

C. Static Frequency Converter Baseplate

The finite element mesh modeling the static frequency converter baseplate is described by 15 grid points and a total of 8 CQUAD4 quadrilateral elements. The thin baseplate is modeled exclusively with CQUAD4 quadrilateral elements and is considered to be a minor structural addition. MPC displacement relations are again used to describe

two tie downs between the baseplate and the cabin floor. This component that occupies a very small space locally on the cabin floor is seen in Figure 29.

D. Adapter Plate Assembly

The finite element mesh modeling the adapter plate and assembly is described by 104 grid points and a total of 83 elements. Of these 83 elements, 55 are CQUAD4s elements and 28 are CTRIA3 elements. In a manner similar to the modeling of the TBS ballast rack, the adapter plate mono-structure with its respective cut outs is modeled with CQUAD4 and CTRIA3 elements. Four grid points describe respective tie-downs to the cabin floor skin. This component mesh is presented in Figure 30.

E. Over Fuel Cell Ballast Assembly (2)

The finite element mesh modeling each over fuel cell ballast assembly (right or left hand side) is described by 35 grid points and a total of 54 elements. Of these 54 elements, 24 are CQUAD4 elements and 30 are CBAR elements. The mounting beam surfaces and ballast support angles of significant area cross section and inertia/material properties are modeled with CBAR bar elements while the lead ballast plate support surface is modeled with CQUAD4 quadrilateral elements. Both RHS and LHS assembly models are presented in Figures 31 and 32 respectively.

4.3 Mass Items

RDAS II Instrumentation System
Pilot, Co-Pilot, Flight Test Engineer
Full Fuel
Laser Cube Assembly (2)
Trimmable Ballast System: Movable/Adjustable Ballast Box Assembly
Observer Station Seat
Tape Recorder I, Tape Recorder II, Formatter, & HALPS Multiplexer
Over Fuel Cell Ballast
MTRAP Instrumented Main Rotor Blades

The distribution of structural and nonstructural weight to the appropriate areas of the finite element model is often a tedious and time consuming task. In the case of rotorcraft, most weight is often of a nonstructural nature. Automated procedures with a NASTRAN interface program are often used in industry to generate the necessary NASTRAN input data. In this current study, special mass items such as flight components listed above and seen in Table V were entered into NASTRAN code separately "by hand" to represent unique items or different weight configurations. In each case of the respective mass item, it was determined that the mass of the component could be represented either as 1) a single point mass located at its center of gravity (F.S., B.L., W.L.) with respect to the global coordinates of the UH-60A model or 2) as a series of point masses distributed uniformly across the appropriate component element mesh surface or line. The mass items mentioned above were modeled in one of these two ways such that 1) an item was specified by a CONM2 concentrated mass at a GRID point corresponding to the item's center of gravity and rigidly connected to a nearby global model with RBE3 elements or 2) the mass of the item was divided into smaller CONM2 concentrated masses and assigned to the corresponding GRID point or points on the existing finite element mesh. For example, the full fuel mass is divided into two equal point masses corresponding to fuel located on right and left hand sides. The two centers of gravity corresponding to these fuel parts is specified by a grid point and connected to the nearby UH-60A global mesh with rigid elements. In another example, the 376 lbs of the TBS ballast rack self weight was divided equally into 78 point masses and distributed uniformly among 78 separate existing grid points along the central portion of the ballast rack finite element mesh. These items were discretized in a manner similar to that used in the previous study by the authors.

For the most of the UH-60A mass model items however, lumped masses are generated by first creating a computer file listing the weight and inertia properties of approximately 5,000 components (both structural and nonstructural) in a MIL-STD tabulation form. Hence, a description of the item (ie. pilot, cabin seat, frame section, etc.), its mass, centroid location, and mass moments of inertia, in terms of the model coordinate system are stored. Second, a volume describing the entire aircraft, again using the model coordinate system, is defined in the mass model generation program and divided into a greater number of smaller, equally sized subvolumes or regions. The interface program assigns each mass item a location in the model volume and respective

region based on its centroidal coordinates. Next, the program calculates a new center of gravity and single lumped mass from the summation and computation of mass items data for each region. Finally, NASTRAN input data lines are written specifying a grid point (GRID) and concentrated mass (CONM2) at the new centroid of each region. This process is repeated for each region over the entire volume. An RBE3 rigid element is created for each concentrated or lumped mass to connect the concentrated mass item to the structural model. The RBE3 element allows the mass to undergo components of motion calculated from the average summation or weighted average of other nearby structural grid points. This mass modeling procedure is depicted in Figure 33. The volume and region size and shape may be arbitrarily chosen based upon the unique structural and mass configuration of different aircraft. For example, the UH-60A NASTRAN model by Sikorsky uses a finite pie shaped inertia region, while Boeing-Vertol uses a rectangular box shape for their finite element models. The combination of the GRID, CONM2, and RBE3 elements are used frequently in the definition of mass items. Alternatively, mass may be specified directly at a pre-existing grid point if the mass occupies that point on the global structure.

5. Summary

The modeling of additional structural/mass components may be divided into three parts: 1) Evaluation of Current Flight Components, 2) Gathering of Component Modeling Data, and 3) the Finite Element Discretization of Component Data. Flight components are categorized in various groups based on their contribution in terms of structural stiffness and additional weight. Component modeling data is generated using existing blueprint or manufacturing data and physical measurements. Component data is used to generate the basic finite element meshes for each respective component.

VII. MODELING CHECKS

1. Objective

To attain a certain level of confidence in the UH-60A finite element discretization, several modeling checks were performed during this task to ensure that the model characterizes the true dynamic behavior of the prototype flight structure. Modeling checks had the purpose of ensuring the proper representation of internal and external constraint conditions in both static and dynamic analyses. Numerous checks have been developed for general rotorcraft finite element analyses through pre-DAMVIBS efforts in industry. Of the several methods used in this modeling task, the *rigid body/enforced displacement check* was the most informative and simplest to apply to the UH-60A dynamic model and warrants a brief description. This form of comprehensive check also maintained a level of physical meaning when applied to the model. We note that other forms of model checks were conducted progressively with the development of the model throughout the initial modeling effort to the processing of final modal results.

2. Rigid Body Check / Enforced Displacement Check

The principal purpose of the *Rigid body / Enforced Displacement Check* is to ensure that there are no inconsistent constraints, primarily unwanted single point constraints (SPCs), applied to the model. If the dynamic model is placed in a free body condition with no inconsistent constraints present, then it must be capable of undergoing rigid body motions without inducing internal forces.

The NASTRAN model is rigidly constrained at grid points corresponding to the main and tail rotor shaft heads in all translational and rotational degrees of freedom excluding the longitudinal degree of freedom (DOF). Single Point Constraints (SPCs) are used to specify the rigid constraints. In the free longitudinal DOF, a unit displacement is applied to the main rotor shaft. A graphical depiction of this check is presented in Figure 34. This applied unit displacement will yield clearly defined zero displacements and notable force reactions at overconstrained grid points. For correctly unconstrained grid points, including the node

specifying the tail rotor shaft head, unit displacements in the longitudinal direction will be computed. Results are easily evaluated from the examination of printed displacement and single point constraint force output. If all grid point displacements on the model are equal to the applied unit displacement and if all internal forces, including SPC forces, are zero or deemed negligible, then the fuselage model will be unrestricted in translation and rotation motions (Table VI). Deviation from these conditions will indicate the presence of unwanted and unspecified constraints not defined by the analyst. The rigid body/enforced displacement check is also conducted along the other five directional axes to verify full free-free body conditions.

3. Additional Modeling Checks

We note that although only one important modeling check is fully described above, other complementary modeling checks have been performed to ensure the reasonability of results. These include, among others, the identification of rigid body or suspension mode frequencies that are close to zero, ensuring that the programmed addition of component or item mass is reflected in the finite element computation of the global mass for the model in the basic coordinate system, and the computation of correct generalized mass matrix components.

VIII. BUILD-UP OF FLIGHT COMPONENT STRUCTURE STUDY (BUCSS)

1. Objective

The main objective of the dynamic study is **to quantify the dynamic effects of cumulatively added flight component structures** through the comparison of modal shapes and frequencies from analytical models. Dynamic characteristics of growing structural configuration are defined and changes in structural behavior, resulting from the cumulative addition of the individual flight components and the respective modeling revisions to the primary/secondary structure model, become evident. Eigenvector/eigenvalue extractions are performed for each configuration giving respective modal deformation states and resonant frequencies. The cumulative build-up of individual component structures also serves a secondary objective as it allows a check-out of each component to be performed with respect to its modeling discretization and the determination of any spurious mechanisms or unreasonable numerical results that may be produced within the solution execution as the structures are added component by component individually.

2. Starting Reference Configuration

A modal study regarding structural contribution and the build-up with individual flight component structures must have a finite element or 'baseline' configuration which serves as a reference point for subsequent comparison. Although the choice for this configuration is arbitrary as we will be observing slight changes in modal frequency relative to a NASA/AEFA mass distribution on a baseline UH-60A primary/secondary structural system has been chosen since it has been studied in some detail and is of a mass configuration quite similar to that of the MTRAP configuration. This starting reference configuration is presented in Figure 35. The model of the suspension system used in ground vibration testing for NASA/AEFA has also been implemented as it is a good general representation of the weight and the type of industrial suspension systems being utilized in modern large scale testing. Clearly, a similar type of suspension system will be used in 1995 testing of the MTRAP configuration. As of the time of this current study, the suspension system to be used in 1995 testing *has yet to be defined.* Over

the UH-60A baseline weight of 10,140 lbs, the NASA/AEFA mass distribution includes the following items with their respective weights:

Mass Item	Weight (lbs)
Pilot	240
Co-Pilot	220
Full Fuel RHS	1,150
Full Fuel LHS	1,150
Cargo Ballast	4,550
Fwd. Instr. Rack	75
Aft. RHS Instr. Rack	175
Aft. LHS Instr. Rack	100
Subtotal	**7,660**
Baseline UH-60A	10,140
TOTAL	**17,800**

This represents the BUCSS starting reference configuration. Using this reference configuration, a structural finite element modeling of individual flight component structures are added cumulatively with eigenvalue analyses being performed at each step.

It is recognized that the modal shape and frequency results at the end of the structural build-up are not representative of the final results because the final mass distribution characteristic of the MTRAP configuration must be added as well in the Build-Up of flight Component Mass (BUCMS) study described in the next section. The final model (FEM III) at the end of the investigation includes updated primary/secondary structure and Sikorsky modeling revisions. Results from this part of the overall study tell us of relative changes in modal response due to slight modifications in model stiffness only.

3. Constraints

In a physical sense, the UH-60A finite element model is constrained through two suspension systems corresponding to the main rotor and tail rotor bungee systems respectively. The grid points corresponding to the top of these bungee systems are rigidly fixed while the rotorcraft grid points are allowed to translate and rotate freely. Although the model is constrained in this manner, it still may be treated as a 'free-free' structure for practical purposes as the bungee suspension system and its corresponding finite element discretization are designed to not interfere with the higher elastic modes of the aircraft. However, the frequency content of the first six 'rigid body modes' in these following data analyses should clearly reflect the addition of this suspension constraint. Thus, not all of the first six rigid body modes are zero but they should be low to reflect the low stiffness characteristic of the bungee system. We also note that the addition of any suspension systems must also include mass corresponding to the respective shaker hardware and cable/chain mass. Hence, a suspension format versus a non-suspension format used in the eigenanalysis is differentiated also by the addition of mass (which may be significant).

4. Loading

In this real eigenvalue/vector analysis, no concentrated or distributed loads are applied to the aircraft model. We note that the inclusion of a uniform gravity load is not present in this analysis. Although a differential stiffness matrix that accounts for a uniform gravity field in the vertical direction may be included, previous studies with the NASA/AEFA configuration have shown that changes in modal frequency are relatively insignificant with the exception of one to two modes. Applying gravity would also interfere with the study of individual component structural or mass additions because one would have to definitively attribute the percent change to either the component addition and/or gravity inclusion quantitatively. A comprehensive gravity analysis is left appropriately to the analyst after the completion of 1995 full scale testing and the definition of the suspension system and suspension mass.

5. Computational Methods & Solutions

In the dynamic analyses, emphasis is placed on the use of eigenvalue analysis in yielding the most informative data in the quantification of additional components and the correlation with shake test results. The studies of this NASTRAN model rely on several matrix decomposition, reduction, and computation techniques to compute the eigenvectors (mode shapes) and eigenvalues (resonant frequencies). NASTRAN Solution 3 for Normal Modes Analysis is used with a modified algorithm based on Givens method of tridiagonalization for the real eigenvalue/eigenvector extraction in the free undamped vibrations case. Solution 3 for Normal Modes is also used for preliminary component studies. This method is chosen from among the other basic Givens and Inverse methods for its computational efficiency and accuracy for large, complex degree of freedom systems where numerous eigensolutions are required after extensive static or dynamic matrix reductions are performed.

With more than 27,000 degrees of freedom specified for each NASTRAN model and restrictions on memory and CPU time, it becomes reasonable to reduce the number of degrees of freedom to a smaller subset, prior to the eigenvalue extraction, which preserves the physical discretization of the actual structure and mathematical integrity of the dynamic formulation. The general method for this type of modal reduction in NASTRAN is called Generalized Dynamic Reduction by which a smaller number of modal degrees of freedom are defined on the basis of their modal participation. Generalized Dynamic Reduction is an extension of the static condensation method (Guyan reduction). The number of degrees of freedom in the subset is approximately equal to the 1.5 times the number of roots found below the maximum frequency of interest in the extraction range. In the case of the UH-60A model (0 to 30 Hz, frequency range of interest), approximately 77 degrees of freedom are used. The details of these reduction and extraction procedures is discussed in the referenced NASTRAN manual [5].

NASTRAN finite element computations and other related operations were performed on Cray Y-MP/832 on site at NASA Ames Research Center's Advance Computing Facility as large memory and CPU time requirements are involved in this structural analysis. Mass storage of the input and output data relevant to this large scale model was located on the facility's Cray X-MP. Editing operations and data transfers were performed on NASA VAX mainframe computers.

6. Eigensystem Results

A real eigenvalue analysis was performed at each separate step or stage when a single flight component discretizations were added **cumulatively** to the global fuselage finite element model from the starting reference configuration (in this case, the NASA/AEFA mass distribution). As described, the first 32 modal frequencies and mode shapes are identified. It is reasonable to be selective in choosing the modes that will be helpful in determining the influence of the component model added respectively. For example, the first six rigid body modes and/or suspension modes that have been identified to be very close to zero frequency and separate from the first elastic mode yield very little information in determining the structural contribution of flight components throughout the overall structural build-up. Having identified the first 27 modes from 0 Hz up to approximately 30 Hz in each component addition stage, experience with the finite element model and ground vibration tests verifying the accuracy of the analytical model has shown the predictive model to be accurate to approximately 20 Hz in most cases. Mode shape descriptions and resonant frequencies are presented in Table VII. Although the first 27 modes have been defined in terms of modal frequency and shape, the influence of structural contribution during structural component build-up may be correctly described using modes starting after rigid body and/or suspension system modes with the first elastic mode to approximately 20 Hz as changes in modal frequency are readily seen with sufficient accuracy and confidence. It is also important to note that these modes contain the basic global fuselage responses that are of great interest including vertical, lateral, and torsion bending. The following flight components are described with respect to percent changes in their modal frequency (Table VIII) with the cumulative addition of each structural contribution from the individual flight components (Table IX) :

6.1 External Structural Components

A. Instrumented Test Boom

The inclusion of the instrumented test boom component influences the global stiffness and hence eigenvalues only slightly. As will be seen section IX, only the introduction of the test boom's distributed mass together n will affect the modal frequency spread in a more notable manner. All modes below the 20 Hz accuracy threshold will undergo a percent less than or equal to 0.098 %.

B. LASSIE Bar

The inclusion of the instrumented LASSIE bar stiffness to the global model also contributes slightly in changing the modal frequency spread. With the exception of the 3rd Vertical Bending / Cockpit/Cabin Torsion mode whose resonant frequency is changed by 0.24 %, all other modes below 20 Hz undergo percent changes below 0.048 %. We note again here that the next build-up including the distributed mass of the LASSIE bar together with its discretized stiffness may cause a greater but not significantly higher percent change.

6.2 Internal Structural Components

A. Trimmable Ballast System

The inclusion of the trimmable ballast system, especially the inclusion of the ballast rack structure, is influential in significantly increasing the in-plane stiffness of a major central portion of the cabin floor. The structural change is evident in the mode frequency changes of the following modes: The 1st Lateral Bending, Stabilator Roll, Cockpit / Cabin Roll, Cockpit / Cabin Roll / 3rd Vertical Bending; all of which are below 20-22 Hz, a generally accepted 'threshold' of accuracy for this specific finite element model. The definition of this approximate threshold is supported by previous ground vibration results. An 80.12% change in modal frequency in the 1st Lateral Bending mode from 4.96 to 8.93 Hz is particularly noteworthy as this indicates the additional stiffness created with the structural inclusion of the component. This significant increase may be reasonable as the singular inclusion of this rack component, with redundant tie-down points, effectively doubles the stiffness of the central portion of the cabin floor. The ballast rack occupies approximately half of the cabin floor area. Some form of experimental verification may be warranted to verify this computed increase.

B.1 Flight Engineer Instrumentation Rack

The inclusion of the primary structural cross support beams that support the flight engineers' instrumentation rack were not expected to contribute significant stiffness to the global model. This is supported by the relatively small percent changes in modal frequency (ie. less than 1 %). The 3rd Vertical Bending/Cockpit/ Cabin Torsion and Cabin Torsion modes are found to change by 0.727 and 0.888 % respectively. The Stabilator Roll, Transmission Pitch/2nd Vertical Bending, and 3rd Vertical Bending modes are also found to change by 0.347, 0.352, and 0.257 % respectively. (As a sidenote, it is observed that all modal frequencies will generally increase, greater than .0001 percent, for the global model with the incorporation of local component finite element models to the global).

B.2 Center of Gravity (C.G.) Rack

Below 20 Hz, the inclusion of the C.G. Rack does not contribute significantly to any changes in the modal frequency and shape. Below the threshold, all modal frequency changes are less than 0.1 %.

B.3 Instrumentation Panel (Aft RHS)

The inclusion of the instrumentation panel in the aft cabin within a bay section between two main frames brings about small minor changes in the modal frequency spread. Only a small number of modes undergoing changes are noteworthy. The Stabilator Roll, Stabilator Roll / Transmisison Roll, and 2nd Vertical Bending / Transmission Vertical modes have mode frequencies that increase 0.499, 0.901, and 1.138 % respectively. Other modes including the 1st Lateral Bending, Transmission Pitch, Transmission Pitch / 2nd Vertical Bending, Transmission Roll / Stabilator Roll, and Cockpit / Cabin Roll modes undergo 0.159, 0.303, 0.176, 0.192, and 0.226 % changes respectively.

B.4 Pallet Rack

The Pallet Rack, a self-supported standing equipment rack, occupying the aft cabin on the left hand side was not considered to change the modal frequency spread significantly through its mounting plate at the cabin floor. This is supported by the observation of two modes below the 20 Hz threshold. The Stabilator / Transmission Roll and 2nd Vertical Bending / Transmission Vertical modes change 0.123 and 0.104 % respectively.

C. Static Frequency Converter Baseplate

Inclusion of the frequency converter baseplate adds minimal in-plane stiffness to the UH-60A cabin floor. All percent decreases for modal frequencies below 20 Hz do not exceed 0.095 % with the exception of the Stabilator Roll / Transmission Roll mode whose frequency increases by 0.22 %. This is reasonable as the frequency converter baseplate is one of the less stiff and smaller components relative to other built-up flight components.

D. Adapter Plate & Assembly

In a similar manner with the ballast rack of the TBS, the inclusion of the adapter plate and assembly contributes in-plane stiffness to the cabin floor. In this case, the structural stiffness contribution is local to the aft right hand side of the floor adjacent to the right cabin door. The following modes change by a small percentage: The Stabilator Roll, 2nd Vertical Bending / Transmission Vertical, and 2nd Vertical Bending / Transmission Pitch modes change 0.545, 0.585, and 0.288 % respectively. Other modes that also change but in a less significant manner include the 1st Lateral Bending, Transmission Pitch / 2nd Vertical Bending, Cockpit/Cabin Roll, and 3rd Vertical Bending / Cockpit/Cabin Torsion modes which undergo 0.131, 0.189, 0.139, and 0.143 % changes respectively.

E. Over Fuel Cell Ballast Assembly

The inclusion of both over fuel cell ballast assemblies on the right and left hand sides is observed to contribute significant in-plane stiffness to the transition section forward of the tail cone sections. Significant percent increases in modal frequency for modes below 20 Hz are evident. The 1st Lateral Bending, Stabilator Roll, Transmission Pitch, Stabilator Roll/Transmission Roll, Cockpit/Cabin Roll, 3rd Vertical Bending / Cockpit/Cabin Torsion, and 3rd Vertical Bending modes undergo a noteworthy 3.29, 1.92, 3.28, 1.98, 1.23, 1.01, and 2.47 % increase in resonant frequency. Other modes including Transmission Roll / Stabilator Yaw, Transmission Roll / Stabilator Roll, 2nd Vertical Bending / Transmission Vertical, 2nd Vertical Bending / Transmission Pitch, and Cockpit/Cabin Roll / 3rd Vertical Bending modes undergo less significant percent changes of 0.19, 0.31, 0.23, 0.22, 0.19 %.

7. Summary

The modal trends observed for the global model in the BUCSS are summarized. Percent changes from the starting reference configuration to the fully built-up structure configuration used in this BUCSS are presented in Table IX for the first 27 modes. Most modes below 20 Hz showed only slight percent changes ranging from 0.539 to 4.027 %. However, the following modes: 1st Lateral Bending, Stabilator Roll, Transmission Pitch, and Cockpit/Cabin Roll; however showed appreciable percent changes. Percent changes of these modes, due to a full structural build-up of the flight components, are 86.6, 15.03, 6.26, and 12.48 % respectively.

The significant percent change of 86.6% in the 1st Lateral Bending frequency may be attributed in most part to the addition of the TBS ballast rack which considerably stiffens the entire length of the UH-60A floor. To a minor extent, the over fuel cell assemblies, on both the right and left hand sides, also contribute to the local stiffness of the top transition section increasing the modal frequency of the mode. Both the Stabilator Roll and Transmission Pitch mode frequencies and their associated percent increases of 15.03 and 6.26 % respectively are also attributed to these two additions. For the Cockpit/Cabin Roll mode, the addition of the TBS ballast rack constitutes the major portion of its 12.48% percent increase in the final built-up configuration frequency from the initial starting reference configuration. The primary flexural action of these global modes are associated with the bending and torsion of the cabin

boxed section. It is reasonable that the addition of the ballast rack has altered the modal frequency of these modes but not the primary global response.

Clearly, while a number of flight components have been added in the final configuration, some structural components, more than others, have contributed more significantly in appreciably increasing the structural stiffness and hence modal frequencies of some basic global displacement patterns such as lateral bending. The majority of the components have 'fine-tuned' the modal frequency to higher frequencies while significant components have effected larger percent changes. The flight component structures are classified as major, minor, and less significant structures in contributing structural stiffness (affecting resonant frequency) to the global model as follows:

Major	Trimmable Ballast System Over Fuel Cell Ballast Assembly (RHS & LHS)
Minor	Flight Engineer's Instrumentation Rack Adapter Plate Assembly Instrumentation Panel
Less Significant	Instrumented Test Boom LASSIE Bar Center of Gravity (C.G.) Rack Pallet Rack Frequency Converter Baseplate

IX. BUILD-UP OF FLIGHT COMPONENT MASS STUDY (BUCMS)

1. Objective

The main objective of this dynamic study is ***to quantify the dynamic effects of added mass representative of the flight component structures and corresponding ballast weight*** through the comparison of modal shapes and frequencies from analytical models. Dynamic characteristics of these configurations are defined and changes in structural behavior, resulting from the cumulative addition of the flight component masses and any respective ballast to the primary/secondary structure model, become evident. Eigenvector/eigenvalue extractions are performed for each configuration giving respective modal deformation states and resonant frequencies. The build-up of individual component masses also serves as a secondary objective as it allows a check-out of each component mass to be performed with respect to modeling discretization and the determination of any spurious mechanisms or unreasonable results that may be produced.

2. Starting Reference Configuration

As in the previous BUCSS, a modal study regarding mass contribution and the build-up of individual component masses **cumulatively** onto their respective flight structures must have a finite element configuration or 'baseline' configuration which serves as a reference point for subsequent comparison. Although the choice for this 'starting point' analytical configuration is again arbitrary as we will be observing slight changes in modal frequency relative to the 'starting point' configuration, a different baseline UH-60A primary/secondary structural system with a *reduced* NASA/AEFA mass distribution has been chosen as a relative known base for comparison. This baseline UH-60A primary/secondary structural system used in the BUCMS also includes the flight component structures **cumulatively** built-up in the previous BUCSS section. Also, this *reduced* mass distribution excludes the weights of several 'overlapping' ballast and instrumentation equipment masses. The BUCMS utilizes this mass distribution since three of the original NASA/AEFA configuration masses would coincide with those internal flight component masses being added in the build-up. These coincident masses

include ballast associated with the trimmable ballast system and two instrumentation rack/panel masses. The availability of data from the previous study of the NASA/AEFA configuration by the authors is also a factor in the selection of this starting configuration. The reduced mass distribution excluding the coincident mass items includes the following with their respective weights:

Mass Item	Weight (lbs)
Pilot	240
Co-Pilot	220
Full Fuel RHS	1,150
Full Fuel LHS	1,150
Cargo Ballast	-
Fwd. Instr. Rack	-
Aft. RHS Instr. Rack	-
Aft. LHS Instr. Rack	100
Subtotal	**2,860**
Baseline UH-60A	10,140
TOTAL	**13,000**

We note that this choice of **'starting reference configuration'** with this unique mass distribution is used in the BUCMS exclusively. Using this reference configuration, flight component mass is added cumulatively with mode frequency and shape being taken at each step. The modal shape and frequency spread and respective percent changes from this mass build-down to this unique starting configuration may be readily seen in the appendix from A-3 and A-4. From A-3 and A-4, one can see that each column shows the change in frequency resulting from the removal of each of the three masses (ie. 'overlapping' ballast, instrumentation rack, instrumentation panel) to create the BUCMS baseline configuration.

It is again recognized that the modal shape and frequency results at the end of the mass build-up are not representative of the *final* results for the MTRAP configuration as the final mass distribution characteristic of the MTRAP configuration with a revised primary/secondary

structural model (FEM III) must be used ultimately. Results from this part of the study tell us of relative changes in modal response due to slight changes in model mass only.

3. Constraints

As in the BUCSS, the UH-60A finite element model includes a discretization of the industrial bungee/chain suspension system used in the ground vibration testing of the DAMVIBS and NASA/AEFA weight distributions. The model is hence not wholly defined as a 'free-free' structure but instead may be simplistically viewed as a spring-mass system where the suspension system at the main and tail rotor shaft serves as a spring to the helicopter mass. The grid points corresponding to the top of these main and tail rotor suspension bungees are rigidly constrained as in the previous structural stiffness study. The suspension system used in ground vibration testing of the DAMVIBS and NASA/AEFA mass distribution has also been implemented since it can be defined as a good general representation of this type of industrial suspension system being utilized in large scale testing. We restate that a similar type of suspension system will be manufactured and used in 1995 testing of the MTRAP configuration.

4. Loading

As in previous build-up study, no concentrated or distributed loads are applied to the rotorcraft model or its respective main and tail rotor systems.

5. Computational Methods & Solutions

Computational methods and solution formats used in the previously described BUCSS are similarly used in this section using the same computational resources.

6. Eigensystem Results

As in the previous BUCSS, the first 27 modes have been identified. Mode descriptions and their modal frequencies with the cumulative addition of respective component masses are presented in Table X. The addition of mass to the components is expected to decrease the

frequencies and equalize the effect of the previous structural build-up. The results show that the inclusion of component mass up to the pre-built stiffness of the flight components result in an overall decrease in frequencies below the 20 Hz threshold. Percent changes in modal frequencies with the BUCMS is presented in Table XI.

6.1 External Structural Components

A. Instrumented Test Boom

Inclusion of the instrumented test boom distributed mass (22 lbs) contributes little to percent changes in the modal frequencies below 20 Hz. Percent changes do not exceed 0.061 %.

B. LASSIE Bar

The inclusion of the distributed mass of the LASSIE bar (10 lbs) likewise does not effect significant percent decreases in resonant frequencies below the 20 Hz threshold. A percent decrease of 0.034 % is not exceeded for all modes below this threshold.

6.2 Internal Structural Components

A. Trimmable Ballast System

The inclusion of the trimmable ballast system and the ballast rack distributed mass cause significant changes in modal frequency response. This is reasonable as trimmable ballast constitutes a major weight contribution to the overall gross weight of the helicopter configuration. This component addition of TBS ballast rack (376 lbs), ballast box (238 lbs), guide shaft (15 lbs), and various peripheral equipment mass and ballast adds 3,539 lbs to the configuration.

Below 20 Hz, the following modes undergo a significant percent decrease in modal frequency: Transmission Pitch / 2nd Vertical Bending, Transmission Roll / Stabilator Yaw, Stabilator Roll / Transmission Roll, Transmission Roll / Stabilator Roll, 2nd Vertical Bending / Transmission Vertical, 2nd Vertical Bending / Transmission Pitch, Cockpit/Cabin Roll, 3rd Vertical Bending, and the Cockpit/Cabin Roll / 3rd Vertical Bending mode. These results reflect the net effect from the **cumulative** addition of component mass onto the pre-existing built-up structure developed from the previous section's BUCSS. Percent decreases for these modes are 5.66, 1.37, 4.81, 3.63, 10.91, 13.97, 7.53, 3.05, and 3.43 % respectively as seen in Table XI. Generally for all modes in this study, the inclusion of mass to the pre-built-up component structures serves to offset the increase in the general frequency spread with the increased stiffness. This offset brings about a better and more realistic estimate of resonant frequency that would be much closer to a given test configuration. We also note that these percent decreases in modal frequency are reasonable if one considers the reduced modal degrees of freedom model to consist of a series of single degrees of freedom whose eigenvalues are subject to the changing ratio of stiffness to mass. Other modes also undergo a less significant percent decrease including the 1st Lateral Bending, Stabilator Roll, Transmission Pitch, and the 3rd Vertical Bending / Cockpit/Cabin Torsion mode which decrease by 0.20, 0.11, 0.063, and 0.99 % respectively as seen in Table XI. Clearly, most of the modes below 20 Hz are affected with the TBS addition of mass.

B.1 Flight Engineer Instrumentation Rack

The mass and stiffness of the flight engineer instrumentation rack (75 lbs) has been considered to contribute only slightly to the overall global frequency response. This is confirmed with minor percent decreases of 0.10, 0.074, 0.25, 0.10, 0.124, 0.19, 0.26, and 0.32 % in the 1st Vertical Bending, 1st Lateral Bending, Stabilator Roll, Transmission Pitch, Transmission Roll / Stabilator Yaw, Cockpit/Cabin Roll, 3rd Vertical Bending / Cockpit/Cabin Torsion, and 3rd Vertical Bending modes respectively.

B.2 Center of Gravity (C.G.) Rack

The inclusion of c.g. rack mass (128.75 lbs) effects a percent decrease in modal frequency of 0.10, 0.25, 0.10, 0.12, 0.19, 0.26 and 0.32 % in the 1st Vertical

Bending, Stabilator Roll, Transmission Pitch, Transmission Roll / Stabilator Yaw, Cockpit/Cabin Roll, 3rd Vertical Bending / Cockpit/Cabin Torsion, and 3rd Vertical Bending modes respectively. To a lesser degree, a percent decrease of 0.074 % is found in the 1st Lateral Bending mode with this component mass added to the pre-existing component stiffness discretization.

B.3 Instrumentation Panel (Aft RHS)

The inclusion of instrumentation panel mass (175 lbs) causes notable decreases throughout the modal frequencies below 20 Hz. The 1st Vertical Bending, Stabilator Roll, Transmission Pitch, Transmission Roll / Stabilator Roll, 2nd Vertical Bending / Transmission Pitch, Cockpit/Cabin Roll, 3rd Vertical Bending / Cockpit/Cabin Torsion, and 3rd Vertical Bending modes undergo percent changes of 0.30, 0.56 0.11, 0.29, 0.28, 0.20, 0.10, and 0.46 respectively. Most of the less significant percent changes are below 0.41 %.

B.4 Pallet Rack

The inclusion of the respective pallet rack mass (90 lbs) does not cause a significant percent decrease in modal results. Below 20 Hz, modal frequencies do not decrease more than 0.074 percent.

C. Static Frequency Converter Baseplate

The inclusion of the static frequency converter and baseplate mass causes minimal decreases in modal frequency. Modes below 20 Hz have percent decreases that do not exceed 0.073 % with the exception of the 3rd Vertical Bending / Cockpit/Cabin Torsion mode which decreases by 0.11 %. These small percent decreases are reasonable as the frequency converter baseplate constitutes one of the less stiff and sizable component members. The static frequency converter weighs of 80 lbs while the baseplate itself weighs 7.5 lbs.

D. Adapter Plate & Assembly

Although the adapter plate and assembly weighs only 44.10 lbs, it does contribute in-plane stiffness to the cabin floor in the same manner that the ballast rack does. This was observed in the BUCSS. In this BUCMS, the inclusion of the adapter plate and assembly includes component masses of the two tape recorders (52.5 lbs each), formatter (143 lbs), and multiplexer (78.90 lbs) payloads and their respective mounting hardware.

Table XI shows percent decreases of 0.11, 0.099, 0.13, 0.09, and 0.11 % are found for the 1st Lateral Bending, Transmission Roll / Stabilator Roll, 2nd Vertical Bending / Transmission Pitch, Cockpit/Cabin Roll, and 3rd Vertical Bending / Cockpit/Cabin Torsion modes. Below 20 Hz, percent decreases do not exceed 0.048 %.

E. Over Fuel Cell Ballast Assembly

Both over fuel cell ballast assemblies on right and left hand sides are specified in the NASTRAN model. Although each assembly can support an additional 750 lbs of ballast, only the assembly self-weight of 130 lbs is specified here. The additional maximum ballast of 1,500 lbs may added optionally pending the definition of the flight test configuration.

The 1st Vertical Bending, Stabilator Roll, Transmission Pitch, Transmission Roll / Stabilator Roll, 2nd Vertical Bending / Transmission Pitch, 3rd Vertical Bending, and Cockpit/Cabin Roll / 3rd Vertical Bending modes under percent decreases of 0.33, 0.40, 0.32, 0.19, 0.31, 0.09, and 0.12 % respectively as shown in Table XI. The 1st Lateral Bending, 2nd Vertical Bending / Transmission Vertical, and 3rd Vertical Bending / Cockpit/Cabin Torsion modes undergo less significant decreases at 0.046, 0.053, and 0.045 % respectively.

6.3 Mass Items

Mass items such as ballast or equipment payload (approximately 4,600 lbs) such that is mounted to structural flight components have been added progressively

within this mass build-up. Other mass items including RDAS II Instrumentation System (133 lbs), Pilot (200 lbs), Copilot (200 lbs), and others that do not have this mounting requirement are to be added in the next sections dealing with the "comprehensive results of the 'best' NASTRAN model".

7. Summary

The modal trends observed for the global model in this BUCMS may be summarized. Percent changes undergone between the starting reference configuration and the fully built-up weight and structure configuration used in this BUCMS are presented in Table XII for the first 27 modes. Most of the modes below 20 Hz undergo only slight percent decreases in modal frequency ranging from 0.564% to 4.927% with the addition of all flight component weight and structure. The following eight modes below 20 Hz have undergone significant percent decreases with the addition of full component masses: Transmission Pitch / 2nd Vertical Bending, 2nd Vertical Bending / Transmission Vertical, 2nd Vertical Bending / Transmission Pitch, Cockpit / Cabin Roll, 3rd Vertical Bending / Cockpit/Cabin Torsion, Cockpit/Cabin Roll / 3rd Vertical Bending, 4th Vertical Bending, and Transmission Pitch / 4th Vertical Bending. The percent decreases for each mode are 5.66, 11.31, 14.66, 11.58, 8.86, 7.22, 9.43, and 7.99 % respectively. Clearly, a full build-up of mass for the flight components alters the modal frequency of these eight modes appreciably. We also note that these percent differences for these eight modes are less than those found in the previous BUCSS highlighting the importance of the flight structure's cumulative stiffness.

The 5.66 % percent decrease in the Transmission Pitch / 2nd Vertical Bending mode may be attributed solely to the addition of Trimmable Ballast System self-weight and ballast payload. The addition of the complete TBS system discretization constitutes a weight increase of 3,539 lbs to the gross weight of the vehicle. Of this 3,539 lbs, 376 lbs is associated with self-weight of the ballast rack, while the ballast box assembly/equipment and lead ballast payload constitute 263 and 2,900 lbs respectively. Hence, the weight contribution of this one flight component addition is considerable. Significant percent changes of 11.31 and 14.66 % for the 2nd Vertical Bending / Transmission Vertical and 2nd Vertical Bending / Transmission Pitch may also be attributed to the addition of the TBS system. The 11.58 percent decrease in the Cockpit / Cabin Roll mode may be importantly attributed to the addition of the TBS system and to the addition of the C.G. Rack to a lesser extent. The converse is true for the the 3rd Vertical Bending / Cockpit/Cabin Torsion mode which undergoes and 8.86 % decrease in modal frequency

due largely to the addition of the C.G. Rack and the TBS system to a much lesser extent. The percent decrease of 7.22 % in the Cockpit/Cabin Roll / 3rd Vertical Bending mode, however, may be attributed equally to the addition of these two flight components. The 4th Vertical Bending mode with a 9.43 % modal frequency decrease occurs in large part to the addition of the TBS system and to a smaller extent, the addition of the pallet rack mass. Finally, the Transmission Pitch / 4th Vertical Bending modes which undergoes a 7.99% decrease is attributed to the addition of Pallet Rack, TBS system, and Instrumentation Panel. These three components listed in order from larger to smaller percent contributions towards the overall decrease constitute the significant addition for this mode.

Clearly, the addition of TBS system and payload weight acts consistently in decreasing the modal frequency of most of the modes below 20 Hz although a handful undergo a more pronounced percent decrease. The addition of component masses such as the c.g. rack, pallet rack, and instrumentation panel to their respective component structures have also contributed in pronouncing this overall decrease. As in the BUCSS, only a few components have affected the frequency of the basic global displacement pattern of the modes while the majority of the flight components have produced only slight 'fine tuning' effects. Again, one sees that modal frequencies about the UH-60A cabin's flexural actions have been altered although the basic global pattern is preserved throughout the build-up. The flight component masses are classified as major, minor, and less significant in contributing mass (affecting resonant frequency) to the global model as follows:

Major	Trimmable Ballast System
Minor	Instrumentation Panel Center of Gravity (C.G.) Rack Over Fuel Cell Ballast (RHS & LHS)
Less Significant	Instrumented Test Boom LASSIE Bar Flight Engineer's Instrumented Rack Adapter Plate Assembly Pallet Rack Frequency Converter Baseplate

X. REFINEMENT OF UH-60A NASTRAN MODEL

1. Objective

Since the DAMVIBS baseline model was originally developed, numerous improvements have been made by Sikorsky Aircraft in support of the UH-60A Black Hawk as a commercial product and research/development tool [6-8]. Many of these improvements have been made since September of 1990 and the authors' previous NASA/AEFA study when NASA Ames received and updated its last finite element model (FEM I) describing the modeling of a limited number of secondary structural additions and the inclusion of the bungee suspension hardware at the main and tail rotors used during ground vibration testing. Using the September 1990 data, the authors have performed a study of the NASA/AEFA weight configuration (FEM I) and the influence of secondary structure contributions which represents the current work. The nature of the modeling revisions and improvements within the last two years to develop the final 'best' model (FEM III) may be described and categorized into seven separate groups:

1) Remodeling of Existing Primary Structure
2) Re-Evaluation of Material or Stiffness Properties
3) Modification of Weight Distribution
4) Additional Modeling of Secondary Structural Components
5) Inclusion of Test Apparatus/Procedures
6) Recent Improvements to Existing Mesh
7) Current MTRAP Configuration

2. Remodeling of Existing Primary Structure

Under this effort, improvements to the existing finite element mesh of the baseline primary structure is evaluated and improved such that the discretization characterizes the true physical behavior of the modeled component or structure. The remodeling or tuning of the stabilator support springs to match experimentally observed behavior is an example of this. FEM I through III carry this type of ongoing improvement.

3. Re-Evaluation of Material or Stiffness Properties

Under this effort, the material or member properties are re-evaluated and modified such that static and dynamic properties of the primary and secondary structures will come closer to those experimentally observed. This task may include rechecking the elastic moduli and area moment of inertia properties of finite element beams. A modification after such a recheck may include changing the Young's Modulus and cross sectional area of the beam to bring data in line with material stock or manufacturing data. The task may also include the recheck and modification of thickness properties of the various plate and shell elements included in the model. The stiffness tuning of the transmission shell on the NASTRAN model is an example of this type of action. The 'best' model or FEM III is a product of such a material property re-evaluation.

4. Modification of Weight Distribution

In support of its own research and development purposes, Sikorsky Aircraft has addressed the support of other aircraft similar to the UH-60A in the existing production fleet. This fleet includes other configurations of the Black Hawk such as the MK-60, the Navy's SH-60B SeaHawk, and the UTTAS versions. Weight configurations of these aircraft are numerous and unique depending on the various mission and operational purposes of the production customer. The modification task of weight distribution may include the addition of concentrated and distributed mass at various respective finite element nodes of the NASTRAN model to reflect the use of weapon packages, extra fuel pods, or the transportation of cargo. The addition of mass to the DAMVIBS baseline configuration (10,000 lbs) to analyze a mission ready configuration of the UH-60A (c. 22,000 lbs) is an example of this type of action. FEM I through III have undergone weight distribution modifications from 'starting point' configurations to the 'best' model.

5. Additional Modeling of Secondary Structural Components

The modeling of secondary structural components to the primary structure of the UH-60A discretization is a common form of model refinement. It has previously been studied by the

authors and Sikorsky Aircraft and shown to provide fine tuning of the overall global vibration response towards improved modal characteristic comparisons. The modeling of the firewall bulkhead is an example of this type of task. FEM I was the first model to have included such additional modeling.

6. Inclusion of Test Apparatus/Procedures

In both the modal testing and subsequent theoretical analysis of a "free-free" structure, two methods may be taken in dealing with the suspension system used in experimental work. In the first method, one may develop and implement a suspension system such that the structure, mass, vibration modes, and practical test setup do not contribute to the experimental response of the tested structure or is relatively negligible. In this case, the tested article may be modeled solely in a subsequent theoretical analysis. In the second method, one may realize that the suspension system does in fact make a limited contribution to the experimental response of the article. Such a contribution would not be uncommon in the vibration testing of a full scale aircraft which cannot be fully isolated from the effects of a modest suspension system. In a practical setup, modal test equipment/hardware and its corresponding mass are added to the aircraft and the suspension system stiffness and/or mass can be significant enough to produce anomalous results in the identification of the lowest elastic modes. In this case, the suspension system must be incorporated into the subsequent theoretical model. The inclusion of the bungee and chain of the suspension system used in DAMVIBS analysis is an example of this task. FEM I through III include such test apparatus.

7. Recent Improvements to Existing Mesh

The Dynamics Group at Sikorsky Aircraft has maintained a continual effort to make model revisions (such as the inclusion of secondary structure) and add improvements to the NASTRAN finite element discretization to reflect the current configuration of the UH-60A Black Hawk. Within the last two years, three noteworthy studies have been accomplished to achieve these goals. The **first** study dealt with improving the pre-existing DAMVIBS NASTRAN model of the UH-60A tailcone and tail rotor pylon for dynamic analyses. Several parts composed this study including: 1) The recalculation of section properties, including the effects of secondary bending and offsets, 2) The revision of the geometric layout of the model for agreement with the current structural configuration of the aircraft, 3) The modeling of additional secondary structural components in these two models, and 4) The representation of these fittings in these

models as assemblages of BAR and QUAD4 elements using weighted averages to compute their section properties. The **second** study dealt with improving the NASTRAN models of the Hover Infrared Suppressor System (HIRSS) and stabilator attachment fittings in order to improve the frequency characteristics predicted by the model. This study was conducted to address the excessive stiffness of the previous model and to update the spring rates of the stabilator to bring predicted stabilator roll mode frequencies into agreement with test estimates. The **third** study was used to correct the NASTRAN distributed mass models of the main and tail rotor heads and engines to bring about an agreement between shake test results and analyses. This effort has resulted in different mass models for longitudinal, lateral, and vertical excitations of the UH-60A test article in the forced response case. We note that these improvements have been included in all models after the DAMVIBS model including FEM I through FEM III.

8. Current MTRAP Configuration

This revision may be generally defined as the imposition of unique structural or weight characteristics on the baseline finite element model. This may include the addition of special flight components or ground vibration test equipment and/or the modification of the mass distribution for some flight or ground test comparison. In this case, a unique flight configuration with structural and weight effects is currently provided. FEM II and III which have the unique MTRAP structural and weight distribution are representative of such models.

9. Summary

The main points regarding the continuing refinement of the UH-60A model used in this study was separated into seven parts: 1) the Remodeling of Existing Primary Structure, 2) the Re-Evaluation of Material or Stiffness Properties, 3) Modifications pertaining to Weight Distribution, 4) previous and current Additional Modeling of Secondary Structural Components, 5) the Inclusion of Test Apparatus/Procedures, 6) the inclusion Recent Improvements to Existing Model Mesh, and 7) the imposition of the Current MTRAP Configuration.

It is important to note that many of the revisions and improvements will continue to be part of an on-going model refinement process by Sikorsky in support of the current UH-60A production line and its numerous mission configurations. It is recommended to update the

primary / secondary structural model with any future improvements to the model before the proposed shake test at NASA Ames.

XI. INCLUSION OF UPDATED PRIMARY/SECONDARY STRUCTURE

INCLUSION OF MODELING REVISIONS

COMPREHENSIVE RESULTS OF 'BEST' MODEL

1. Objective

An additional study is required after the BUCSS and BUCMS to generate the final results. The main objective of this study is **to include the dynamic effects of updated primary/secondary structure and the addition of Sikorsky modeling revisions.** This task is achieved through the generation of data for the comparison of modal shapes and frequencies from both analytical models (FEM II and FEM III). Dynamic characteristics of these configurations are defined and changes in structural behavior, resulting from the addition of the flight component masses, ballast, and their respective modeling revisions to the primary/secondary structure model, become evident. Eigenvector/eigenvalue extractions are performed for each configuration giving respective modal deformation states and resonant frequencies.

The September 1990 finite element model previously used in the study of the NASA/AEFA mass distribution and the influence of secondary structural components consisted of a primary structural system composed of 8,819 elements, specified geometrically by 4,379 grid points, and utilized 25,509 degrees of freedom. With the previous study by the authors, the number of grid points and elements increased with a refined mesh and the addition of secondary structure to 9,742 elements, 4,669 grid points, and 26,547 degrees of freedom. This revised September 1990 model (FEM I) received in part from the Dynamics Group at Sikorsky Aircraft and revised towards the NASA/AEFA distribution and configuration is described by the following types and numbers of finite elements in Table XIII.

With recent modeling revisions and material property revisions, the UH-60A model has been refined to include a finer finite element mesh. Without adding the MTRAP flight component models, the updated primary/secondary structural fuselage with suspension systems is described by 5,860 grid points and 12,100 elements. The following number of elements are

used in this configuration and may be reviewed in Table XIV. (A preliminary NASTRAN run of the baseline configuration, with updates only as received from Sikorsky Aircraft, yields the basic modal frequency spread and is presented with the unidentified mode numbers for reference purposes in the appendix in A-5 and A-6.)

Together with the 987 grid points and 937 elements developed for the MTRAP flight component models, a total of 6,847 grid points and 13,037 finite elements described the updated UH-60A model including the MTRAP flight components and mass distribution. The following table denotes the type and numbers of elements required to model the internal and external structural flight components in Table XV.

2. Updates

The following updates to the primary and secondary structural model (FEM II) have been enacted under a parallel effort at Sikorsky Aircraft's Dynamics Group resulting in the 'best' model (FEM III) available:

1) Revision of Main Rotor Transmission Housing shell stiffness
2) Revision of Aft Main Rotor Pylon Fairings
3) Addition of rigid bearins and output shaft to Main Rotor Transmission
4) Revision of Tailcone stiffness
5) Inclusion of tail rotor power and drive train systems components
6) Modification to Tail Rotor Pylon including cambered fairings
7) Modifications to Stabilator inertia and mass model
8) Re-evaluation of model material properties
9) Re-evaluation of finite element tapers
1 0) Inclusion of Tail Rotor Shaft service cover and shaft casing

These items are described in the following:

1) Revision of Main Rotor Transmission Housing shell stiffness

The UH-60A main rotor transmission housing had been modified with respect to stiffness. The previous UH-60A models had included the doubling of housing shell

thickness to obtain improved correlation with ground vibration test results. The housing shell thickness has been downgraded to 1.5 times the actual shell thickness.

2) Revision of Aft Main Rotor Pylon Fairings

Parts of the aft main rotor pylon fairing have been revised with respect to element structure and layout.

3) Addition of rigid bearins and output shaft to Main Rotor Transmission

A rigid bearing and output shaft has been added to the main rotor transmission at the tail rotor take-off. The main rotor pylon contains an RBE2 rigid element to act as a bearing at the drive shaft take-off of the main transmission housing and an RBAR rigid bar element to simulate the output shaft. Torque from the tail rotor drive shaft is distributed by the RBE2 element to the transmission housing and not to the internal bearing which is not represented in the finite element model. It is noted that this simulation will be corrected in a future Sikorsky Dynamics Group study to improve the main rotor transmission model.

4) Revision of Tailcone stiffness

The UH-60A tailcone model has been modified with respect to its stiffness properties. In addition to the primary aluminum fuselage, composites materials covering the outer shell of the primary tailcone have been included to define the physically correct 'double deck' nature of this shell. Tailcone property and material cards have also been revised accordingly.

5) Inclusion of tail rotor power and drive train systems components

Several components of the tail rotor power & drive train systems that are situated between the main rotor transmission and stabilator sections have been included in the updated NASTRAN model.

6) Modification to Tail Rotor Pylon including cambered fairings

The tail rotor pylon model in the UH-60A finite element discretization has also been modified with respect to additional secondary structure. Cambered fairings including leading and trailing edges of the tail rotor pylon have been included. The accompanying inertia and mass model has been superimposed on the structure respectively.

7) Modifications to Stabilator inertia and mass model

The UH-60A stabilator model has been updated with respect to structure. The accompanying inertia and mass model has been superimposed in an appropriate manner.

8) Re-evaluation of model material properties

Estimation of material properties constitutes an important aspect of the finite element model where the global stiffness matrix may be improved greatly with relatively little effort. Sikorsky Aircraft has re-evaluated the element properties of the model. Element data describing the material properties of the fuselage components are modified to reflect a better estimation of those manufacturing materials used in practice, in place of code or text book estimates of those properties. NASTRAN data describing the various types of aluminum used in the load bearing fuselage components include better estimates of Aluminum 7075-T6, 2024-T3, and 7075-T73 manufactured stock and also the different grades of magnesium and steel. Unique materials such as aluminum webs with lightening holes, fold bulkhead webs, and beaded panels have also been estimated in a similar manner. Material estimates of composite materials including orthotropic woven fiberglass, various isotropic and orthotropic forms of woven kevlar, and honeycomb core have been revised.

9) Re-evaluation of finite element tapers

Element connectivity has also been rearranged for a handful of quadrilateral elements to improve previous element tapers. For those elements affected, conditioning of the local and subsequent global stiffness matrices will be limited upon model execution.

10) Inclusion of Tail Rotor Shaft service cover and shaft casing

Elements detailing structural features of the UH-60A tailrotor shaft service cover and casing components that are situated on top of the revised tailcone have been included.

The inclusion of these recent revisions may be viewed as the currently updated model as seen in Figure 36.

3. Constraints

As in the previous structural and mass build-up studies, the UH-60A finite element model includes an element discretization of the main and tail rotor bungee suspension systems. The rotorcraft model main and rotor hubs are again attached to the respective lower section of the suspension systems element wise. Two MTRAP configurations (FEM II and FEM III) with and without the bungee systems are studied for the previous model received in September 1990 versus the currently updated model received this last November 1992. These two different configurations for the updated November 1992 model (FEM III) are presented in Figures 37 and 38 respectively.

4. Loading

As in previous sections using real eigenvalue/vector analysis, no concentrated or distributed loads are applied to the aircraft model.

5. Computational Methods & Solutions

Computational methods and solution formats used in the previously described BUCSS and BUCMS are similarly implemented in this section with the same computational resources.

6. Eigensystem Results

Although we have used starting reference configurations in the separate structural and mass build-up studies, we must consider the 'best' practical model for MTRAP flight test purposes regardless of the previous component studies. This model is to include the most recent and updated baseline finite element model with the additional MTRAP structural flight components. The 'best' model also includes a modified mass distribution characteristic of the unique MTRAP flight test configuration The mode shape and frequency results of the 'best' model (current study) compared with the initial primary/secondary structural model (previous study by authors) under suspended/no-bungee suspension conditions are presented in Table XVI. The following describes the mode shapes and frequencies of the 'best' model for the MTRAP configuration.

6.1 Updated Secondary Structure & Modeling Revisions for the 'Best' Model

With the BUCSS and BUCMS completed, we can generate modal results for FEM III, the 'best' model for the MTRAP Configuration, which consists of our updated primary and secondary structure, the added MTRAP flight components, and the imposition of the MTRAP flight test weight distribution. The twelve mode shapes below an accuracy threshold of 20 Hz and their corresponding resonant frequencies for this 'best' model are described in the following:

1st Vertical Bending

The *1st Vertical Bending* mode is placed at 6.322 Hz in the MTRAP structural configuration (Figure 39). This fundamental shape is signified by major upward vertical deformations centered about the midcabin section. Full fuselage bending is present. Vertical displacements in the stabilator region are due to the upward deflection of the tail rotor pylon base at the fold joint.

1st Lateral Bending

Figure 40 shows the 1st Lateral Bending mode. The *1st Lateral Bending* mode is located at 9.122 Hz in the MTRAP configuration. Notable lateral deflections about the midcabin section is evident with rolling of the tail rotor pylon. Significant torsion in the tail rotor pylon that was encountered in previous NASA/AEFA results using FEM I are minimized. This mode also exhibits the first of many antisymmetric bending behaviors of the stabilator although such behavior has been limited with the inclusion of new revisions to the stabilator inertia model and tail rotor shaft and pylon. Stabilator movement in this mode is due solely to the rolling of the tail rotor pylon. This rolling of the tail rotor pylon may be attributed to the significant lateral bending of the tailcone section.

Stabilator Roll

The *Stabilator Roll* mode at 11.268 Hz is characterized by isolated anti-symmetric bending of the stabilator wing (Figure 41). Minor lateral bending in the aft tailcone before the pylon fold joint is present.

2nd Vertical Bending / Transmission Pitch

This mode shape at 11.657 Hz is characterized by the pitch rotation of the transmission section and main rotor hub shaft (Figure 42). Significant vertical bending in tailcone with antisymmetric bending of stabilator is also present. Longitudinal displacements are found in the tail rotor pylon with additional but limited vertical bending in the cabin areas.

Transmission Pitch / Stabilator Roll & Yaw

At 12.444 Hz, this mode is characterized by notable vertical displacements in the nose and cockpit/cabin transition section to the aft cabin transition section (Figure 43). Limited vertical bending of the fuselage is exhibited is found. Pitching of the transmission shaft is a dominant feature of this mode shape. Limited vertical bending of

general tailcone section is also present. Antisymmetric vertical bending and yaw rotation of stabilator are also present.

Transmission Roll / Stabilator Yaw

The *Transmission Roll / Stabilator Yaw* mode at 12.778 Hz is characterized by isolated antisymmetric bending with yaw rotation of the stabilator wing and the significant roll rotation of the transmission structure (Figure 44). Isolated and limited vertical and lateral displacements near the cockpit nose and tailcone aft regions are included in this mode.

Stabilator Roll/Transmission Roll

The *Stabilator Roll/Transmission Roll* mode at 12.938 Hz exhibits vertical displacements in the cockpit and tailcone regions (Figure 45). Significant displacements are due to rolling of the main rotor hub and transmission support structure. A limited antisymmetric roll and yaw rotation of the stabilator is a prevalent feature of this mode. Minor vertical bending displacements are contributed to the midcabin floor from the rolling of the transmission structure.

Tailcone Lateral Bending/Transmission Roll/Stabilator Roll & Yaw

At 13.259 Hz, the *Tailcone Lateral Bending / Transmission Roll / Stabilator Roll & Yaw* mode is defined on the basis of the well pronounced lateral bending of the full tailcone (Figure 46). Roll translation of the transmission structure and main rotor hub is also found. Anti-symmetric bending and yaw rotation of the stabilator is exhibited.

2nd Vertical Bending/Transmission Vertical

At 14.536 Hz, the *2nd Vertical Bending/Transmission Vertical* mode is defined on the basis of the well pronounced vertical bending and translation of the full fuselage and tailcone (Figure 47). Uniform vertical translation of the transmission structure and

main rotor hub is found. No stabilator bending is present in this mode unlike NASA/AEFA results which had exhibited some antisymmetric vertical bending and yaw rotation of stabilator.

Cockpit/Cabin Roll

The Cockpit/Cabin Roll mode at 14.651 Hz is characterized by an apparent roll of the cockpit and cabin regions (Figure 48). Limited lateral bending in tailcone section coupled with a limited roll rotation of the tail rotor pylon base is also present. Isolated lateral displacements in the nose also occur. Minor roll and yaw rotations in the stabilator include antisymmetric bending are also present.

Cockpit/Cabin Torsion/3rd Vertical Bending

This mode at 18.779 Hz seen in Figure 49 is characterized by torsion behavior from the cockpit through the aft cabin areas as a dominant displacement feature. There are considerable and concerted deformations of the main frames in the forward through aft cabin sections. Limited lateral translation of the tailcone section is evident as is a limited yaw and antisymmetric bending of the stabilator. A limited transmission roll due to the torsion behavior is apparent as well. Some vertical displacements are also evident through such displacements are related more to the full torsion displacement.

3rd Vertical Bending

The 3rd Vertical Bending mode at 19.554 Hz also includes vertical deformation of the tail rotor pylon top section. Significant vertical bending of the fuselage is clear as are deformations of the individual main station frames. A slight roll in the cockpit section accompanies this primary flexural action. Limited yaw of the stabilator is also present as is a respective transmission pitch. This mode may be seen in Figure 50.

6.2 Definition of 'best' model

Through predictive means, we have described the first twelve mode shapes that the modal test analyst should find in the 1995 in-house ground vibration test of the MTRAP configuration. One model has been clearly defined as representative of the **'best' model** for the MTRAP configuration (FEM III) which includes: **1)** An updated and revised primary and secondary fuselage structure, **2)** Modeled MTRAP flight components and respective mass, and **3)** The MTRAP weight and ballast distribution.

We have also defined the 'best' model (FEM III) as a model that does not include a bungee suspension system and its respective mass for several reasons:

First, the inclusion of the suspension system may signify an additional weight up to 1,665 lbs (the total weight of bungees, chains, fasteners, and related suspension hardware) which may not be representative of the future shake test experimental set-up. While we have included a suspension system in both the BUCMS and BUCSS, our study was planned to look at *relative* changes in modal frequency for the individual components for an *arbitrary* starting configuration.

Second, details regarding suspension system requirements at the main and tail rotor shafts of the UH-60A may be different from customary suspension set-ups used in previous UH-60A helicopter ground vibration tests. It is conceivable that the 1995 shake test requirements may be similar to that of the NASA Ames Bell-Textron XV-15 Tiltrotorcraft shake test which required bungee suspension running from the tail *to a ground tie-down point.*

Third, modal results generated in a free-free condition without suspension systems are representative of shake test results that employ suspension systems that will not generate significantly high suspension system "pendulum" or "plucked-string" modes. This is the ideal experimental set-up that the good modal analyst hopes to employ.

Clearly, with many details lacking regarding the overall set-up of the future shake test, predictive results (including those that include gravity effects and a respective differential stiffness matrix) should be open to future revision. We note again that a linear gravity analysis with a suspension system for the MTRAP

configuration should be performed only after the 1995 shake test and set-up requirements have been clearly defined.

7. Summary

The major points of the last portion of the study describing modal results with the inclusion of the updated primary/secondary structural model and other flight component modeling revisions leading up to the those results for the 'best' model are summarized.

Two types of models, with and without an arbitrary shake test suspension system, have generated four sets of modal shape and frequency results and have been considered in this section. The first UH-60A finite element model is composed of basic primary/secondary structural model with the appropriate MTRAP structural flight components and weight configuration. This first model was used the authors in a previous study in September 1990. The second model is a fundamentally revised primary/secondary structural model again with the appropriate MTRAP structural flight components and weight configuration. This second model has been altered with respect to the re-evaluation of the primary structure and the inclusion of important secondary components as of Novemner 1992. This model also carries very important revisions including that of the stabilator structural and inertial model, (which has been critically reviewed in all studies since the DAMVIBS Program), and the *re-estimation of material properties* for most of the primary structural materials.

The definition of those modal results that indicate the 'best' model currently available has been considered. The use of suspension systems in the model will be an important modeling point. The inclusion of the main and tail rotor bungee suspension systems as used in past NASA/AEFA ground vibration testing may be clearly deemed as an 'arbitrary' choice, as the form of suspension for future MTRAP ground vibration testing will likely be dissimilar than that used for the NASA/AEFA configuration. *While the use of a suspension system has been a good choice in the build-up of component structure and mass studies (BUCSS and BUCMS respectively), the UH-60A model executed as a free-free structure without such suspensions should be considered to define the 'best' model, as the suspension geometry and mass distribution remains as yet to be defined.* This aspect of the 'best' model is a better estimation as we assume that the test engineers at the future MTRAP GVT will work to isolate and lower their suspension system modal frequencies and not allow them to interfere with elastic modes. We also assume

that the test engineers at the future MTRAP GVT will minimize the effect of the suspension mass on the modal frequencies.

One should again take note that this preliminary 'best' model eigensolution analysis, in advance of the actual GVT, may not reflect the planned ground vibration test configuration. However, the NASTRAN finite element model may be modified to include any slight modifications without great difficulty. Pending final definition and shake testing of current flight configuration, brief modal analyses may be performed to describe mode shapes and frequencies to obtain results within reasonable proximity to these 'best' modal values.

XII. CONCLUSIONS

1. Influence of Flight Component Structure

Among the total number of MTRAP flight components that have been added in the BUCSS, it is clear that some components effect a much more significant percent change than others for a limited number of modes. The inclusion of the TBS system ballast rack is an example of such a case. With this component, the larger portion of the cumulative percent increase may be attributed to the addition of the ballast rack. The inclusion of the TBS ballast rack alone effects a significant 80.12 % increase in modal frequency for the 1st Lateral Bending mode in the BUCSS. With this inclusion, the 1st Vertical Bending mode becomes the first elastic mode instead of the second elastic mode. This is significant as the inclusion of a singular stiff component has moved the first 'default' global fuselage mode to a higher frequency requiring a higher energy state for resonance. Verification of this frequency change should be performed during the 1995 modal test.

Clearly, other components such as the over fuel cell ballast assemblies contribute to this percent increase to a lesser extent at some instances for a much smaller number of modes. Cumulatively with all component structures added, the 1st Lateral Bending, Stabilator Roll, Transmission Pitch, and Cockpit/Cabin Roll modes have shown appreciable percent changes. Percent changes of these modes, due to a full structural build-up of the flight components, are 86.6, 15.03, 6.26, and 12.48 % from the initial starting reference configuration to the final configuration in the BUCSS respectively.

2. Influence of Flight Component Mass

The results found in the BUCMS are analogous to those for the BUCSS. Among the total number of MTRAP flight masses added to their respective flight structures, it again becomes clear that some component masses effect a much more significant percent decrease than others for a limited number of modes. Most of the modes below 20 Hz undergo cumulative percent decreases in modal frequency ranging from 0.564% to 4.927% with the addition of all flight

component weight and structure. The following eight modes below 20 Hz have undergone significant percent decreases with the addition of full component masses: Transmission Pitch / 2nd Vertical Bending, 2nd Vertical Bending / Transmission Vertical, 2nd Vertical Bending / Transmission Pitch, Cockpit / Cabin Roll, 3rd Vertical Bending / Cockpit/Cabin Torsion, Cockpit/Cabin Roll / 3rd Vertical Bending, 4th Vertical Bending, and Transmission Pitch / 4th Vertical Bending. The percent decreases for each mode are 5.66, 11.31, 14.66, 11.58, 8.86, 7.22, 9.43, and 7.99 % respectively.

The imposition of a significant gross weight change attributed the inclusion of the TBS system: ballast payload, movable ballast box, ballast rack, and related equipment is an example of such a case. With this component mass, the larger portion of the cumulative percent decrease in modal frequency may be attributed to the addition of this sole component. The 5.66 % percent decrease in the Transmission Pitch / 2nd Vertical Bending mode may be attributed solely to the addition of Trimmable Ballast System self-weight and ballast payload. Significant percent changes of 11.31 and 14.66 % for the 2nd Vertical Bending / Transmission Vertical and 2nd Vertical Bending / Transmission Pitch may also be attributed to the addition of the TBS system. The addition of the complete TBS system discretization had constituted a weight increase of 3,539 lbs to the gross weight of the vehicle. Of this 3,539 lbs, 376 lbs was associated with self-weight of the ballast rack, while the ballast box assembly/equipment and lead ballast payload constituted 263 and 2,900 lbs respectively.

Clearly other component masses, namely those of the c.g. rack, pallet rack, and instrumentation panel contributed on varying levels towards the overall decrease in modal frequency for a limited number of modes. The 11.58 percent decrease in the Cockpit / Cabin Roll mode may be importantly attributed to the addition of the TBS system and to the addition of the C.G. Rack to a lesser extent. The converse was true for the the 3rd Vertical Bending / Cockpit/Cabin Torsion mode which had undergone and 8.86 % decrease in modal frequency largely in part to the addition of the C.G. Rack and the TBS system to a much lesser extent. The percent decrease of 7.22 % in the Cockpit/Cabin Roll / 3rd Vertical Bending mode, however, may be attributed equally to the addition of these two flight components. The 4th Vertical Bending mode with a 9.43 % modal frequency decrease occured in large part to the addition of the TBS system and to a smaller extent, the addition of the pallet rack mass. Finally, the Transmission Pitch / 4th Vertical Bending modes which had undergone a 7.99% decrease was attributed to the addition of Pallet Rack, TBS system, and Instrumentation Panel.

3. Influence of Updated Structure & Modeling Revisions

The inclusion of updated primary and secondary structural components, the revision of inertia models (ie. stabilator model), and re-evaluation of material element properties for FEM III have caused a significant difference as to the types of mode shapes and resonant frequencies from those for FEM II. If one looks at the mode descriptions of both MTRAP configurations under FEM II and FEM III in Table XVI, one will see that the Transmission Pitch mode as found in FEM II results is not found in FEM III results. The updates to the primary/secondary structure including the revision of transmission housing properties have served to effect changes in modes that have or had transmission activity as a predominant displacement feature of the mode. Likewise, updates of the tailcone have limited and modified the bending behavior of the tailcone section for fuselage vertical and lateral bending modes. In a similar example, changes to the stabilator inertia model have limited stabilator activity including antisymmetric and symmetric vertical bending and yaw rotation to more realistic levels. Fundamental changes such as those brought about through the re-evaluation of material element properties on a global level would serve to modify resonant frequencies overall. Clearly, some form of experimental verification will be required to confirm and validate these model changes.

In this part of the study, we have not tried to study and quantify the modal frequency changes due to individual updates or revisions but rather update the pre-existing primary/secondary structure as found in FEM II to generate better results for the 'best' model in FEM III. We also note that the definition of the 'best' model should require, at a future date, the inclusion of a suspension system that will be defined in the 1995 modal test. A gravity analysis may then be included if the modal test engineer believes that the suspension mass and geometry will contribute some effect the overall modal shape and frequency spread.

Through this study, one was allowed to classify those basic structure/mass or unique configuration revisions (the modeling of primary, secondary, tertiary, or unique flight components/weight distribution) that succeed in effecting significant modal frequency changes for the global model's response. It has also become clear that a global finite element model cannot be considered equivalent to a given test configuration unless its unique mass distribution and structural configuration is included. This preceding fact can also be said of variations on a unique mass configuration.

4. Future Studies Using NASTRAN Data

With the modeling of MTRAP flight components and an updated primary/secondary structural model of the UH-60A, one may reconfigure the model to analyze a specific flight or shake test configuration in the near future. The flight component structures and their respective masses may be included or excluded from the NASTRAN solution data, piece by piece, in a manner similar to mass and ballast distribution modifications. Flight components may be revised as secondary structural components have been in past studies. Clearly, some form of experimental verification is recommended to verify the accuracy of the model.

XIII. RECOMMENDATIONS

1. Validation of Component Model Additions

With respect to the added flight components, several recommendations may be made that will be of interest to the model analyst and GVT engineer at the time of MTRAP testing. To ascertain and confirm the influence of the ballast rack addition in increasing the in-plane stiffness of the UH-60A cabin floor, a limited case study is recommended during the MTRAP GVT. This involves the minimum identification of the first few elastic modes of the MTRAP configuration with and without the ballast rack. This would confirm the component structure's significance and possibly determine the influence of assumed displacement boundary conditions that have been implemented in the NASTRAN model with components. As the component weighs only 376 lbs which is small relative to the gross weight of the aircraft, it is not expected that the ballast rack mass will significantly play a part relative to a greater stiffness role. Clearly, one of the main objectives of the proposed shake test will be to verify any analytical models or codes including NASTRAN model data.

In a similar manner, the influence of the addition of the complete TBS system weight (3,163 lbs) needs to be ascertained. Such a significant addition to the overall gross weight may be important especially when one considers the objectives of the MTRA Program regarding aspects of the changing center of gravity of the aircraft. Again, the identification of a limited number of modes under the program configuration with and without this addition are of importance. Clearly, both these case studies are contingent upon the total time alloted to testing and resources.

2. Stabilator Model

In discussion with Sikorsky Aircraft test engineers and based upon experiences with past NASTRAN models and the current 'best' model, a more expansive case study of the stabilator is recommended during the proposed ground vibration tests. In past NASTRAN models, (DAMVIBS, NASA/AEFA, and other mission configurations), the motions of the stabilator model have been

excessive although its influence on the global flexural action of the length of the rotorcraft remains to be determined. With the update of the structural and inertial features of the local model, a verification of the stabilator model through modal tests is recommended. An identification of modes, not limited to just a select few, with and without the physical stabilator during shake testing may produce informative results useful to many analysts that have encountered such anomalous behavior previously. As much of the revisions are based on improved discretization of the stabilator using manufacture data or upon limited system identification techniques, an experimental verification would be helpful in understanding this form of 'difficult component'.

We note here that two forms of component model verification are available here. In the *first* form, an individual physical component may be dynamically tested such that the component's modal frequency and shape are determined thus confirming or denying the accuracy of the NASTRAN component model. In this case, the finite element model of interest is that of the individual component itself. In the *second* form, the contribution of the added flight component structure and mass to the global stiffness, mass, and subsequent modal response is assumed to be correct. A modal test of the global structure is performed to verify the component's contribution to the global stiffness and mass. With this physical test, the NASTRAN component model may be modified if there is disagreement between analytical and experimental results. With limited time and resources, it would be deemed appropriate to use this second form of component model verification as it has been used in past studies.

3. Pre- Ground Vibration Test Stage

In addition, a close dialogue between the model analysts and modal test engineers is recommended in the pre-GVT stage since many of the ground vibration test objectives will be similar to those required for model verifications. For example, if the modal test analyst is interested in accurate estimates of modal damping values, the finite element analyst may recommend the use of time domain methods as a post-test and consistent technique for extracting damping values. The finite element analyst may also be able assist in other aspects such as the determination of appropriate accelerometer transducer locations. Clearly, a good dialogue is required.

4. Maintenance of Component Fabrication Records

Clearly, good manufacturing plans and final blueprints describing the additional equipment or ballast components necessary for finite element modeling are important to maintain an accurate UH-60A NASTRAN model for the MTRAP. This is especially true for those components that were made by NASA for the research program. However, flight components, such as those fabricated through the Army Engineering Activity (AEFA) including the instrumented test boom, instrumented LASSIE bar and two instrumentation racks, were manufactured with little or no documentation. Physical measurements of these components describing their geometry and material composition were taken by the authors prior to component modeling. A continued maintenance of all records related to flight component manufacture or test weight distribution is recommended.

ACKNOWLEDGMENTS

Special acknowledgments and thanks go to Karen Studebaker of the Rotorcraft Technology Branch for her guidance and technical support regarding this study, Dave Jordan of the UH-60A Project Office at NASA Ames for making UH-60A flight component and ballast data available to the authors, and to Tim Chen and Peter Dinyovszky of the Sikorsky Aircraft Dynamics Group for their continued efforts in making UH-60A modeling data available to the Rotorcraft Technology Branch.

REFERENCES

[1] Idosor, F.R. and Seible, F. : Comparison of NASTRAN Analysis with Ground Vibration Results of UH-60A NASA/AEFA Test Configuration, SSRP - No. 90/03, NASA Research Grant Number NCC2-598, University of California at San Diego, September 1990

[2] Fifth Design Analysis Methods for Vibrations (DAMVIBS) Meeting, Part I : NASA Langley Research Center, Hampton, Virginia, September 11-12 1990.

[3] Howland, G.R., Durno, D.A., and Twomey, W.J. : Plan, execute, and discuss vibration measurements and correlations to evaluate a NASTRAN finite element analysis model of the UH-60A helicopter airframe, Task 3 Report, NASA CONTRACT NAS1-17499, Sikorsky Aircraft, October 1986.

[4] Loney, Daniel J. : ADAS Implementation Plan, NASA Ames Research Center Fabrication Document, November 5, 1990

[5] The MacNeal-Schwendler Corporation, : MSC/NASTRAN User's Manual Vol. I & II. , November 1985

[6]* Dinyovszky, P. : Improvements to the NASTRAN Model of the UH-60A Stabilator for Static and Dynamic Analysis, Internal Correspondence TEM-G2-8601, United Technologies Sikorsky Aircraft, September 25, 1989

[7]* Dinyovszky, P. : Comparison of Mode Shapes for Test and NASTRAN for the 10,000 Pound (DAMVIBS) Gross Weight Configuration Using Modal Assurance Procedures, Internal Correspondence TEM-G2-8143, United Technologies Sikorsky Aircraft, Undated.

[8]* Dinyovszky, P. : Effect of the Main Rotor Pylon on the Vibration Characteristics of the UH-60A Black Hawk Airframe, Internal Correspondence TEM-G2-8639, United Technologies Sikorsky Aircraft, December 21, 1989

[9]* Dinyovszky, P. : Improvements to the NASTRAN Model of the UH-60 Black Hawk Airframe for Dynamics Analysis, Internal Correspondence TEM-G2-9183, United Technologies Sikorsky Aircraft, April 3, 1991

* Internal Document Relevant to MTRAP Flight Components Modeling Effort

FIGURES

Figure 1.
UH-60A Black Hawk Airloads Program Flight Test Configuration
Modern Technology Rotor Airloads Program

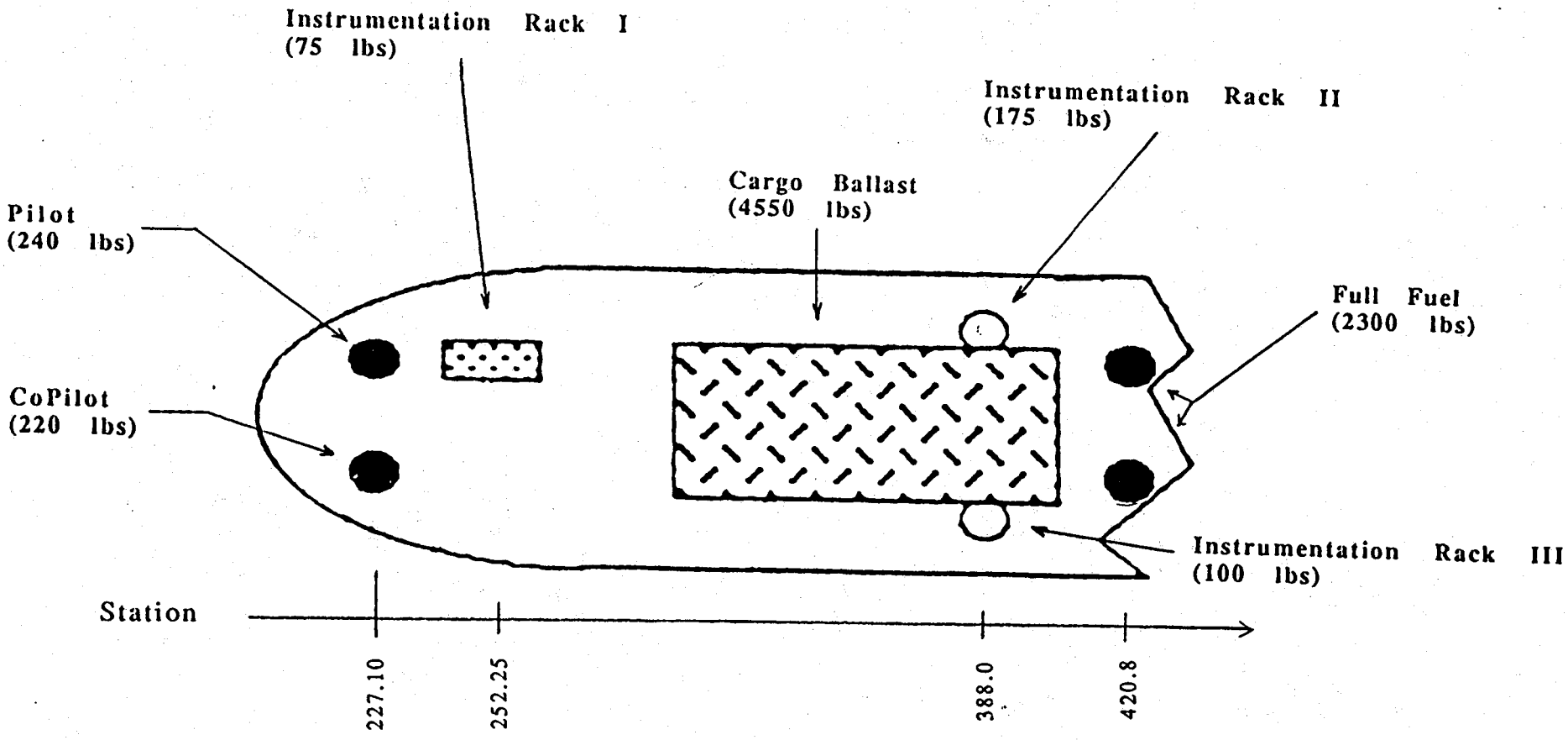

Figure 2.
NASA/AEFA Ground Vibration Test Weight Distribution

PRIMARY/SECONDARY STRUCTURAL SYSTEMS

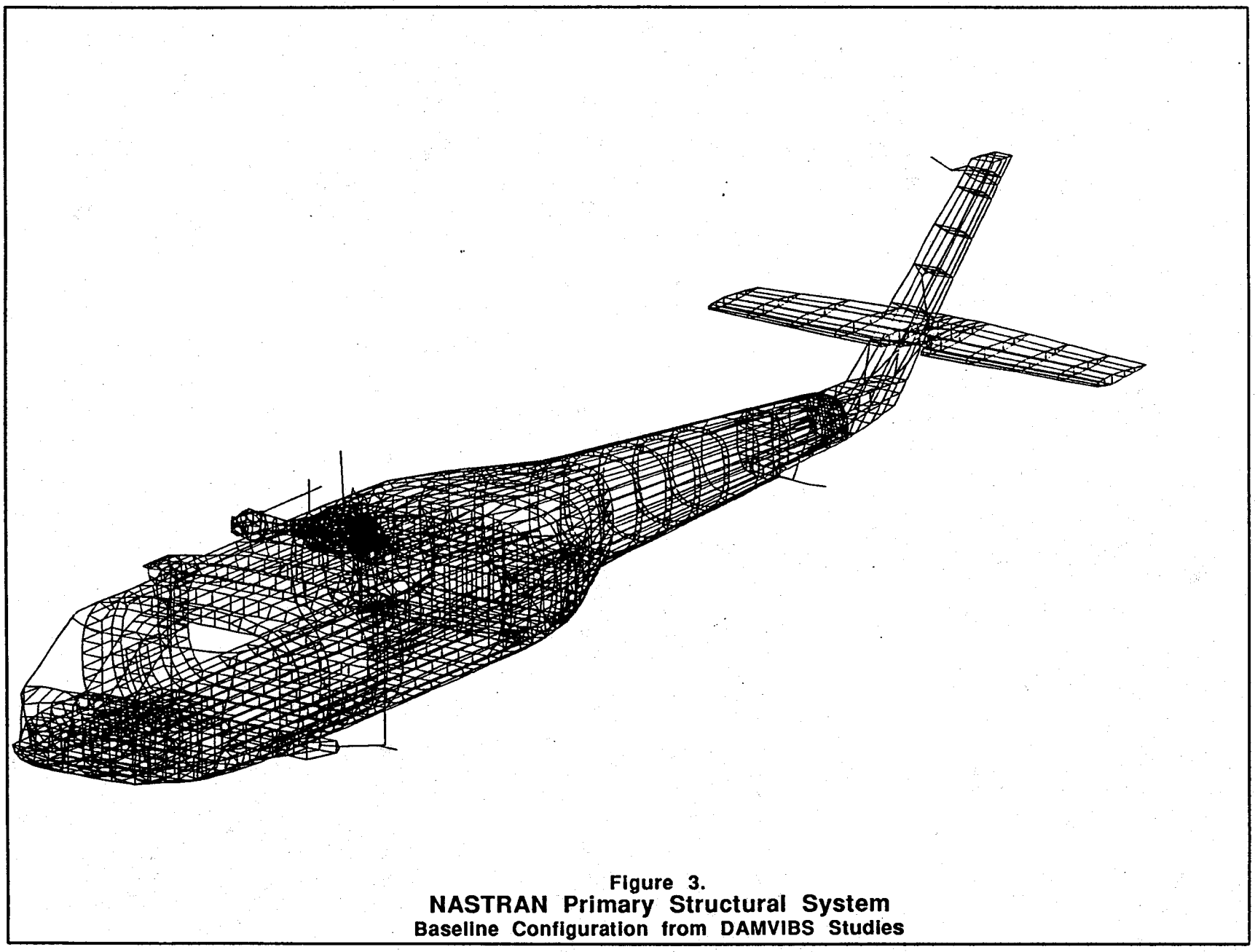

Figure 3.
NASTRAN Primary Structural System
Baseline Configuration from DAMVIBS Studies

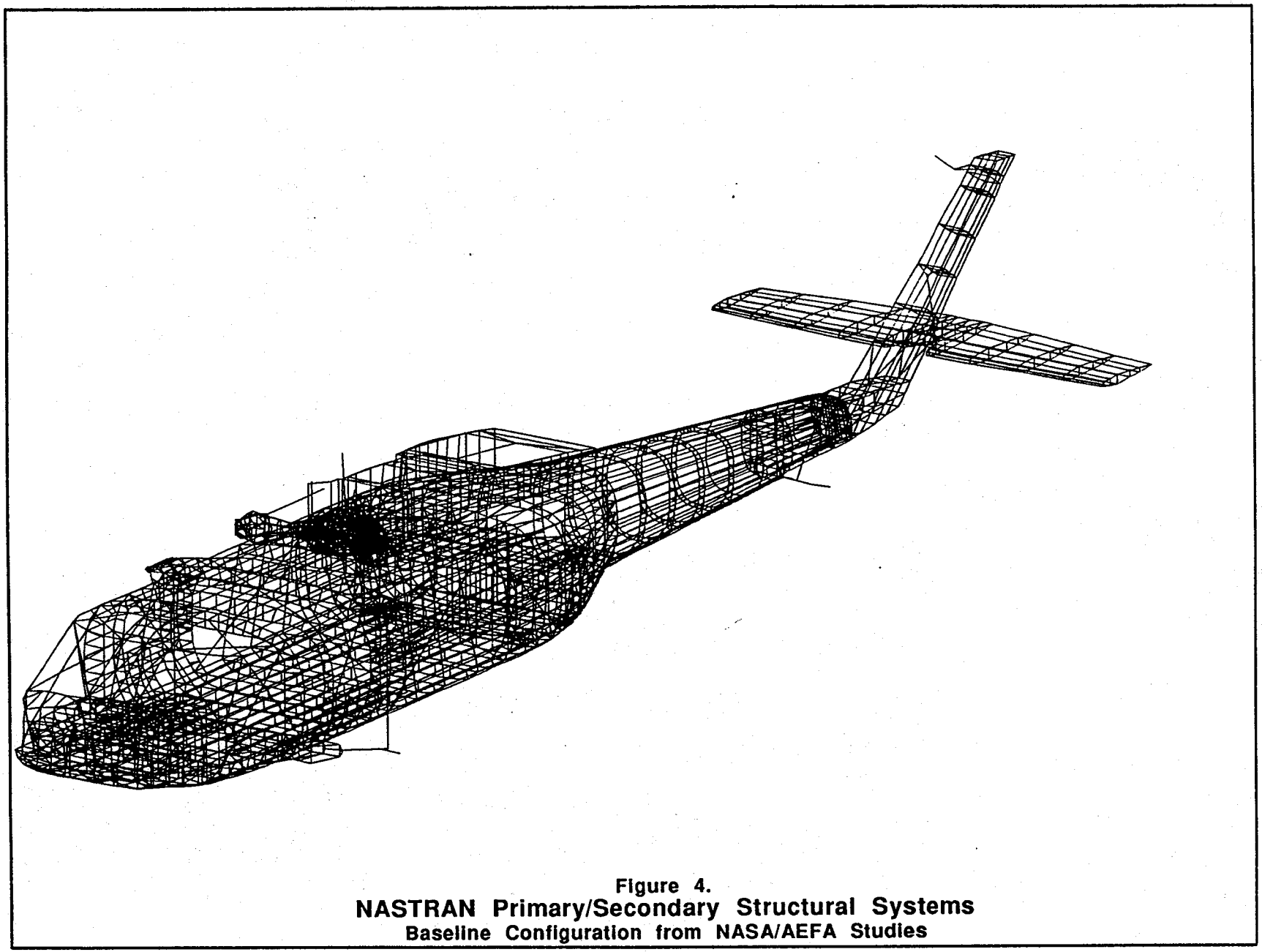

Figure 4.
NASTRAN Primary/Secondary Structural Systems
Baseline Configuration from NASA/AEFA Studies

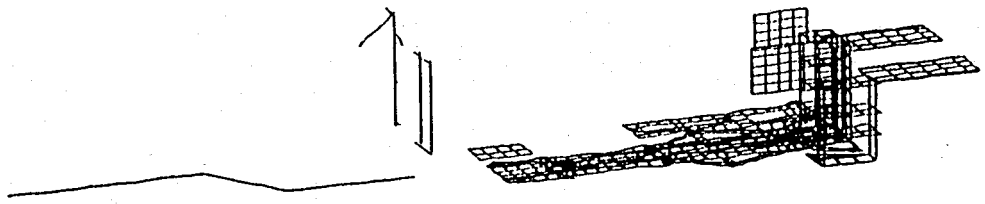

Flight Component Structure and Mass

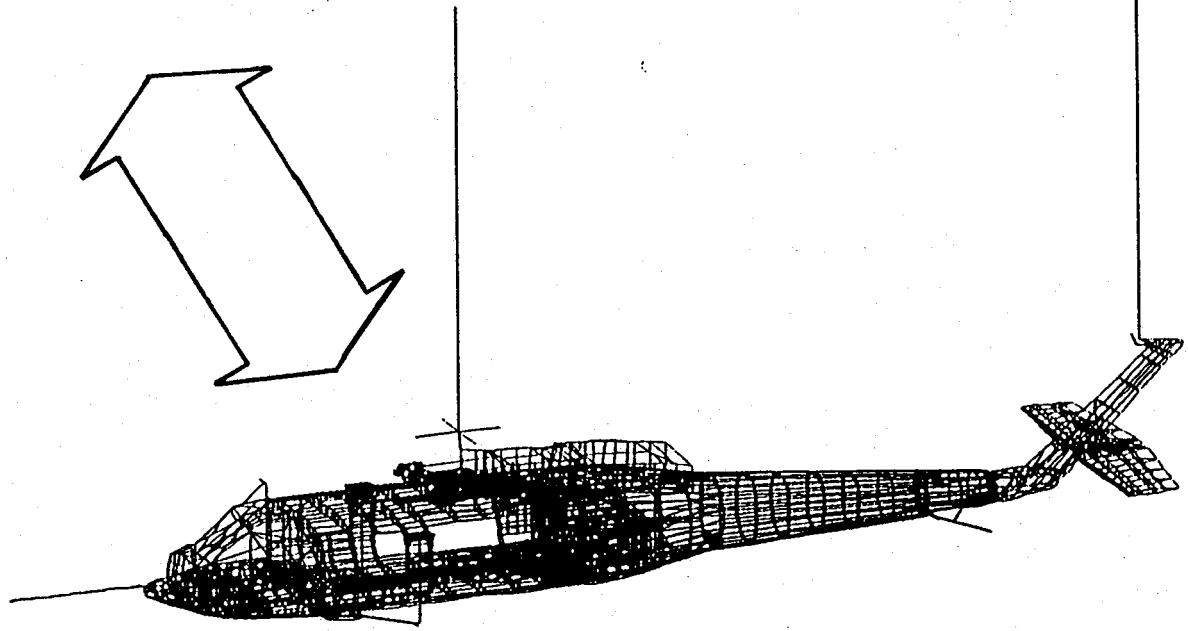

Baseline UH-60A with MTRAP Mass Item Distribution

Figure 5.
NASTRAN Primary/Secondary Structural Systems w/ Flight Components
Baseline Configuration for MTRAP Study

EXTERNAL STRUCTURAL COMPONENTS

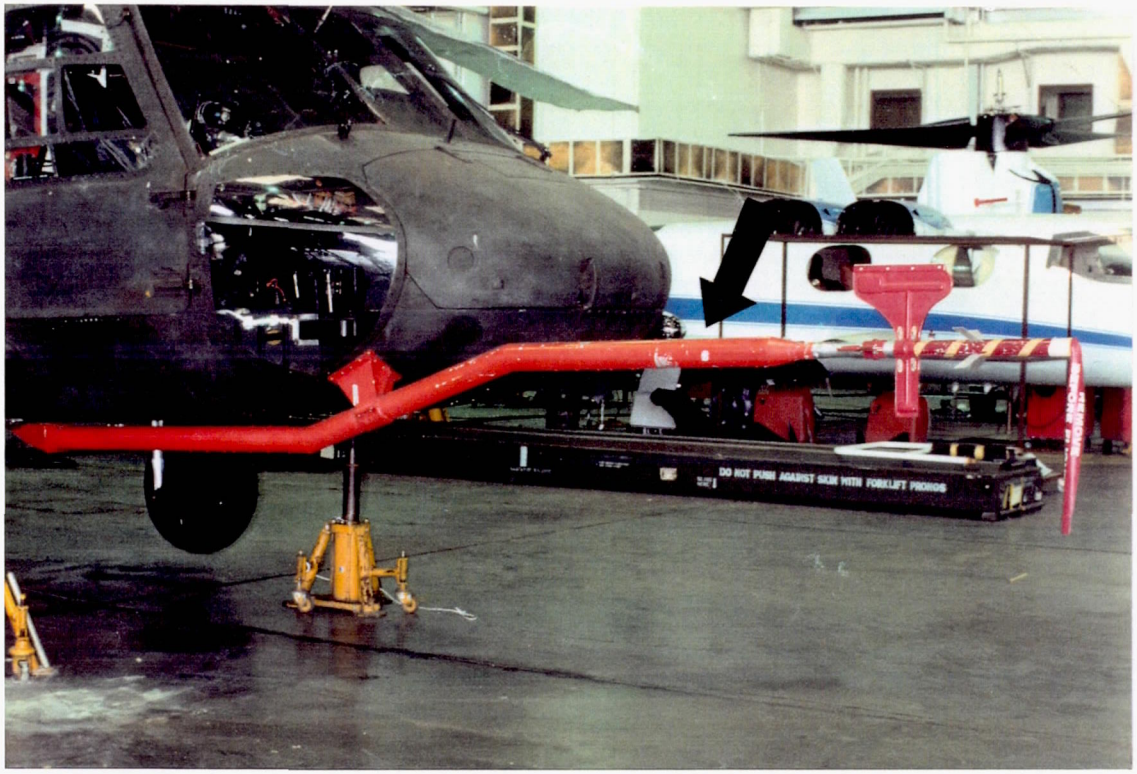

Figure 6.
Instrumented Test Boom
UH-60A Airloads Program Flight Component

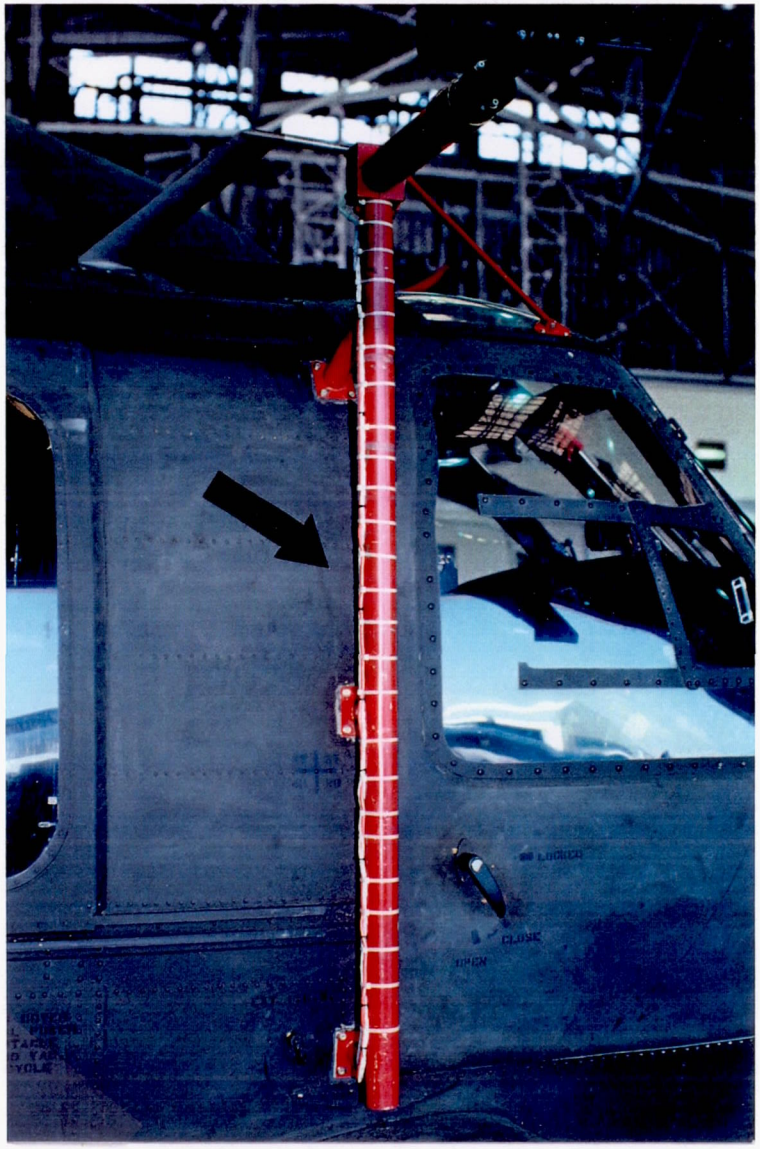

Figure 7.
Instrumented LASSIE Bar
JH-60A Airloads Program Flight Component

INTERNAL STRUCTURAL COMPONENTS

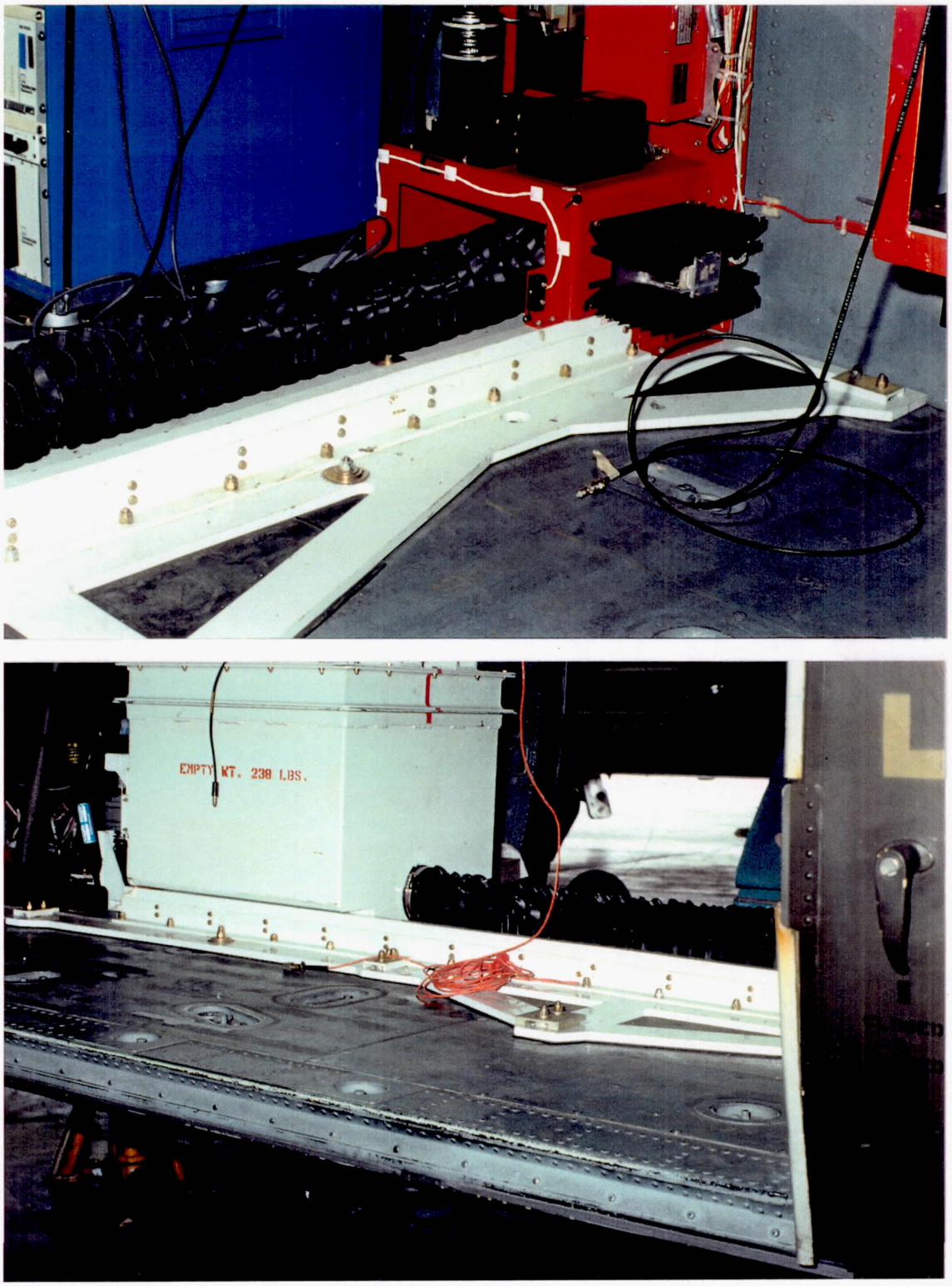

Figure 8.
Ballast Rack
UH-60A Airloads Program Flight Component

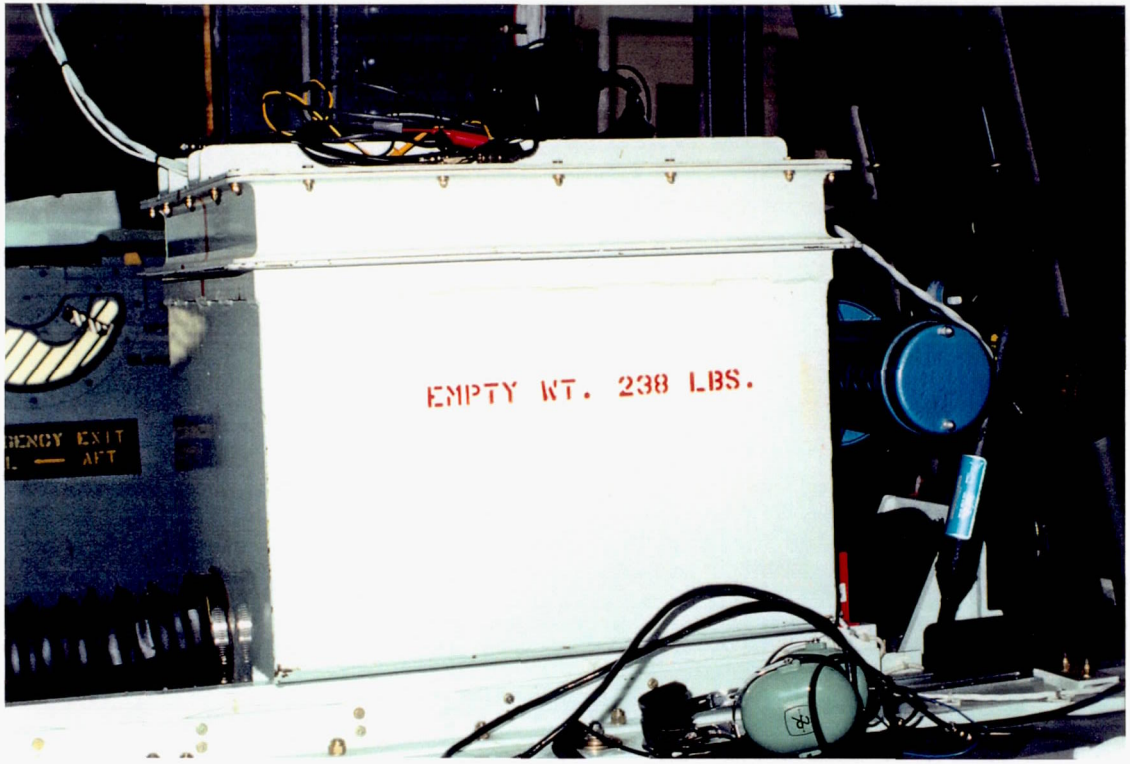

Figure 9.
Movable Ballast Cart
UH-60A Airloads Program Flight Component

Figure 10.
Flight Engineer's Instrumentation Rack
UH-60A Airloads Program Flight Component

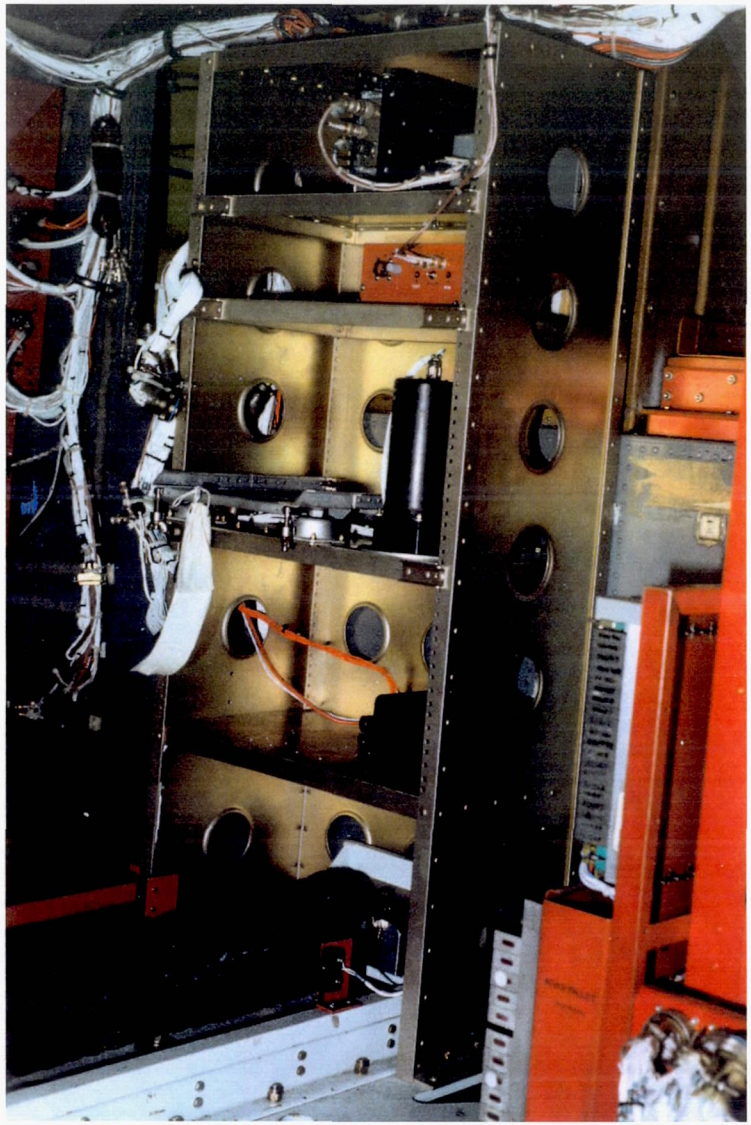

Figure 11.
C.G. Rack
UH-60A Airloads Program Flight Component

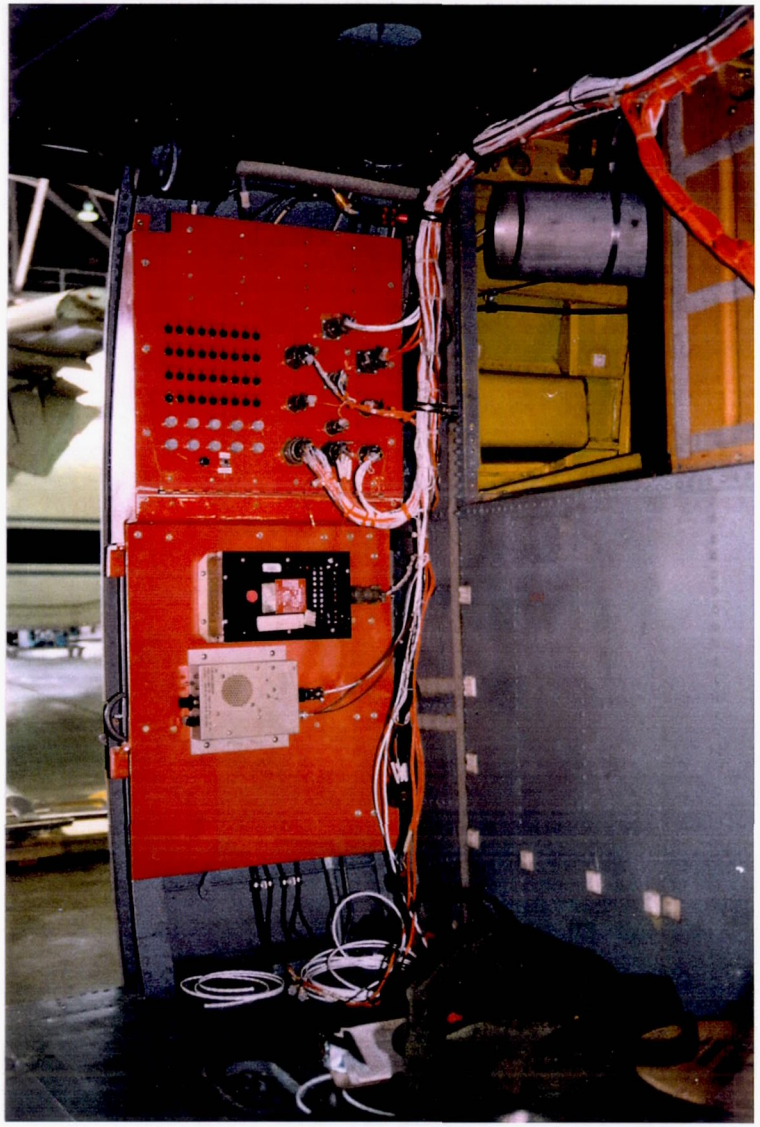

Figure 12.
Instrumentation Panel (AFT RHS)
UH-60A Airloads Program Flight Component

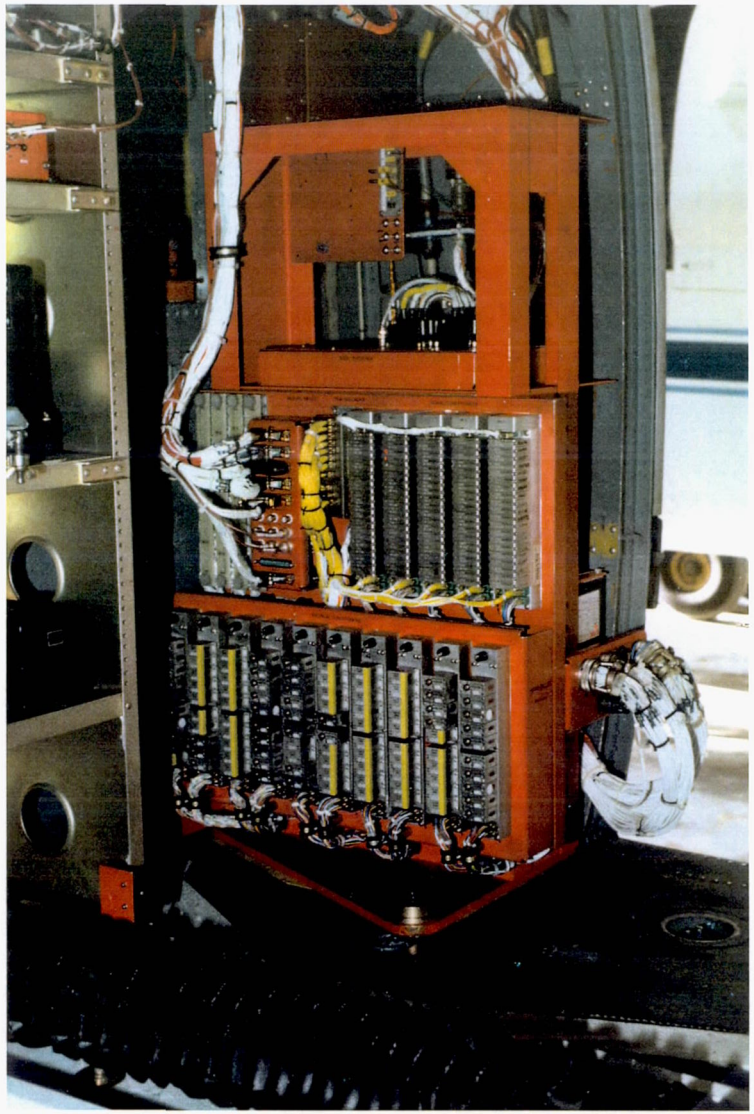

Figure 13.
Pallet Rack
UH-60A Airloads Program Flight Component

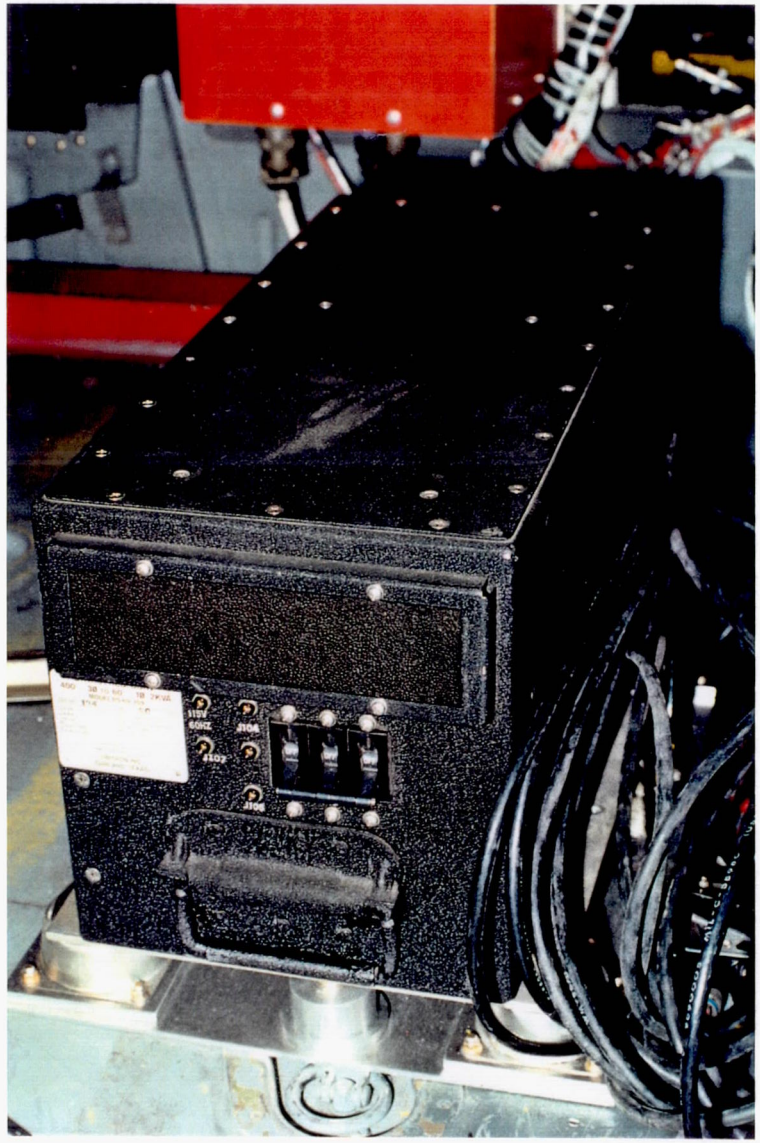

Figure 14.
Static Frequency Converter
UH-60A Airloads Program Flight Component

ORIGINAL PAGE
COLOR PHOTOGRAPH

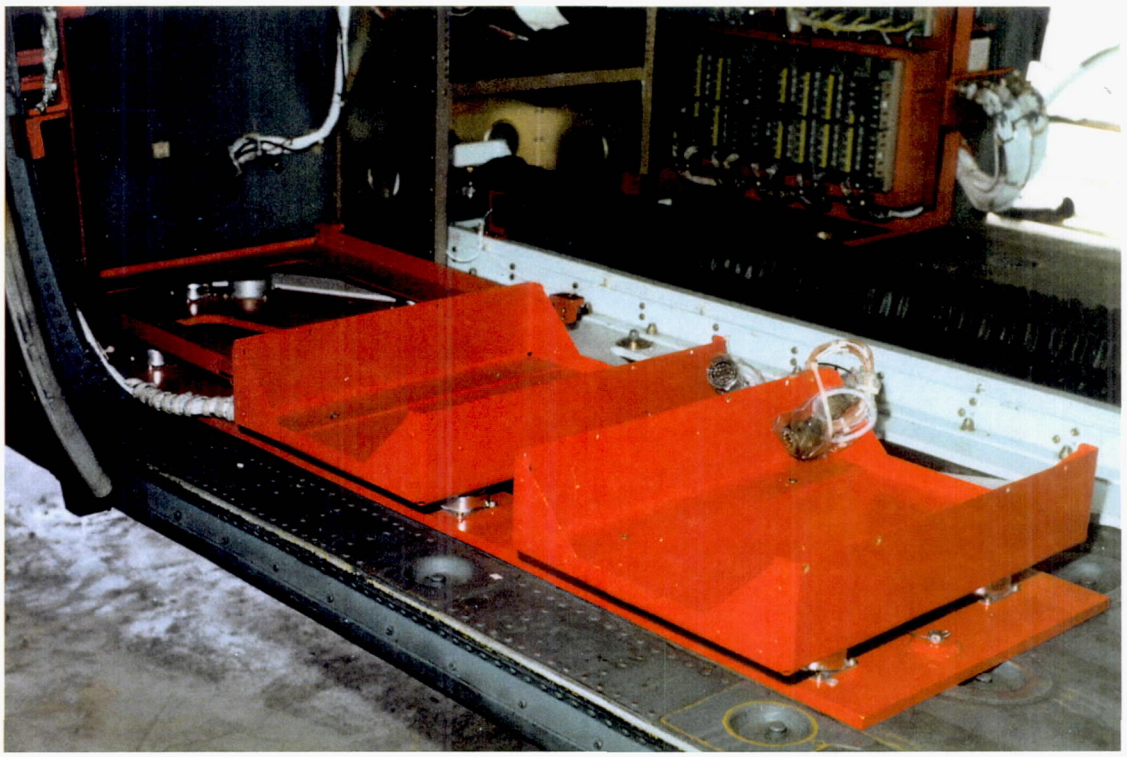

Figure 15.
Adapter Plate Assembly
UH-60A Airloads Program Flight Component

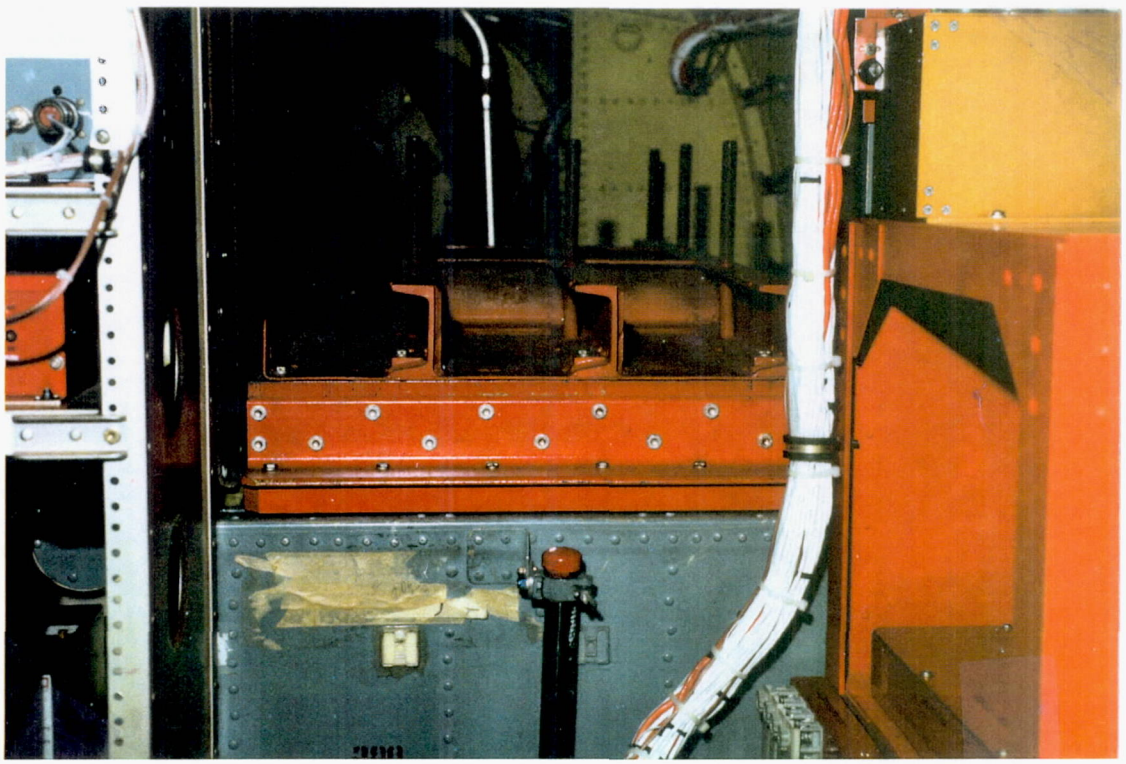

Figure 16.
Over Fuel Cell Ballast (RHS & LHS)
UH-60A Airloads Program Flight Component

Figure 17.
RDAS II Instrumentation Bucket
UH-60A Airloads Program Flight Component

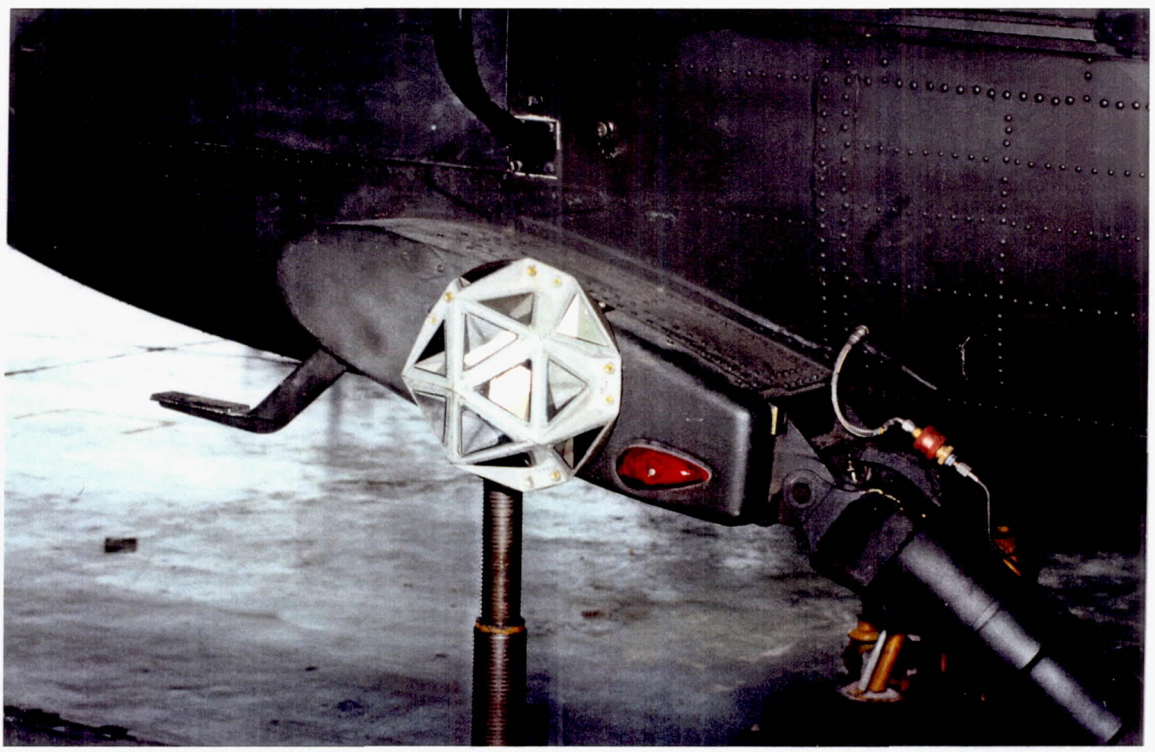

ORIGINAL PAGE
COLOR PHOTOGRAPH

Figure 18.
Laser Cube Assembly (2, RHS & LHS)
UH-60A Airloads Program Flight Component

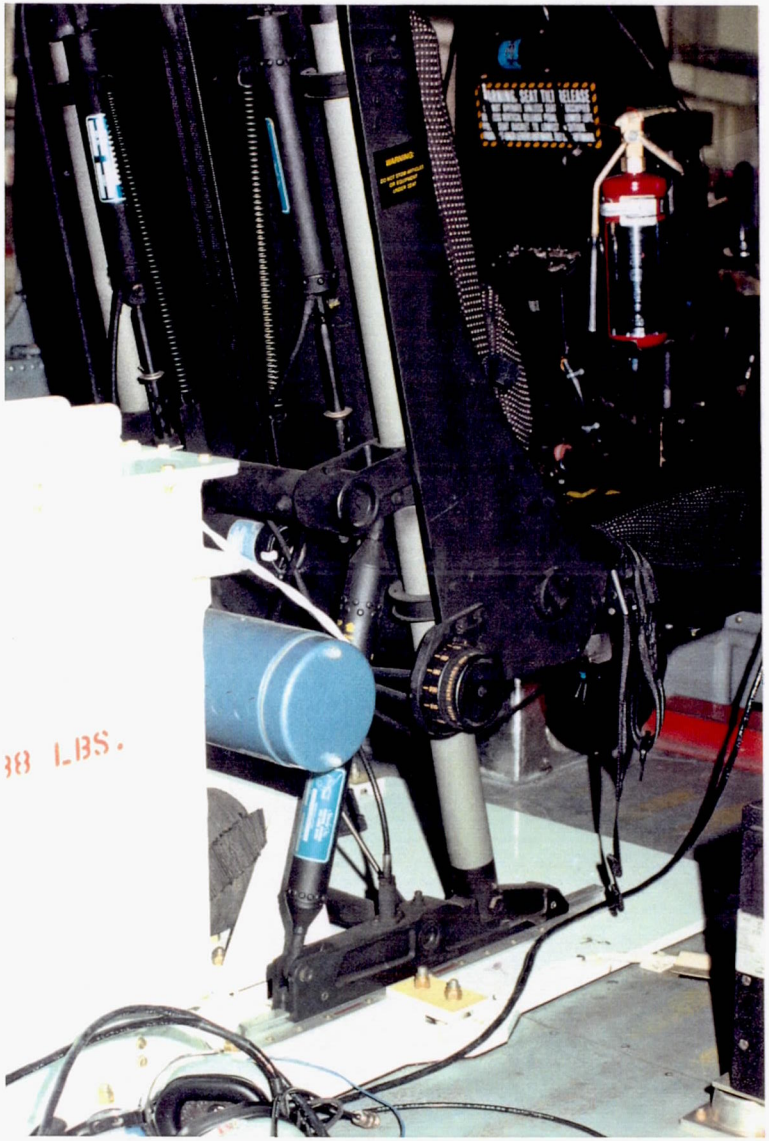

Figure 19.
Observer Station Mount and Seat
UH-60A Airloads Program Flight Component

Figure 20.
Formatter, Multiplexer, and Tape Recorders (2)
UH-60A Airloads Program Flight Component

MODELING OF COMPONENTS

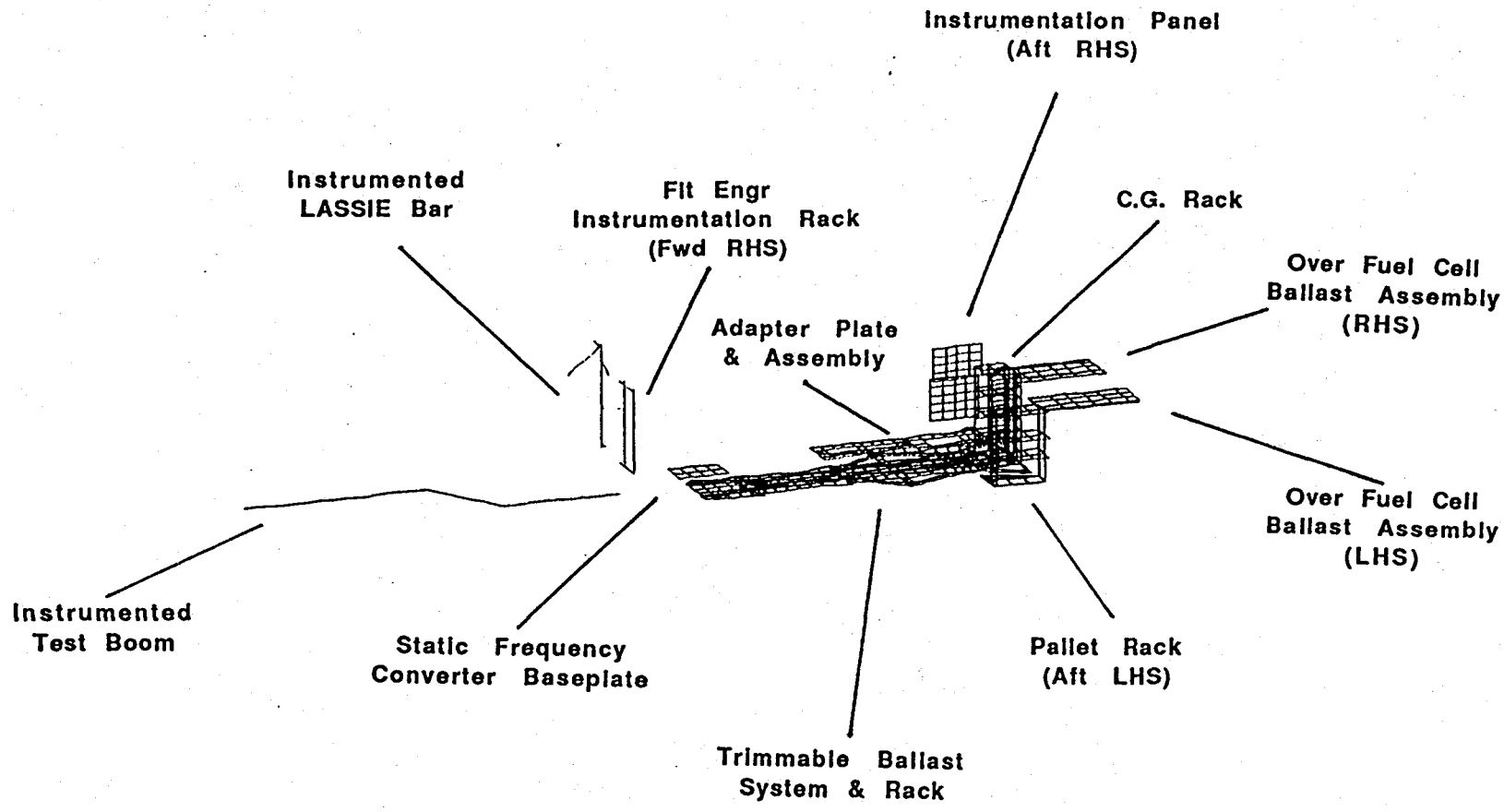

Figure 21.
Summation of Flight Components - Finite Element Representation
UH-60A Airloads Program Flight Components

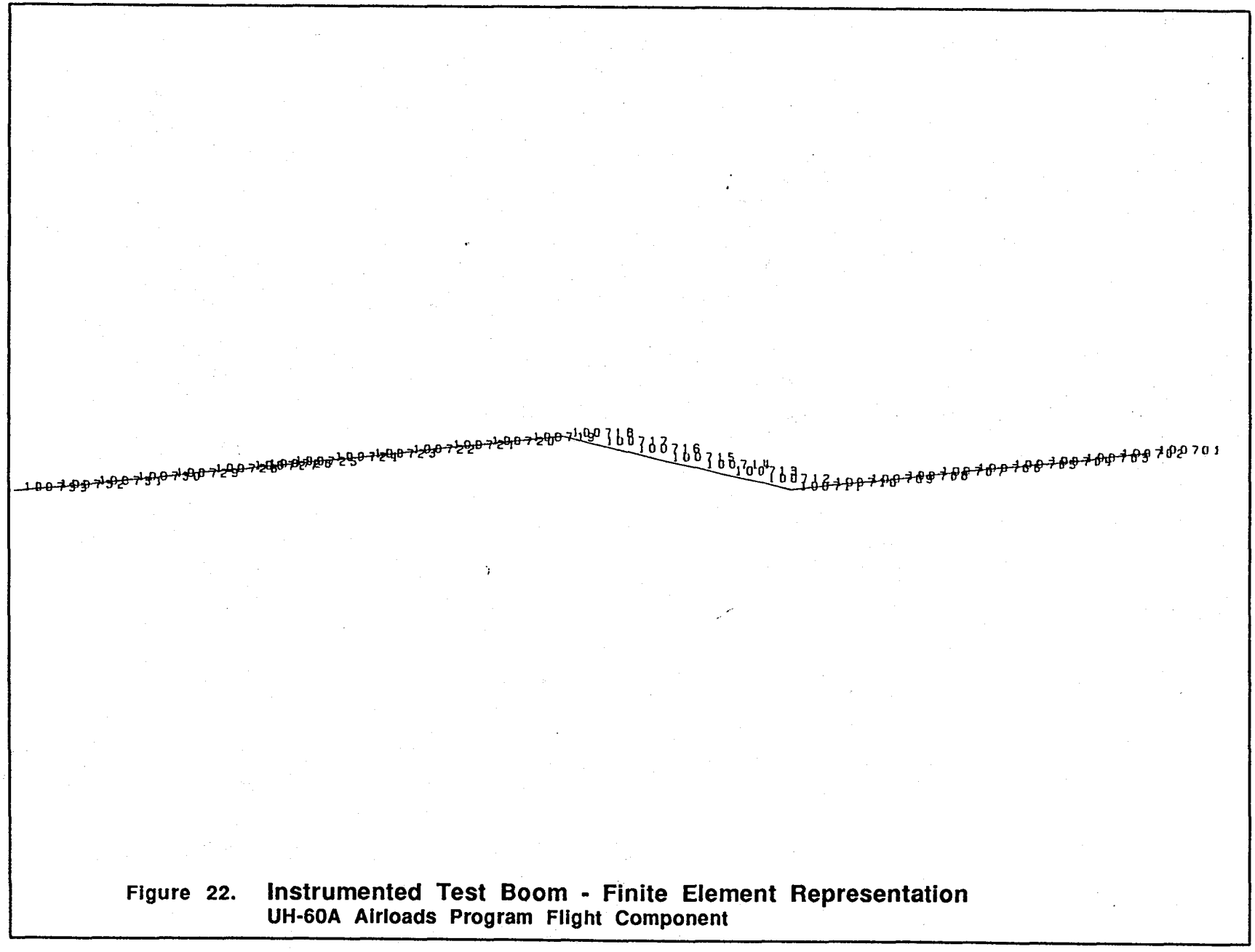

Figure 22. **Instrumented Test Boom - Finite Element Representation**
UH-60A Airloads Program Flight Component

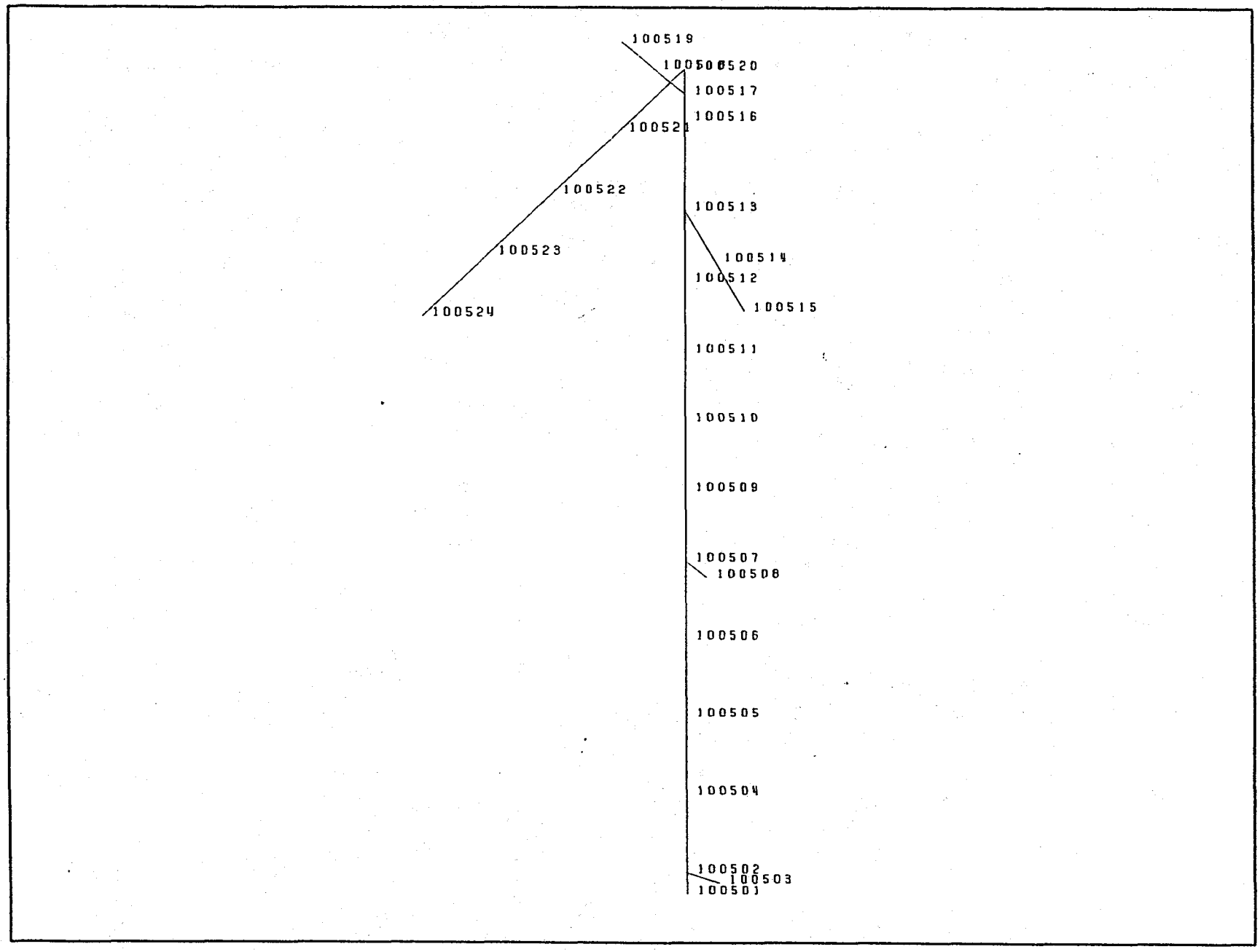

Figure 23. Instrumented LASSIE Bar - Finite Element Representation
UH-60A Airloads Program Flight Component

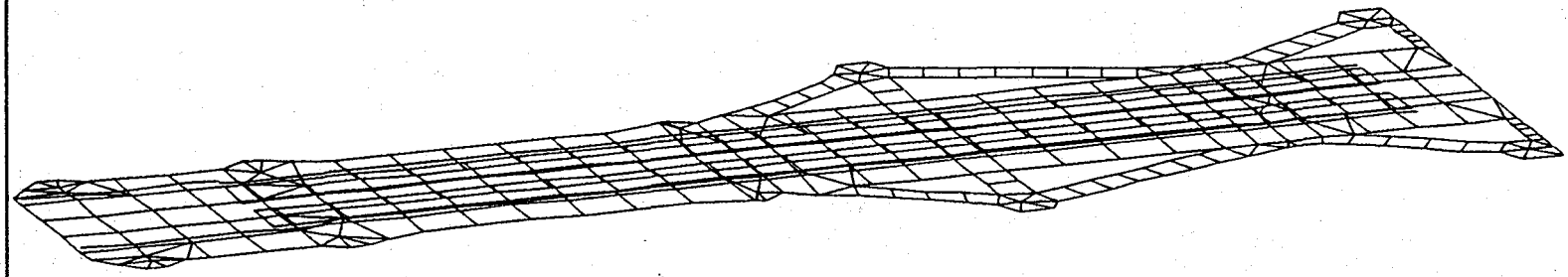

Figure 24. **Ballast Rack - Finite Element Representation**
UH-60A Airloads Program Flight Component

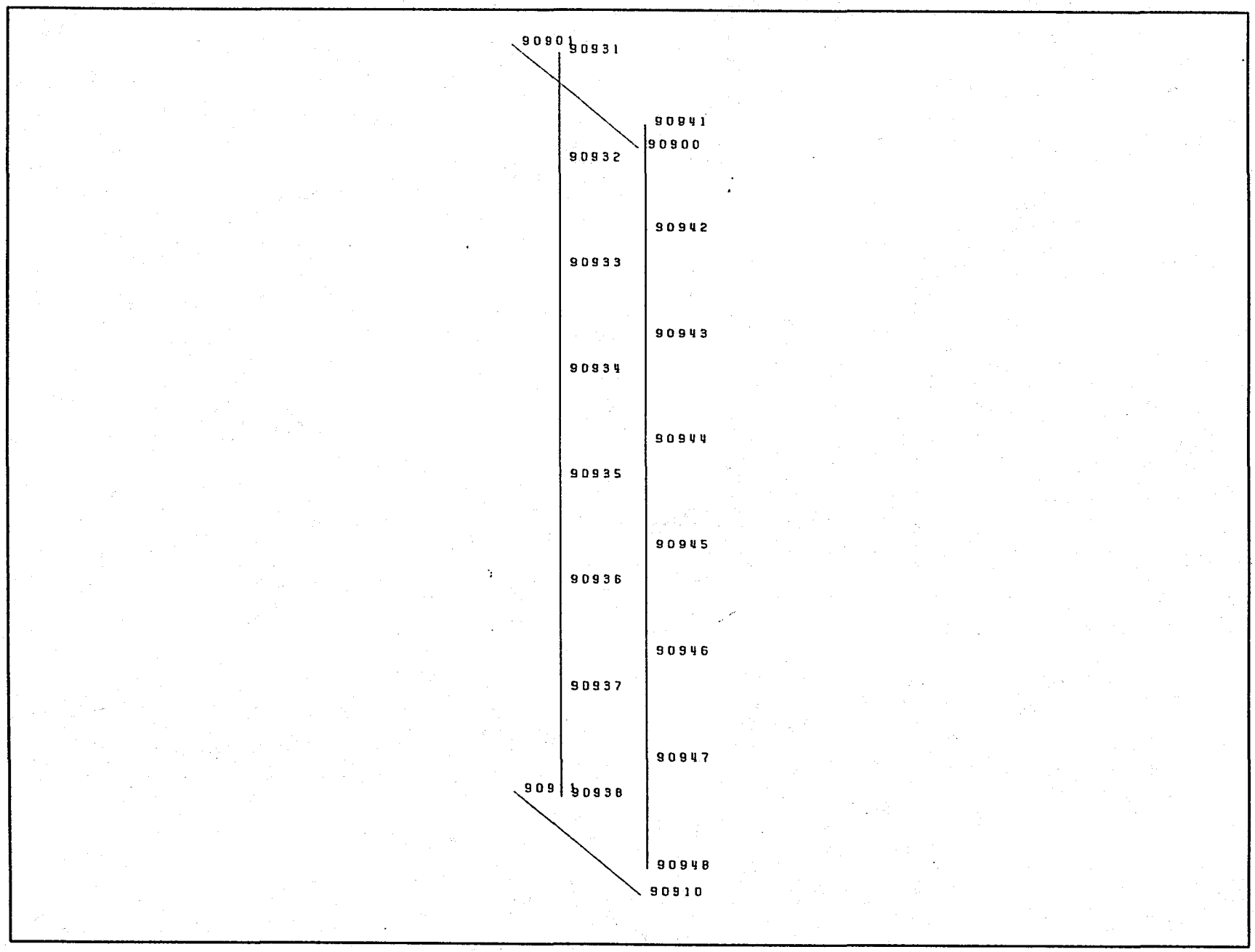

Figure 25. Flight Engineer's Instrumentation Rack - Finite Element Representation
UH-60A Airloads Program Flight Component

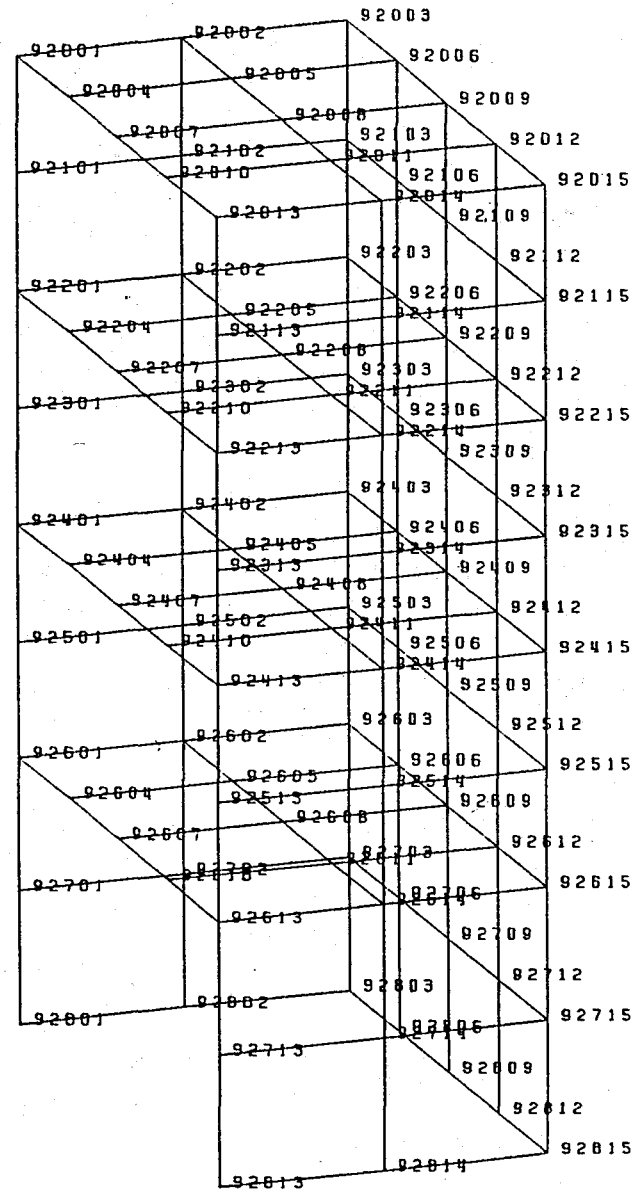

Figure 26. C.G. Rack - Finite Element Representation
UH-60A Airloads Program Flight Component

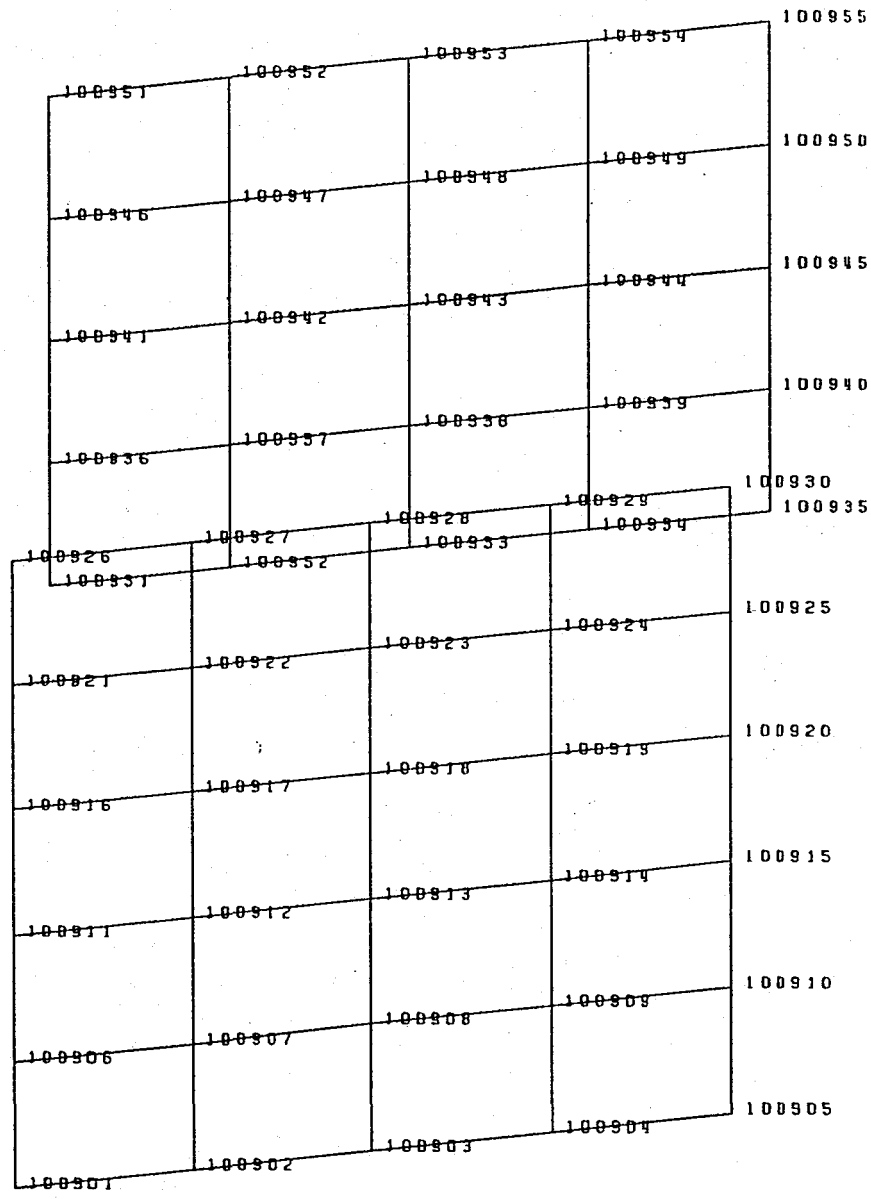

Figure 27. Instrumentation Panel (AFT RHS) - Finite Element Representation
UH-60A Airloads Program Flight Component

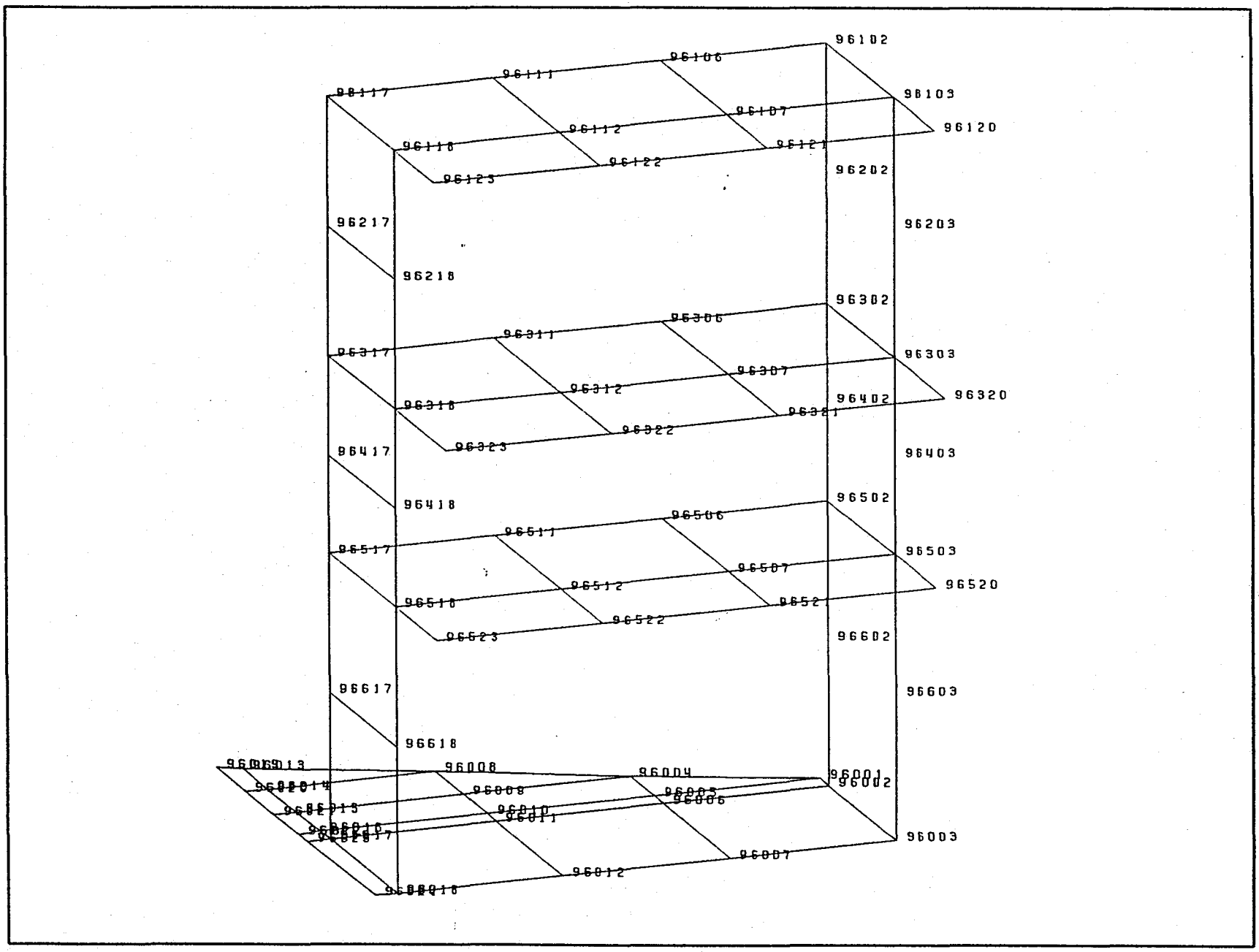

Figure 28. Pallet Rack - Finite Element Representation
UH-60A Airloads Program Flight Component

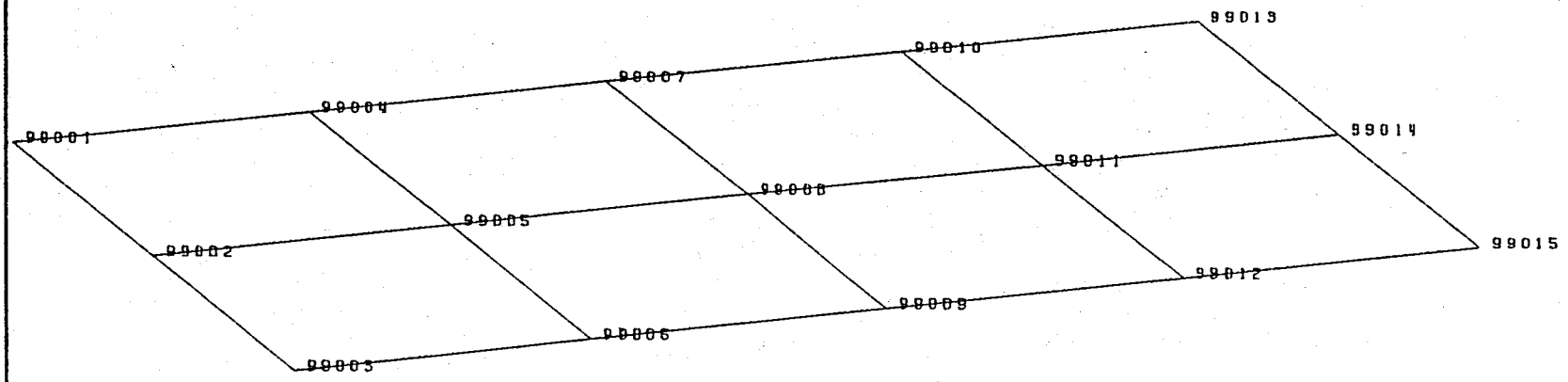

Figure 29. Static Frequency Converter Baseplate - Finite Element Representation
UH-60A Airloads Program Flight Component

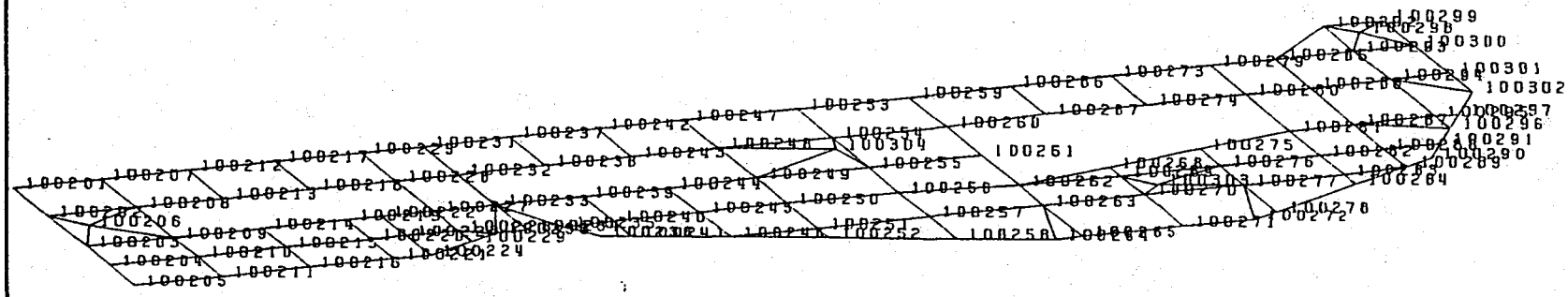

Figure 30. Adapter Plate Assembly - Finite Element Representation
UH-60A Airloads Program Flight Component

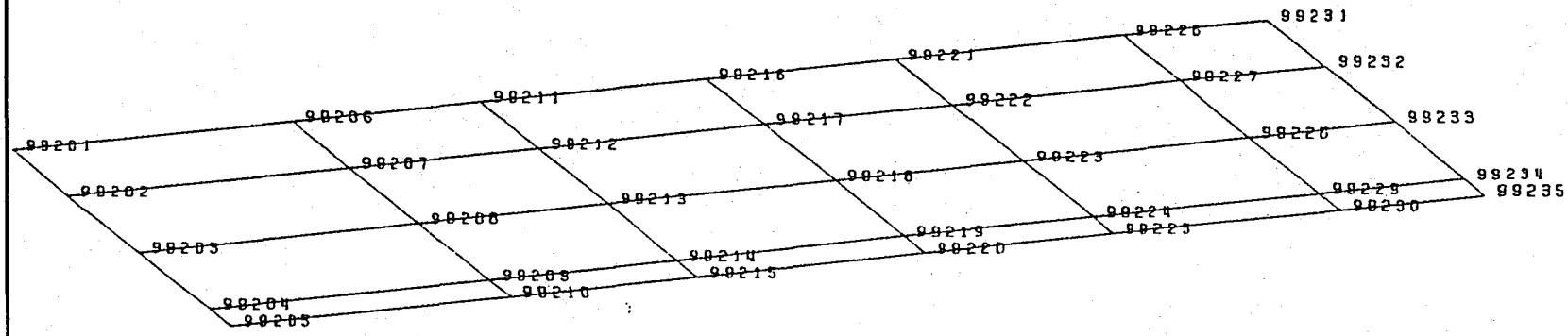

Figure 31. Over Fuel Cell Ballast (RHS) - Finite Element Representation
UH-60A Airloads Program Flight Component

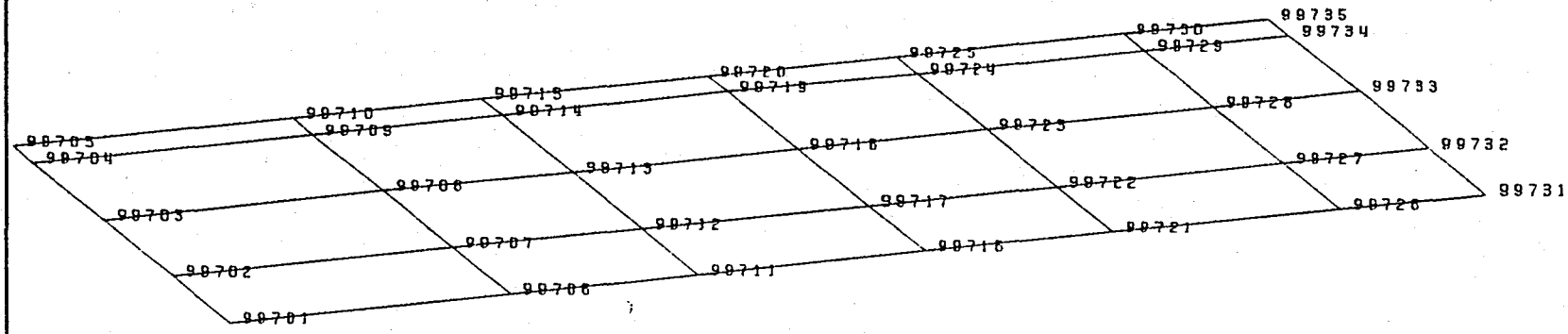

Figure 32. Over Fuel Cell Ballast (LHS) - Finite Element Representation
UH-60A Airloads Program Flight Component

Mass Items

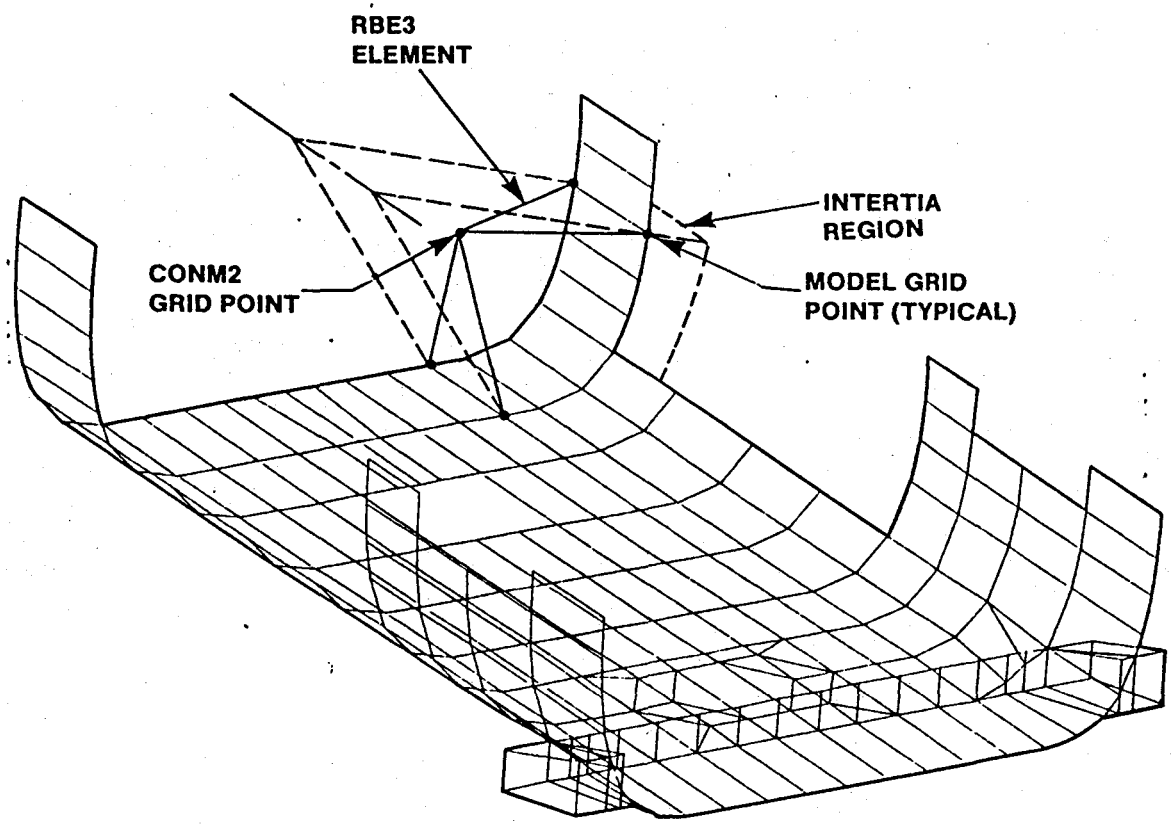

Figure 33. Mass Modeling: Representation of Distributed Mass

MODELING CHECKS

Prescribed Displacement $U_{longitudinal}$

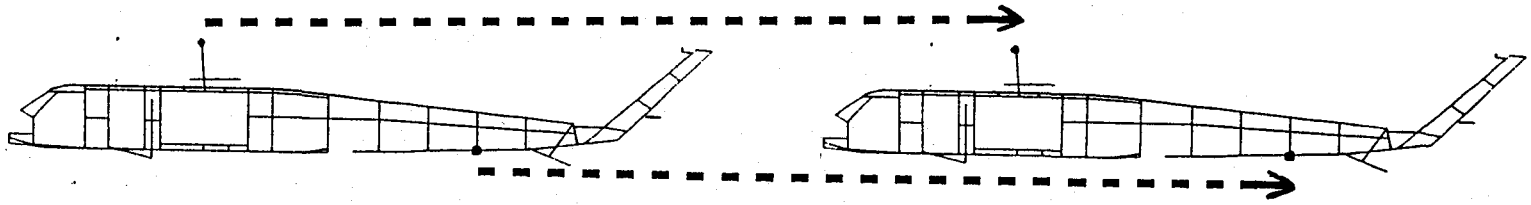

Grid Point i

Resulting Displacement $U_i = U_{longitudinal}$

Figure 34. Rigid Body Check Diagram - Example

BUILD-UP OF FLIGHT COMPONENT STRUCTURE STUDY
BUILD-UP OF FLIGHT COMPONENT MASS STUDY

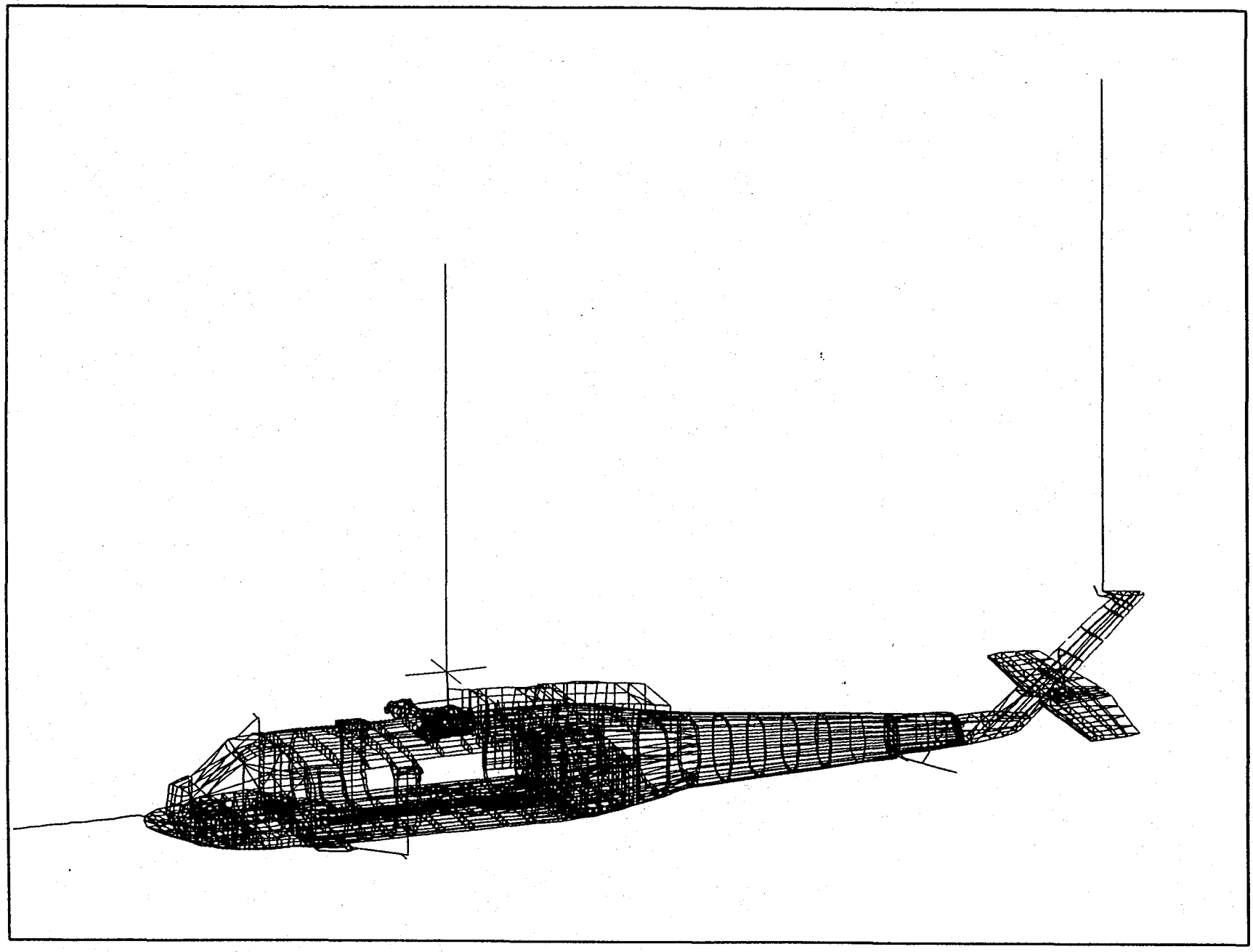

Figure 35. **Starting Reference Configuration w/ Suspension System**
Build-Up of Flight Component Structure & Mass
NASTRAN Finite Element Model

INCLUSION OF UPDATED PRIMARY/SECONDARY STRUCTURE
INCLUSION OF MODELING REVISION
COMPREHENSIVE RESULTS OF 'BEST' MODEL

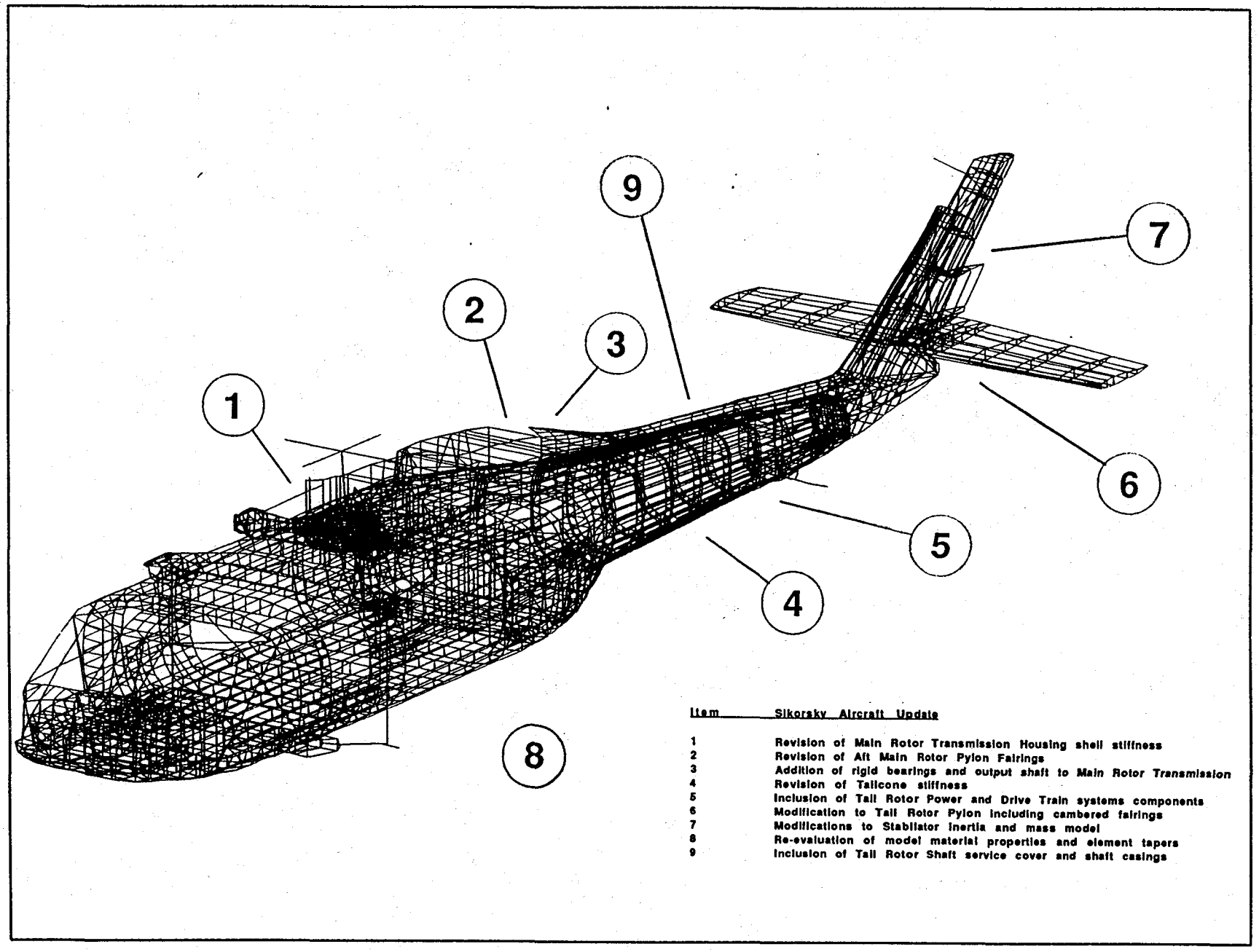

Figure 36. **Updated Primary/Secondary Structural Model**
NASTRAN Finite Element Model

Figure 37.

'Best' Model for MTRAP Flight Test Configuration

Updated Primary/Secondary Structural Model

MTRAP Structural Flight Components and Mass Distribution w/ Suspension System

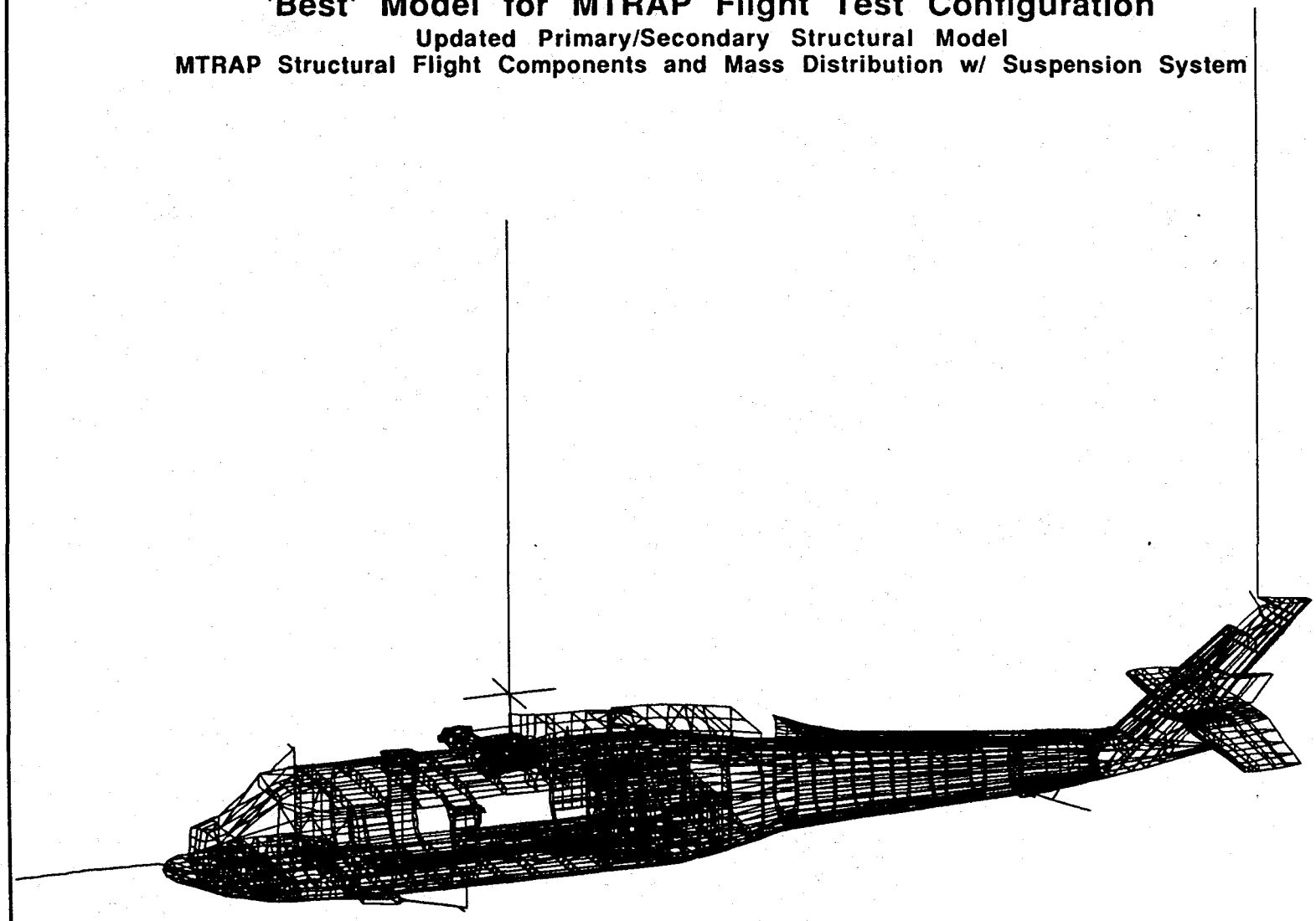

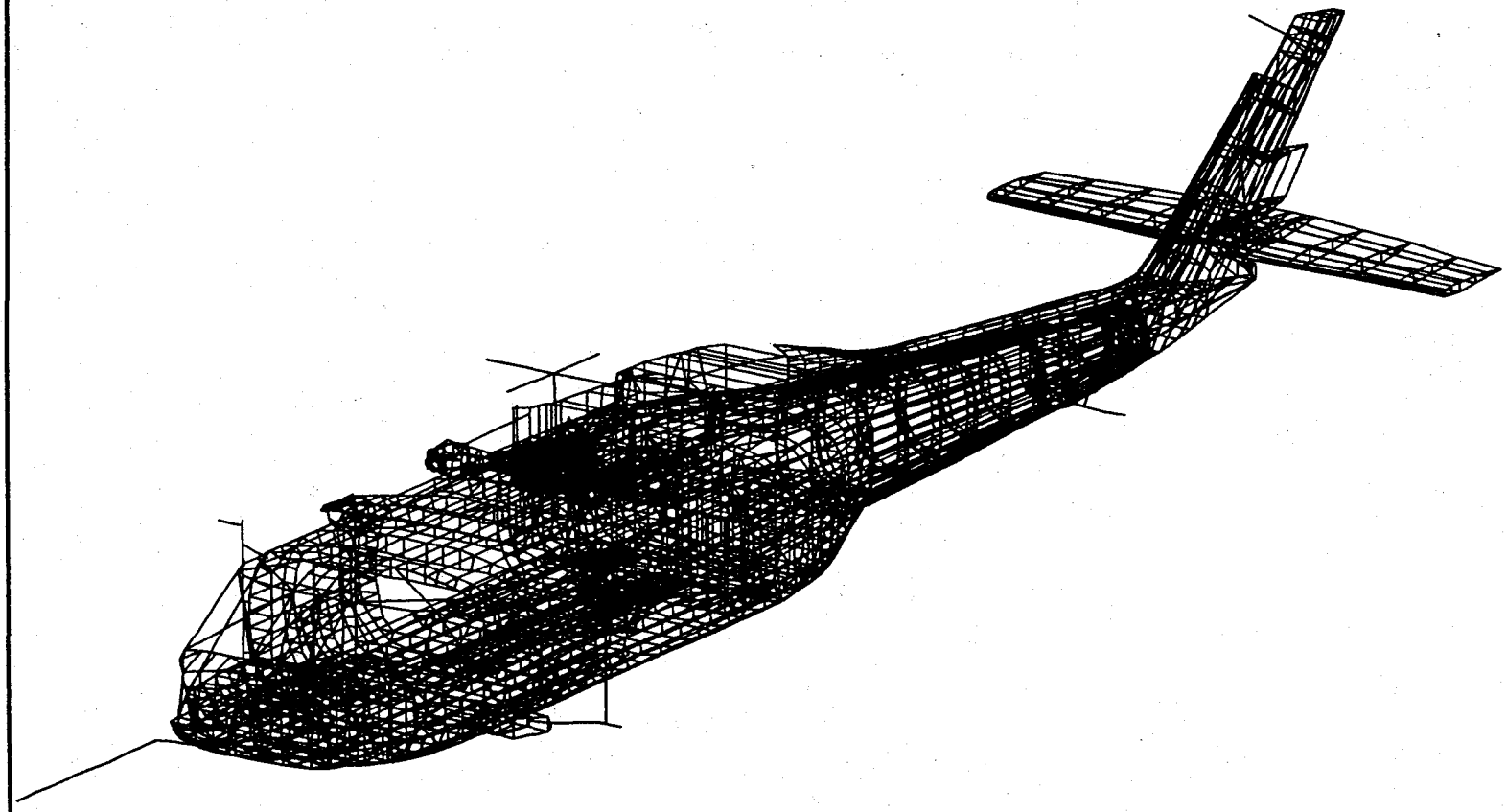

Figure 38.
'Best' Model for MTRAP Flight Test Configuration
Updated Primary/Secondary Structural Model
MTRAP Structural Flight Components and Mass Distribution wo/ Suspension System

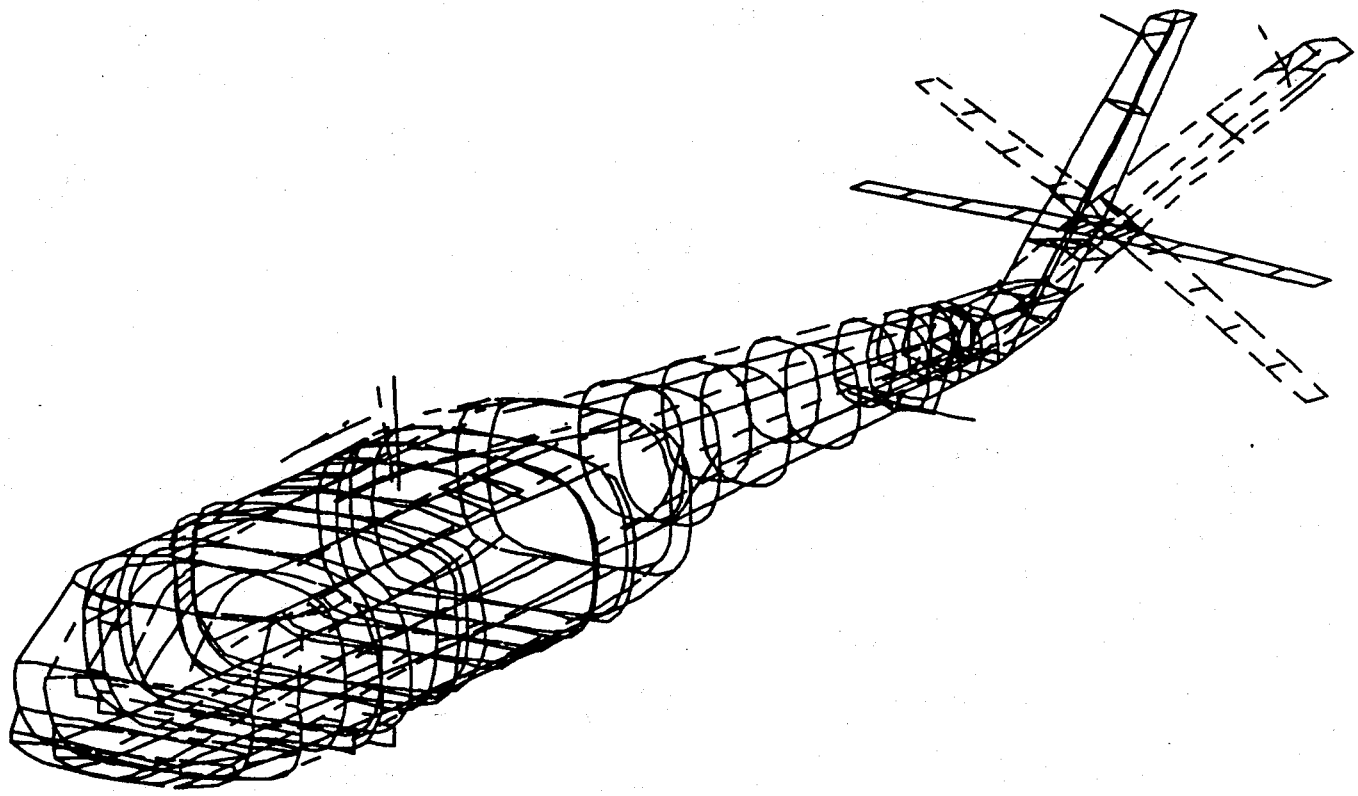

Figure 39.
Mode Shape 1 - 1st Vertical Bending
Mode Frequency: 6.322543 Hz
"Best" Model for MTRAP Flight/Shake Test Configuration

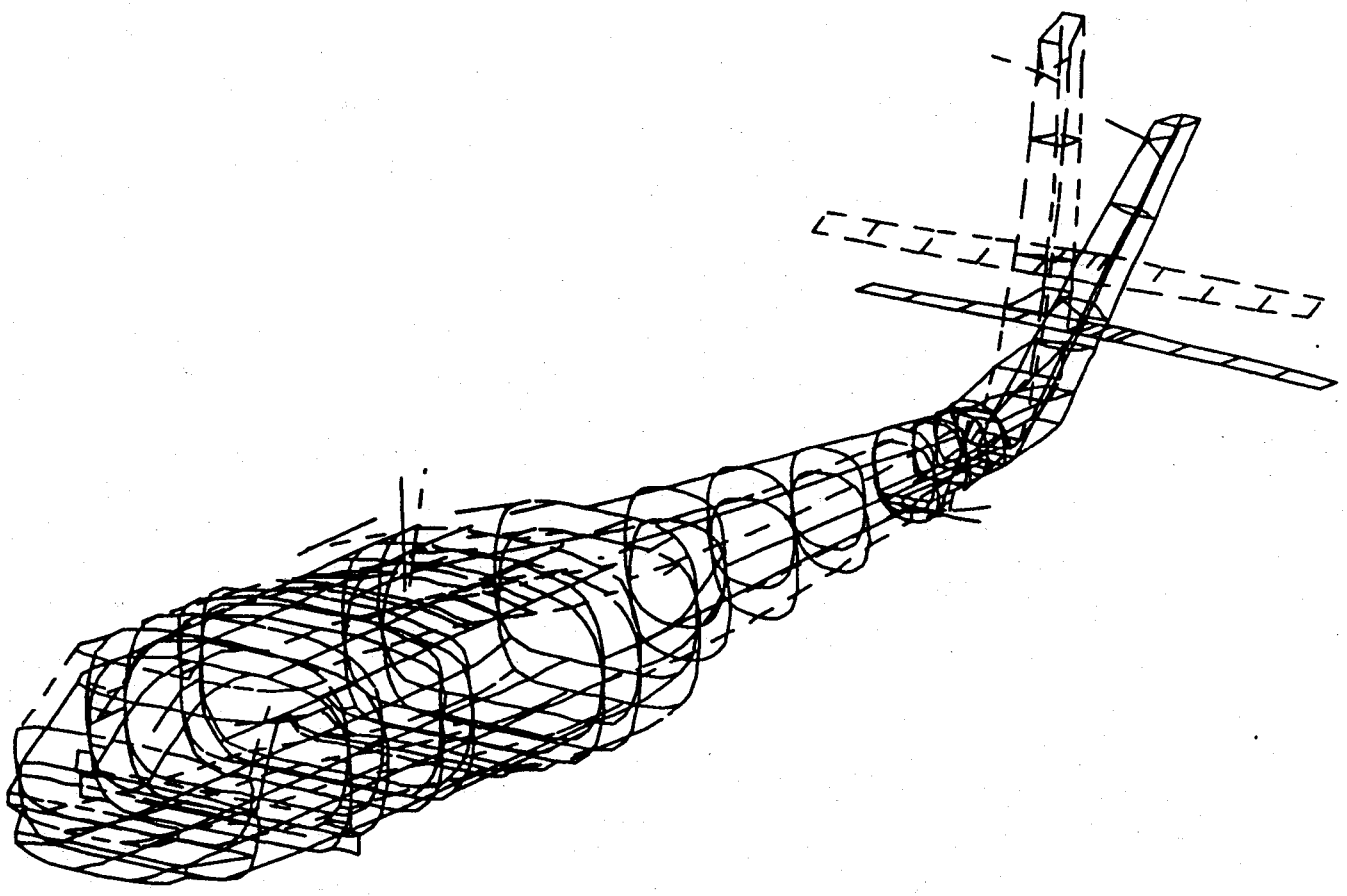

Figure 40.
Mode Shape 2 - 1st Lateral Bending
Mode Frequency: 9.121788 Hz
"Best" Model for MTRAP Flight/Shake Test Configuration

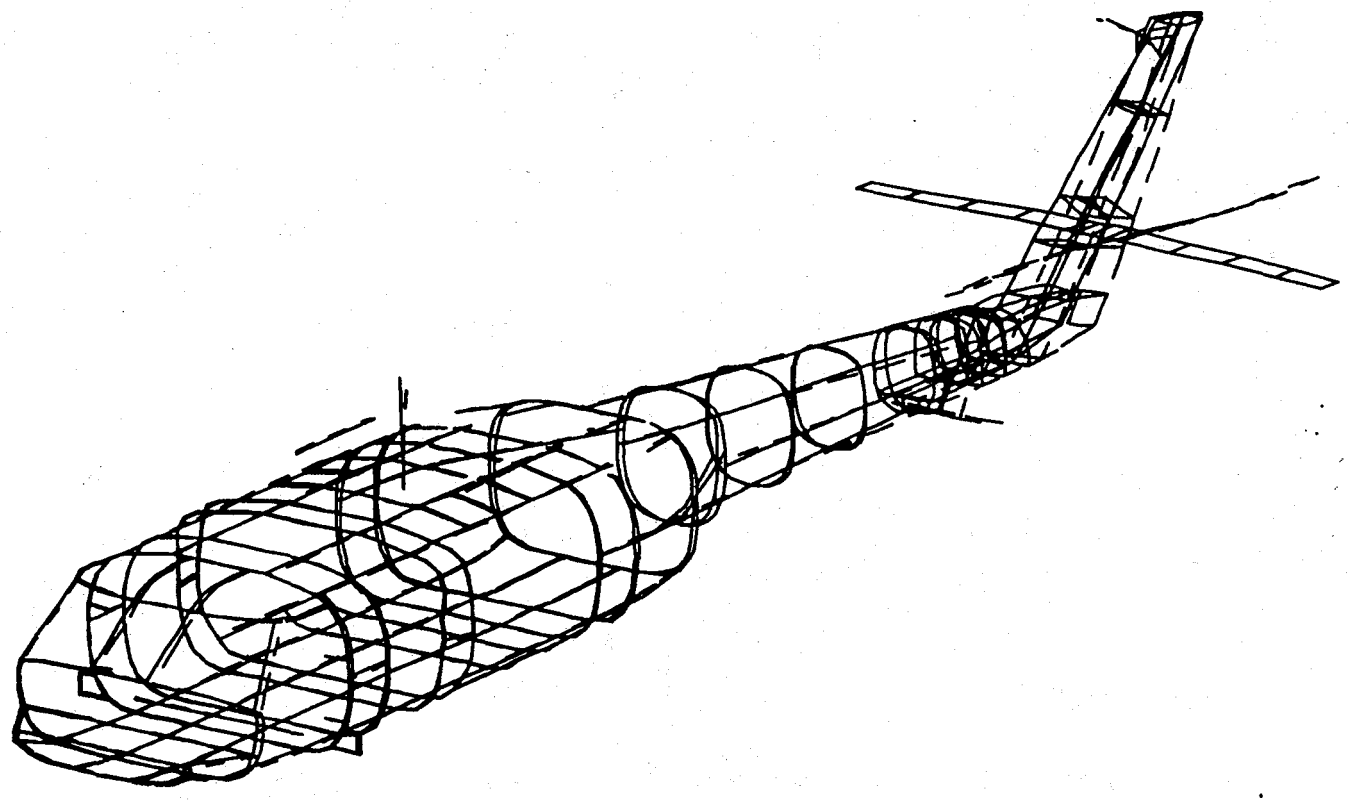

Figure 41.
Mode Shape 3 - Stabilator Roll
Mode Frequency: 11.26758 Hz
"Best" Model for MTRAP Flight/Shake Test Configuration

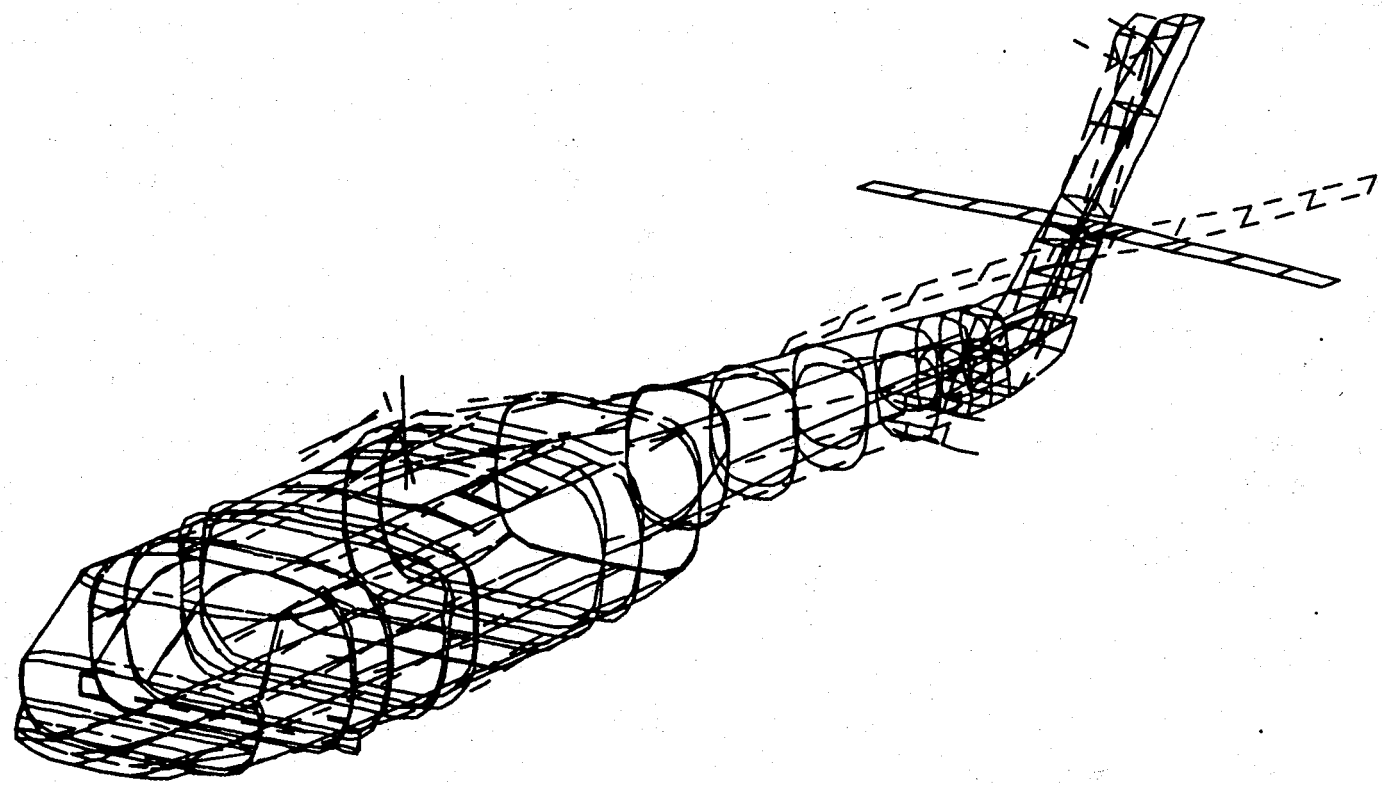

Figure 42.
Mode Shape 4 - 2nd Vertical Bending / Transmission Pitch
Mode Frequency: 11.65715 Hz
"Best" Model for MTRAP Flight/Shake Test Configuration

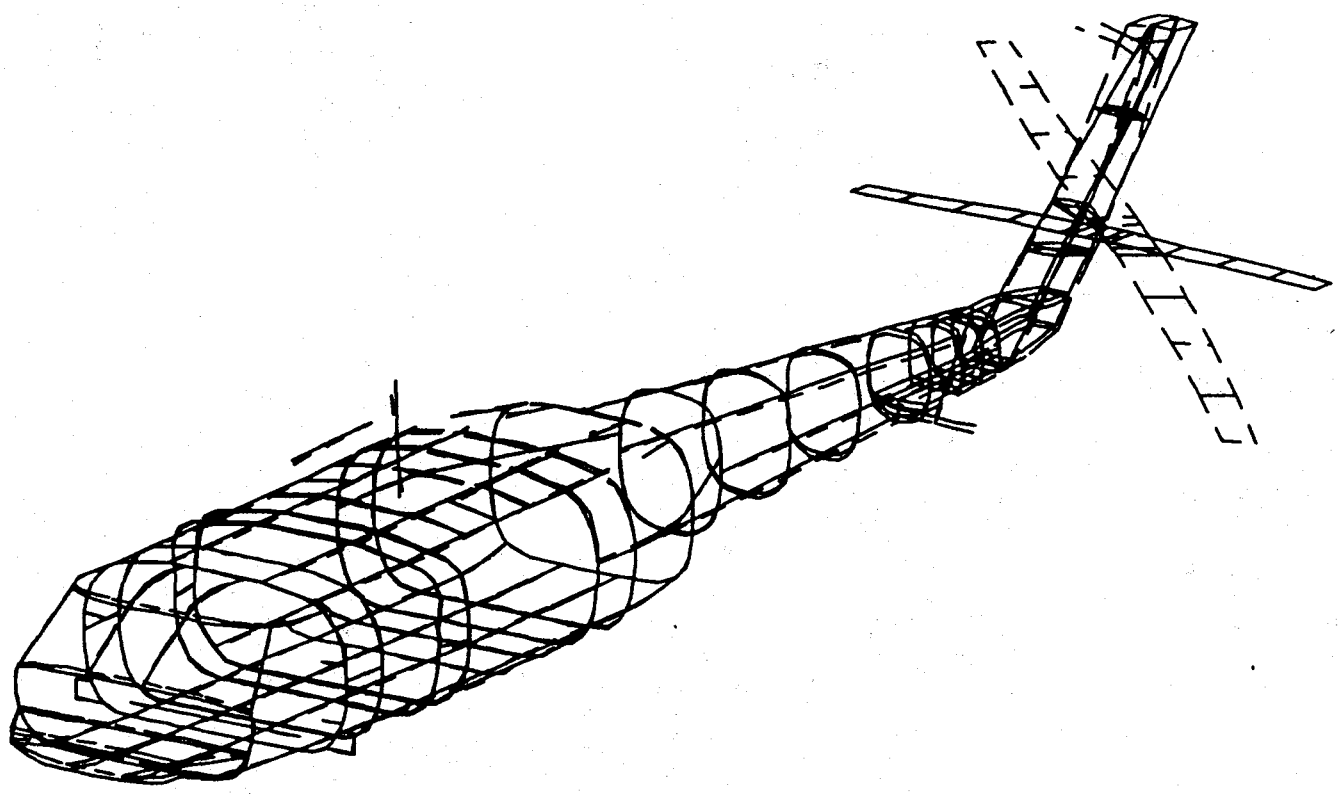

Figure 43.
Mode Shape 5 - Transmission Pitch / Stabilator Roll & Yaw
Mode Frequency: 12.44405 Hz
"Best" Model for MTRAP Flight/Shake Test Configuration

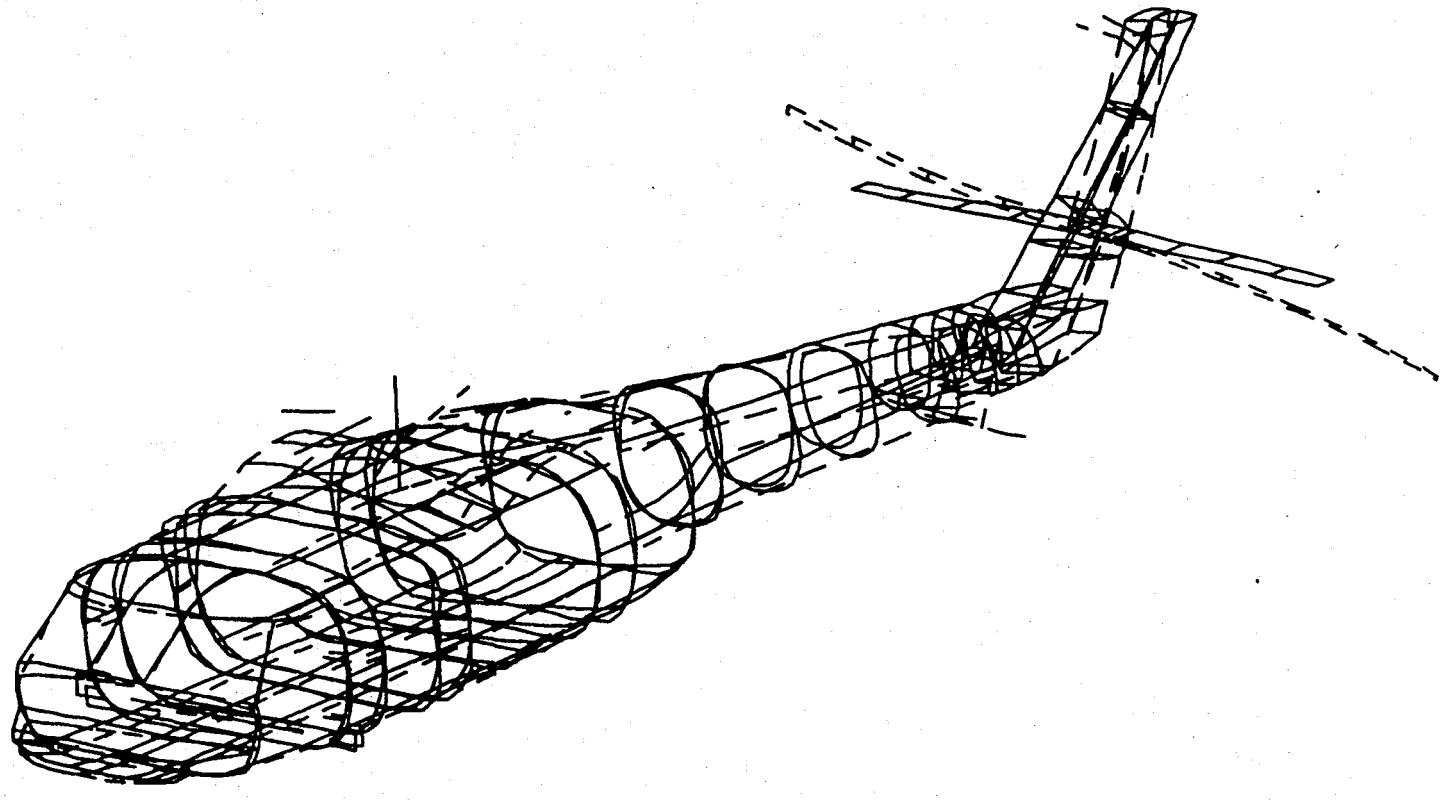

Figure 44.
Mode Shape 6 - Transmission Roll / Stabilator Yaw
Mode Frequency: 12.77752 Hz
"Best" Model for MTRAP Flight/Shake Test Configuration

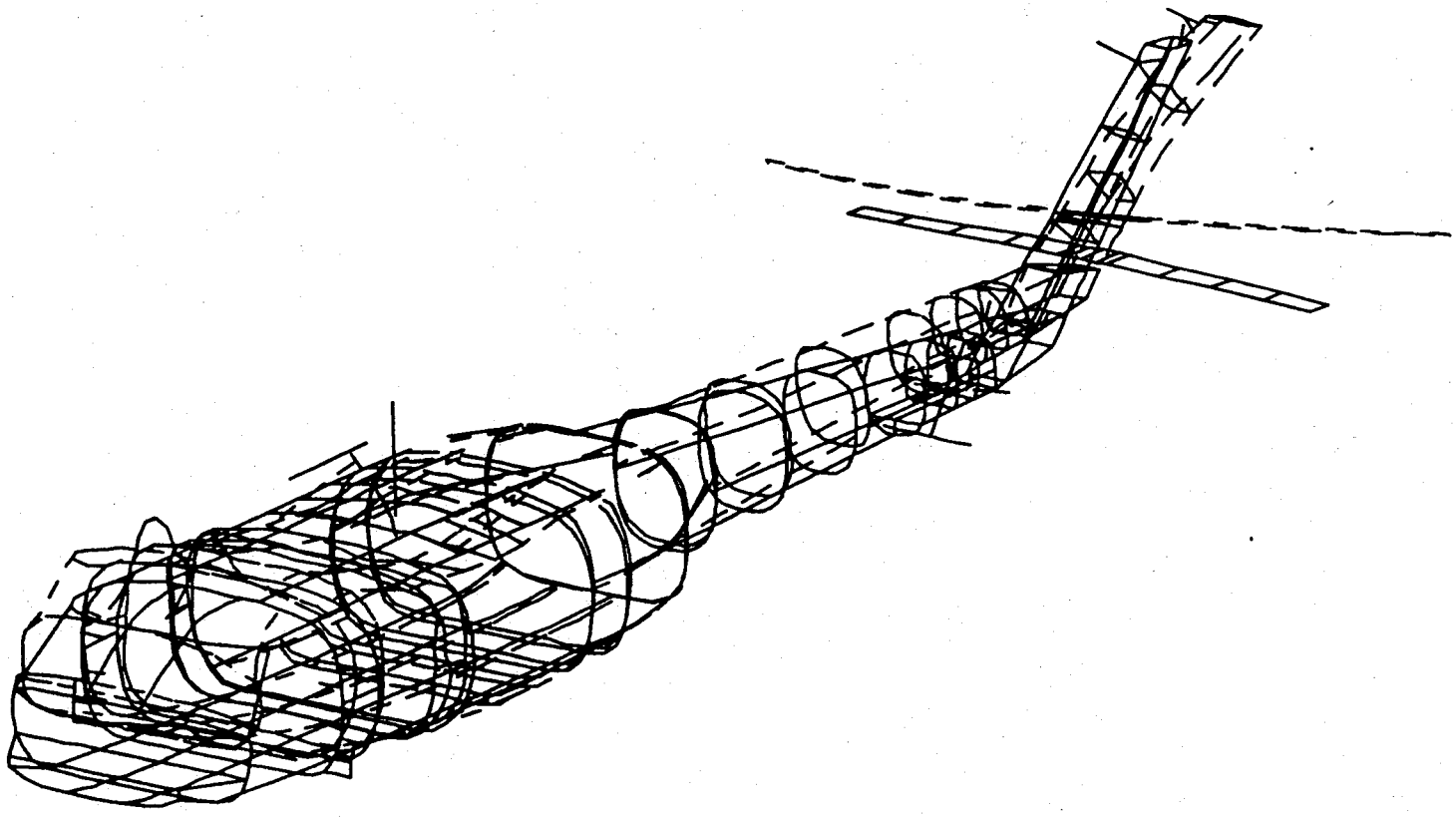

Figure 45.
Mode Shape 7 - Stabilator Roll / Transmission Roll
Mode Frequency: 12.93762 Hz
"Best" Model for MTRAP Flight/Shake Test Configuration

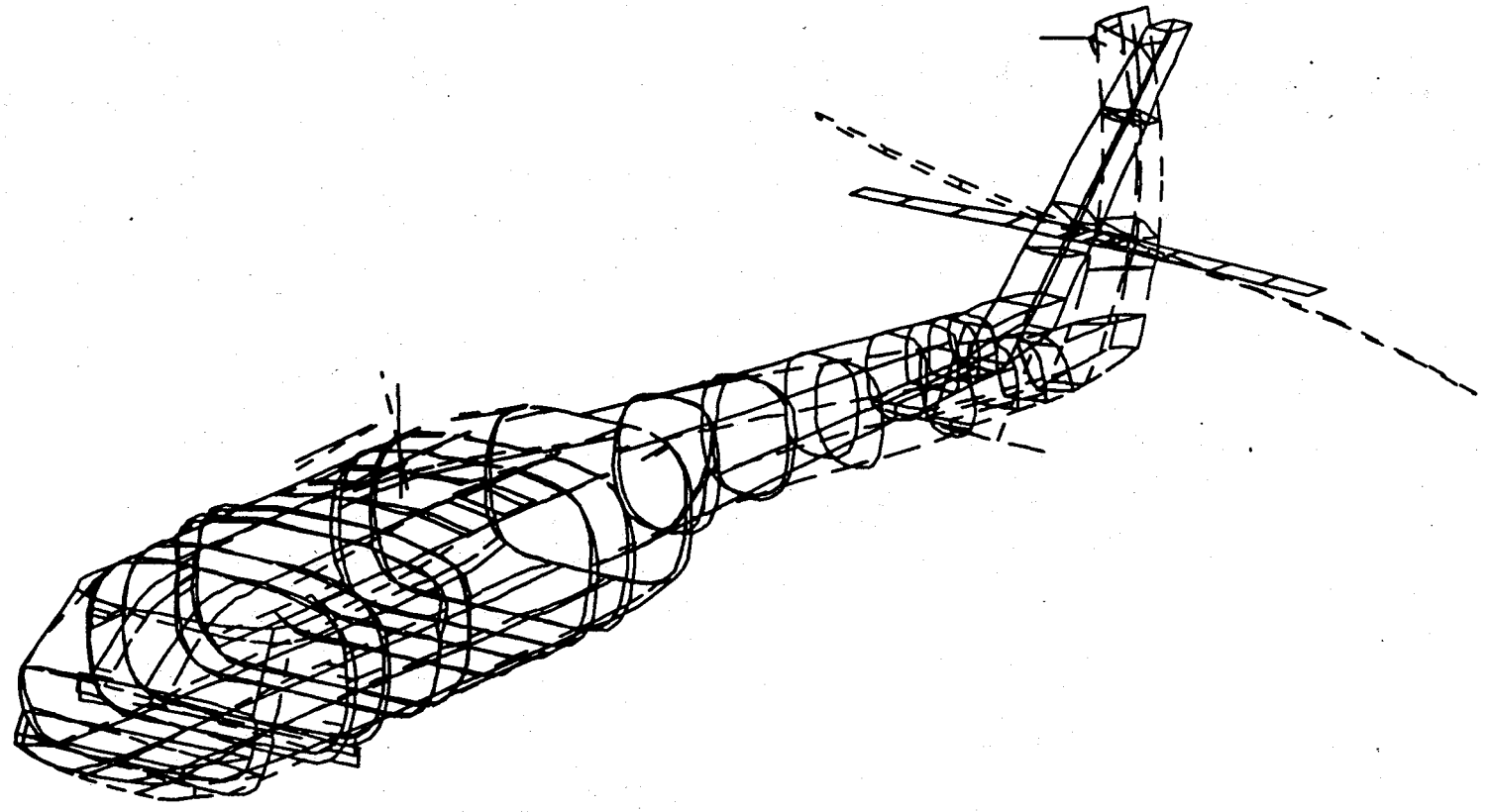

Figure 46.
Mode Shape 8 - Tailcone Lateral Bending/Transmission Roll/Stabilator Roll & Yaw
Mode Frequency: 13.25998 Hz
"Best" Model for MTRAP Flight/Shake Test Configuration

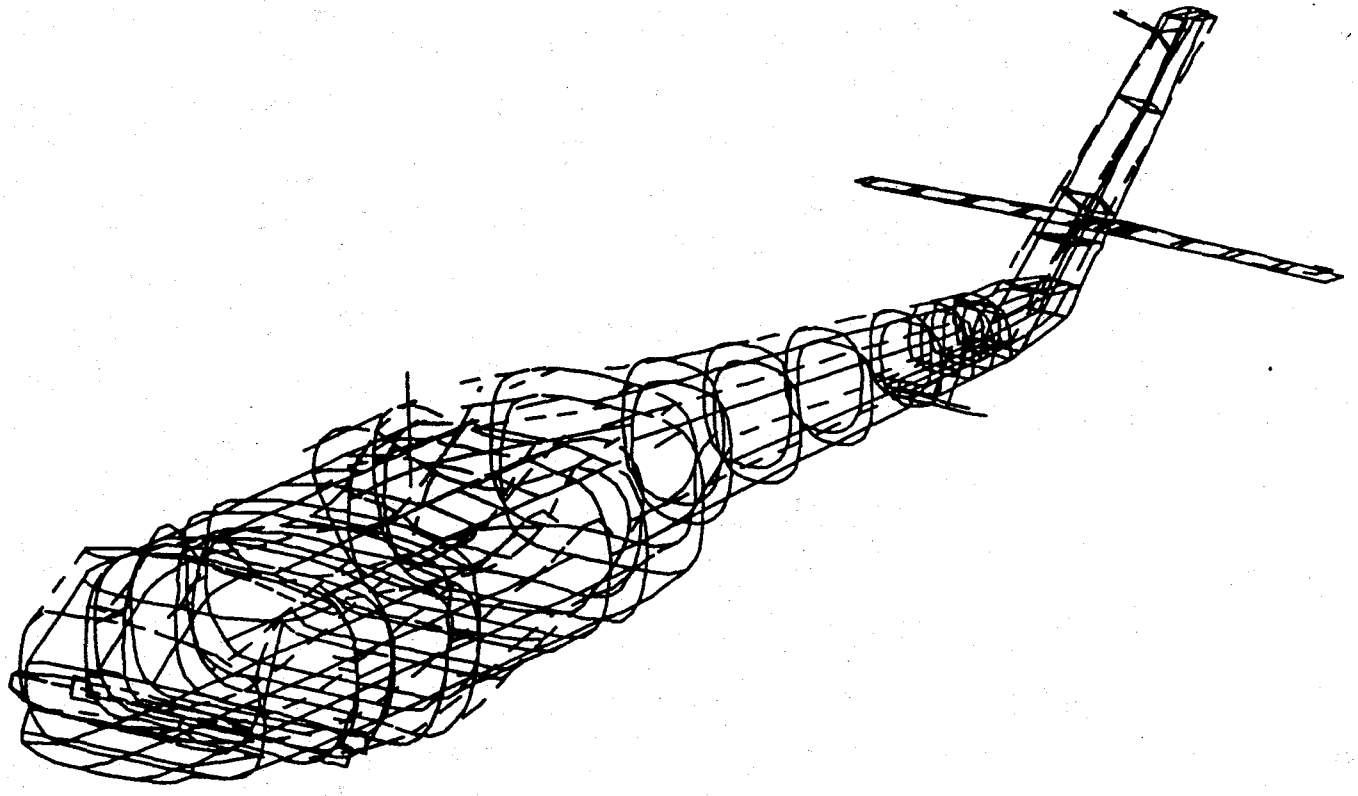

Figure 47.
Mode Shape 9 - 2nd Vertical Bending / Transmission Vertical
Mode Frequency: 14.53610 Hz
"Best" Model for MTRAP Flight/Shake Test Configuration

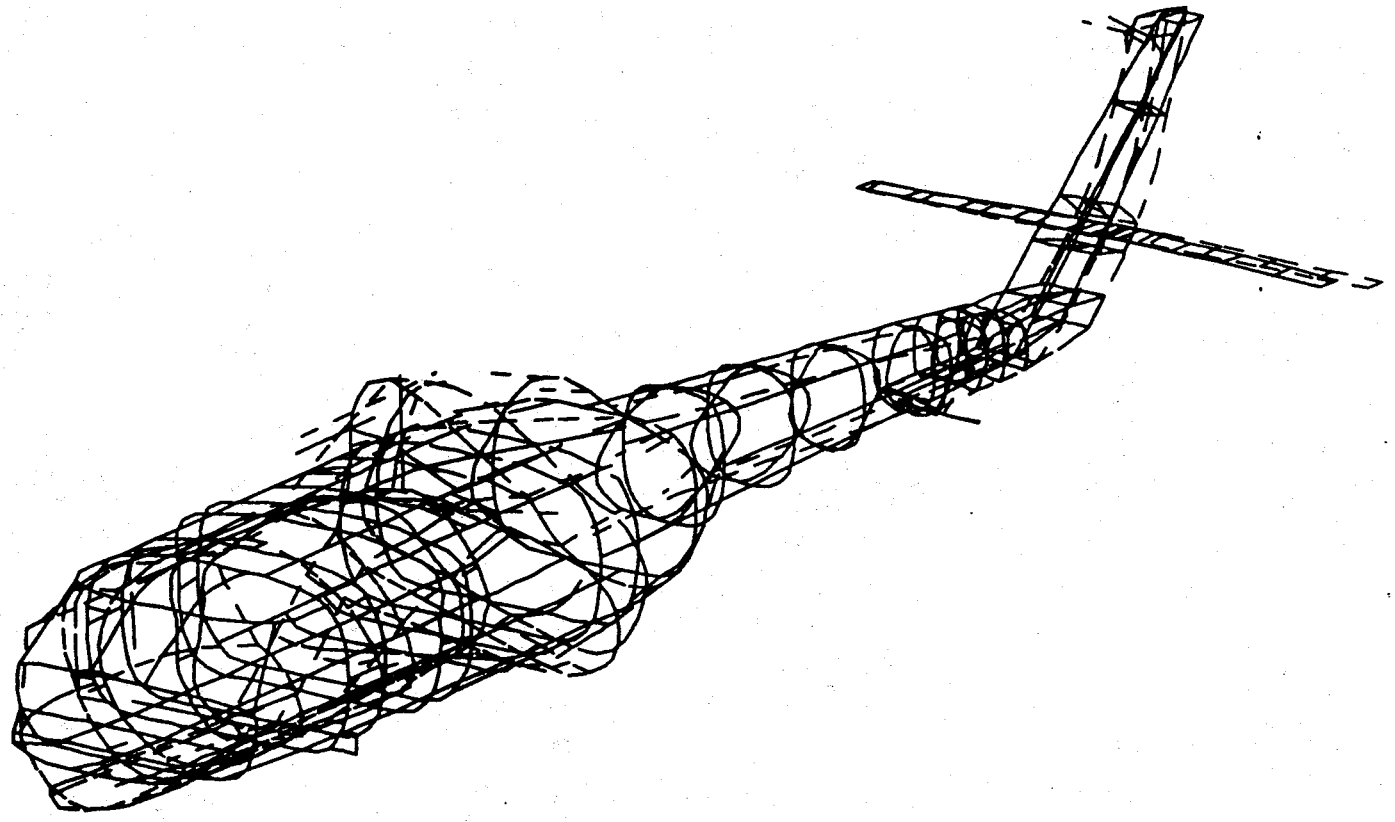

Figure 48.
Mode Shape 10 - Cockpit/Cabin Roll
Mode Frequency: 14.65144 Hz
"Best" Model for MTRAP Flight/Shake Test Configuration

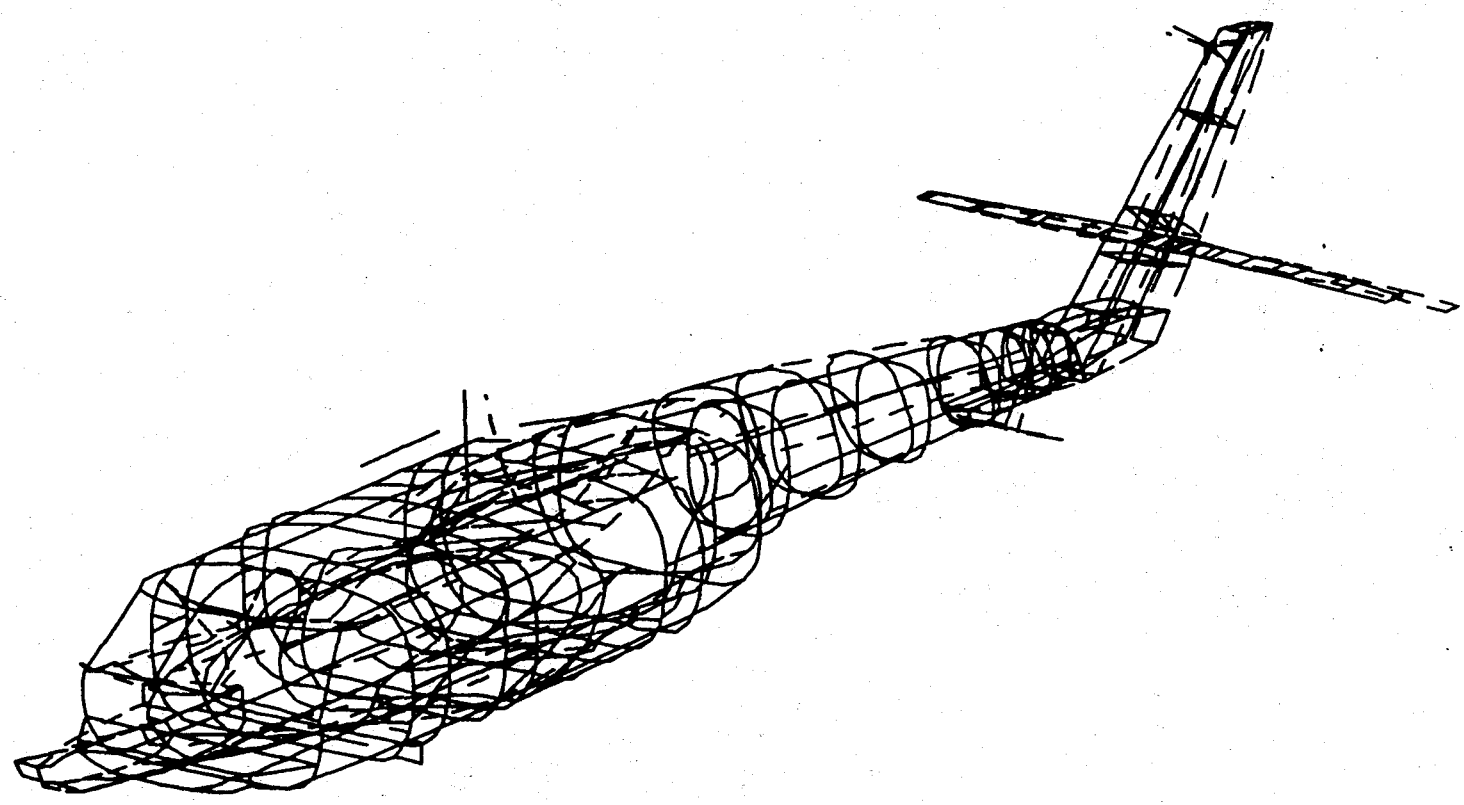

Figure 49.
Mode Shape 11 - Cockpit/Cabin Torsion/3rd Vertical Bending
Mode Frequency: 18.77941 Hz
"Best" Model for MTRAP Flight/Shake Test Configuration

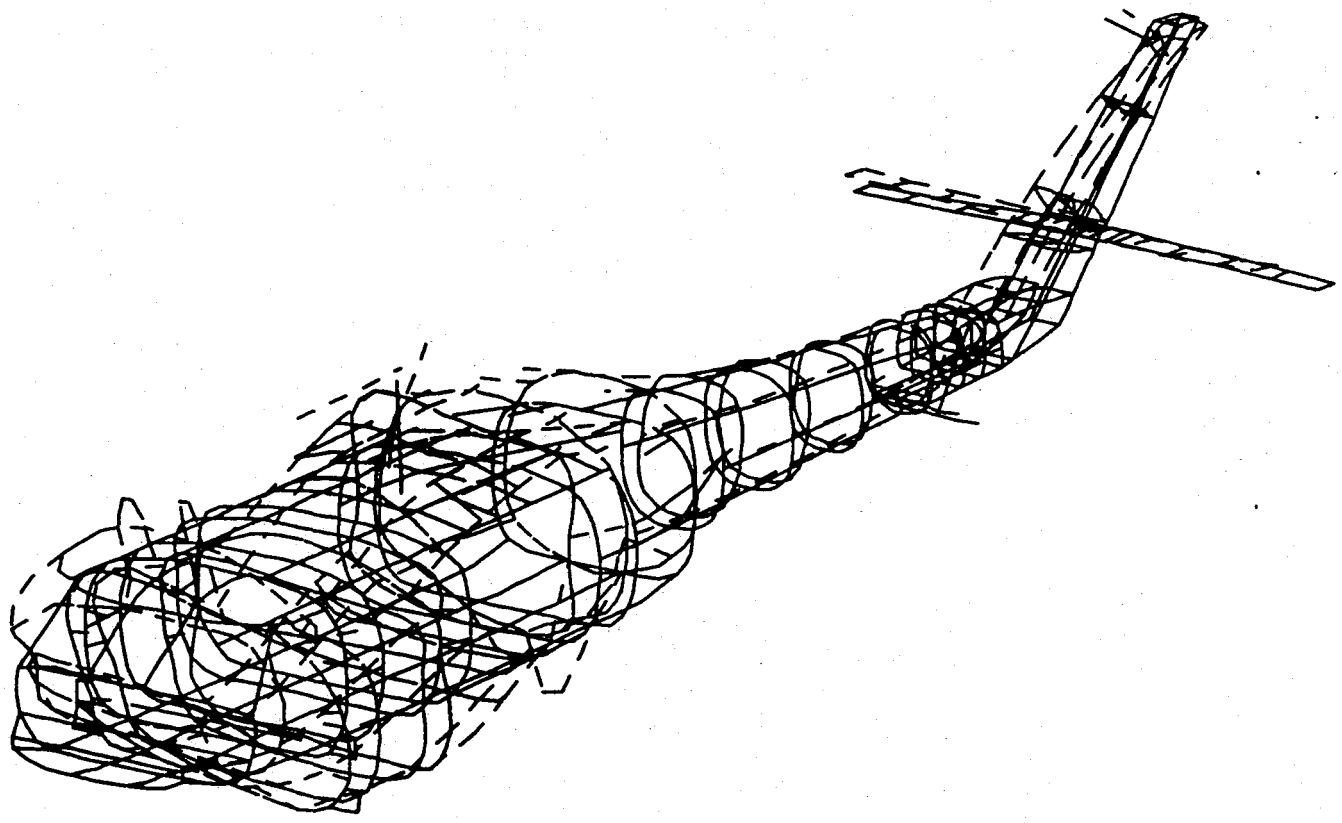

Figure 50.
Mode Shape 12 - 3rd Vertical Bending
Mode Frequency: 19.55370 Hz
"Best" Model for MTRAP Flight/Shake Test Configuration

TABLES

Table I

Comparison of NASTRAN Configurations* with Shake Test Results

NASA/AEFA Weight Configuration (4 to 14 Hz, 2.0% critical damping ratio)

		NASTRAN Model:		*Shake Test:*	
Mode #	Mode Description	Primary	Primary & Secondary	Imperial College Software Est.	Modal 3 SE Software Est.
1	1st Lateral Bending w/ Torsion	4.810	4.839	5.4	5.4
2	1st Vertical Bending	5.650	6.055	6.3	6.3
3	Stabilator Roll	9.067	9.129	9.9	10.0
4	Transmission Pitch	11.035	11.049	11.6	11.6
5	Transmission Pitch/2nd Vertical Bending	10.181	12.045	13.0	12.9
6	Transmission Roll/Stabilator Yaw	12.969	13.115	13.6	13.5
7	Stabilator Roll/Transmission Roll	11.442	13.297	*	13.9

*Mode not detected by Imperial College Software

Table II

List of MTRAP Flight Components
UH-60A MTRAP Flight Configuration

Internal Structural Components

Trimmable Ballast System
Flight Engineer Instrumentation Rack (Fwd RHS)
C.G. Rack
Instrumentation Panel (Aft RHS)
Pallet Rack (Aft LHS)
Static Frequency Converter Baseplate
Adapter Plate & Assembly
Over Fuel Cell Ballast Assembly (RHS & LHS)

External Structural Components

Instrumented Test Boom
Instrumented LASSIE Bar

Mass Items

RDAS II Instrumentation System
Laser Cube Mounts (2; RHS & LHS)
Tape Recorder I
Tape Recorder II
Formatter
HALPS Multiplexer
Static Frequency Converter
Observer Station Seat
Trimmable Ballast
Pilot
CoPilot
Flight Engineer/Observer

Table III

Secondary Structure, MTRAP Flight Components, & Modeling Revisions
NASTRAN Finite Element Model

MTRAP Flight Test Configuration

FEM I.

Primary/Secondary Structure
(Includes primary baseline model and following)

Secondary Components (Previous September 1990 study by authors)

Added Firewall
Added Transmission Bridge
Simulated Windshield
Gunner's Window Approximation
Simulated Cockpit Doors
Cabin Doors Approximation
Revised Shell Properties for Transmission
Revised Stabilator Springs

FEM II.

Primary/Secondary Structure
with MTRAP Flight Components
(Includes FEM I and following)

Build-Up of Flight Components (Current Study by authors)

Addition of MTRAP Structural Flight Components
Imposition of MTRAP mass distribution

FEM III.

Updated & Revised Primary/Secondary Structure
with MTRAP Flight Components
(Includes new, updated baseline model, FEM II flight components, and following)

Sikorsky Aircraft Upgrades (November 1992 updates for Current Study)
for *'Best' Model*

Revision of Main Rotor Transmission Housing shell stiffness
Revision of Aft Main Rotor Pylon Fairings
Addition of rigid bearins and output shaft to Main Rotor Transmission
Revision of Tailcone stiffness
Inclusion of tail rotor power and drive train systems components
Modification to Tail Rotor Pylon including cambered fairings
Modifications to Stabilator inertia and mass model
Re-evaluation of model material properties and element tapers
Inclusion of Tail Rotor Shaft service cover and shaft casing

Table IV

General Arrangement
Longitudinal Center of Gravity Expansion Program

Mass Item	Weight (lbs.)	Station (in)
Trimmable Ballast:		
Baseplate	376.0	333.2
Adjustable Weight Box	2800.0	350.6 to 303.4
Pilot/Copilot Seat	450.0	229.0
Nose 'E' Bay	310.0 to 256.0	177.0
Forward Cabin	750.0 to 650.0	260.0
Middle Cabin	1420.0 to 480.0	281.0
Aft Cabin	1140.0	354.0
Over Fuel Cell	1760.0 to 274.0	421.0

Table V

Weights of Flight Components
MTRAP UH-60A Flight Test Configuration

Item #	Component	Weight (lbs)
1	Trimmable Ballast System	376.00
2	TBS Ballast	3,163.00
3	Flight Engr./Observer	200.00
4	Flight Engr./Observer Seat	63.40
5	Flight Engr. Instrumentation Rack (FWD-RHS)	75.00
6	C.G. Rack w/ 75% Max Load	128.75
7	Instrumentation Panel (AFT-RHS)	175.00
8	Pallet Rack (AFT-LHS) w/ 100% Max Load	90.00
9	Adapter Plate & Assembly	44.10
10	Tape Recorder I	52.50
11	Tape Recorder II	52.50
12	Formatter	145.50
13	HALPS Multiplexer & Enclosure	81.40
14	Over Fuel Cell Ballast Assembly (RHS)	130.00
15	Over Fuel Cell Ballast Assembly (LHS)	130.00
16	Over Fuel Cell Ballast (optional up to 1,500 lbs)	0.00
17	Static Frequency Converter & Baseplate	87.50
18	Instrumented Test Boom	22.00
19	LASSIE Bar	10.00
20	RDAS II Instrumentation System	133.00
21	Pilot	200.00
22	CoPilot	200.00
23	Full Fuel	2,448.00
24	Laser Cube Assembly (RHS)	8.00
25	Laser Cube Assembly (LHS)	8.00
26	Nose Ballast (optional up to 100 lbs)	0.00
27	Baseline UH-60A	10,140.00
	GROSS WEIGHT	**18,163.65**

Table VI

Rigid Body Check/Enforced Displacement Output
'Excerpt from Printed Output'

D I S P L A C E M E N T V E C T O R

POINT ID.	TYPE	T1	T2	T3	R1	R2	R3
2531	G	-9.999993E-01	1.843909E-09	-4.194581E-07	-6.273821E-12	-7.315051E-09	4.242626E-12
2533	G	-9.999993E-01	1.829559E-09	-4.195052E-07	-1.464132E-11	-7.313072E-09	1.867273E-11
2534	G	-9.999993E-01	1.906437E-09	-4.194866E-07	-1.652777E-11	-7.333439E-09	7.027879E-12
2535	G	-9.999994E-01	2.062021E-09	-4.193898E-07	-3.205319E-11	-7.357449E-09	3.655100E-11
2536	G	-9.999994E-01	2.237121E-09	-4.193437E-07	-4.663989E-11	-7.346390E-09	5.606718E-11
2537	G	-9.999995E-01	2.614731E-09	-4.192902E-07	-5.080231E-11	-7.354289E-09	7.562560E-11
2538	G	-9.999995E-01	2.929490E-09	-4.192610E-07	-6.029688E-11	-7.337942E-09	9.639514E-11
2543	G	-9.999997E-01	2.121393E-09	-4.261821E-07	3.762904E-10	-7.404110E-09	-4.457607E-11
2544	G	-9.999998E-01	6.674328E-10	-4.243097E-07	3.985719E-10	-7.402421E-09	2.083921E-11
2545	G	-9.999998E-01	1.494967E-10	-4.220117E-07	3.952850E-10	-7.369316E-09	-4.794650E-11
2546	G	-9.999998E-01	-3.319056E-10	-4.194091E-07	3.506480E-10	-7.338067E-09	2.857024E-11
2547	G	-9.999998E-01	-4.362239E-10	-4.174445E-07	2.598342E-10	-7.199496E-09	2.741126E-11
2548	G	-9.999998E-01	-1.884627E-10	-4.162764E-07	1.565624E-10	-7.469614E-09	-1.285486E-11
2549	G	-9.999998E-01	7.317303E-14	-4.155699E-07	7.474716E-11	-7.659618E-09	7.628036E-12
2580	G	-9.999993E-01	1.894557E-09	-4.195199E-07	0.0	0.0	0.0
2582	G	-9.999993E-01	1.881496E-09	-4.194563E-07	0.0	0.0	0.0
2583	G	-9.999993E-01	1.875301E-09	-4.194713E-07	0.0	0.0	0.0
2584	G	-9.999993E-01	1.856366E-09	-4.194441E-07	0.0	0.0	0.0
2586	G	-9.999993E-01	1.834586E-09	-4.193792E-07	0.0	0.0	0.0
2587	G	-9.999993E-01	1.801581E-09	0.0	0.0	0.0	0.0
2590	G	-9.999993E-01	1.766603E-09	0.0	0.0	0.0	0.0
2591	G	-9.999993E-01	1.733208E-09	-4.189397E-07	0.0	0.0	0.0
2593	G	-9.999993E-01	1.710687E-09	-4.186985E-07	0.0	0.0	0.0
2594	G	-9.999993E-01	1.690717E-09	-4.184030E-07	0.0	0.0	0.0
2596	G	-9.999993E-01	1.683684E-09	-4.180936E-07	0.0	0.0	0.0
2597	G	-9.999993E-01	1.669326E-09	-4.178557E-07	0.0	0.0	0.0
2601	G	-9.999998E-01	1.574726E-10	-4.153305E-07	-9.875194E-12	-7.648250E-09	1.211921E-10
2602	G	-9.999998E-01	-7.671498E-12	-4.156502E-07	-9.505627E-11	-7.369642E-09	2.740051E-10
2603	G	-9.999998E-01	-2.133126E-10	-4.165990E-07	-2.090327E-10	-7.071729E-09	1.579859E-10
2604	G	-9.999998E-01	-6.194700E-10	-4.180181E-07	-3.133643E-10	-7.103414E-09	-2.142892E-10
2605	G	-9.999998E-01	-1.193469E-09	-4.203450E-07	-3.534826E-10	-7.393227E-09	-1.300910E-11
2606	G	-9.999997E-01	-1.584604E-09	-4.223729E-07	-3.347312E-10	-7.420058E-09	2.619176E-11

Constraints to be checked

Unit Displacements

Negligible translation/rotations (zero)

Table VII

Cumulative Build-Up of Flight Component Structure
MTRAP Flight Test Configuration

Mode Shape Descriptions & Resonant Frequencies
(Structural Modeling of Added Components Only)

Mode #	Mode Description	Baseline Primary & Secondary Structure	+ Trimmable Ballast System	+ Instr. Test Boom	+ LASSIE Bar	+ Flight Engineer's Instr. Rack	+ Adapter Plate Assembly	+ Instrument. Panel	+ C.G. Rack	+ Pallet Rack	+ Over Fuel Cell Ballast (RHS & LHS)	+ Frequency Converter Baseplate
1	1st Vertical Bending	6.063642	6.083213	6.083291	6.083208	6.085915	6.088786	6.092916	6.092890	6.092899	6.096100	6.096318
2	1st Lateral Bending	4.957316	8.929302	8.929351	8.929282	8.931107	8.942788	8.957086	8.957186	8.957090	9.251421	9.251403
3	Stabilator Roll	9.952858	11.15489	11.15446	11.15450	11.115740	11.17630	11.23205	11.23209	11.23105	11.44719	11.44917
4	Transmission Pitch	11.25954	11.53868	11.53911	11.53782	11.538740	11.54761	11.58259	11.58354	11.58275	11.96312	11.96494
5	Transmission Pitch/2nd Vertical Bending	13.16711	13.25069	13.25170	13.25115	13.29784	13.32301	13.34647	13.34691	13.34419	13.35407	13.35577
6	Transmission Roll/Stabilator Yaw	13.75548	13.85037	13.84907	13.84883	13.84892	13.86065	13.86032	13.86055	13.85986	13.88641	13.88671
7	Stabilator Roll/ Transmission Roll	13.99202	14.03104	14.02572	14.01900	14.01423	14.01915	14.14552	14.15911	14.14171	14.42176	14.45312
8	Transmission Roll/ Stabilator Roll	14.50045	14.84086	14.84154	14.84000	14.84667	14.85963	14.88819	14.89047	14.88775	14.93454	14.93354
9	2nd Vertical Bending/ Transmission Vertical	14.94998	15.25165	15.25601	15.25590	15.25475	15.34401	15.51870	15.52309	15.50691	15.54255	15.55206
10	2nd Vertical Bending/ Transmission Pitch	15.86694	15.97392	15.97575	15.97414	15.98181	16.02788	16.05552	16.05520	16.05270	16.08725	16.09477
11	Cockpit/ Cabin Roll	17.29366	19.12816	19.12657	19.12920	19.15076	19.17729	19.220683	19.20180	19.19718	19.43398	19.45244
12	3rd Vertical Bending/ Cockpit/Cabin Torsion	19.72595	20.16723	20.17759	20.12891	20.27515	20.24624	20.26369	20.25642	20.25274	20.45789	20.45733
13	3rd Vertical Bending	20.19662	20.30918	20.30693	20.30674	20.35894	20.36956	20.42193	20.41819	20.41778	20.92211	20.85241
14	Cockpit/ Cabin Roll/ 3rd Vertical Bending	21.78833	21.95951	21.98097	21.96131	21.97723	21.98427	22.01493	22.02393	22.03545	22.07778	22.08623
15	Transmission Pitch/ Cockpit/ Cabin Roll /3rd Vertical Bending	22.02608	22.79570	22.80187	22.80755	22.80089	22.80423	22.80737	22.80760	22.80728	22.81785	22.81499
16	Cockpit Vertical/ Stabilator Bending	22.74864	23.05958	23.06347	23.06003	23.07939	23.08149	23.08375	23.08447	23.08358	23.09179	23.08910
17	Cockpit Vertical I	23.00541	23.26716	23.31112	23.28654	23.29355	23.31995	23.32309	23.32817	23.32656	23.35227	23.36225
18	4th Vertical Bending	23.08513	23.72699	23.73140	23.76539	23.73146	23.75327	23.75444	23.75418	23.75789	23.79686	23.79668
19	Transmission Pitch/ 4th Vertical Bending	23.70768	24.05830	24.02432	23.97186	24.07777	24.01445	24.13367	24.14339	24.08575	24.21400	24.24128
20	Cabin Torsion	23.96991	24.12998	24.16432	24.11234	24.32640	24.16846	24.22813	24.20359	24.17909	24.74720	24.62076
21	Transmission Pitch/ Cabin Torsion	24.51000	25.57570	25.52606	25.52020	25.55589	25.72226	25.78482	25.77613	25.77284	25.85728	25.84827
22	Stabilator Vertical Bending/ Transmission Pitch	25.92649	25.96182	25.98936	25.96106	25.99169	25.95750	25.96513	25.97474	25.98294	26.15745	26.11708
23	Stabilator Vertical Bending	26.72463	26.74528	26.72134	26.71498	26.70498	26.73145	26.69935	26.72055	26.74810	26.73210	26.79098
24	Forward Cabin Bending	28.15631	28.23271	28.29127	28.25981	28.27703	28.27702	28.24989	28.30713	28.29865	28.30224	28.44996
25	Transmission Yaw/ 2nd Lateral Bending	28.75642	29.11828	29.14348	29.14004	29.38151	29.05932	29.27343	29.20204	29.21391	29.40591	29.38551
26	Forward Cabin Torsion	29.87710	29.95713	29.97084	30.02891	29.96915	29.93467	29.99742	30.02092	29.98920	30.07135	30.03727
27	5th Vertical Bending	30.19905	30.63908	30.39568	30.83676	31.14047	30.65480	30.73852	30.72368	30.69698	30.94743	30.84510

Table VIII

Cumulative Build-Up of Flight Component Structure
MTRAP Flight Test Configuration

Percent Change of Mode Frequency with Component Structural Build-Up
(Structural Modeling of Added Components Only)

Mode #	Mode Description	+ Trimmable Ballast System	+ Instr. Test Boom	+ LASSIE Bar	+ Flight Engineer's Instr. Rack	+ Adapter Plate Assembly	+ Instrument. Panel	+ C.G. Rack	+ Pallet Rack	+ Over Fuel Cell Ballast (RHS & LHS)	+ Frequency Converter Baseplate
1	1st Vertical Bending	0.32275982	0.00128222	-0.0013644	0.04449955	0.0471745	0.06782961	-0.0004267	0.00014771	0.05253657	0.00357606
2	1st Lateral Bending	80.1237202	0.00054876	-0.0007727	0.02043837	0.13079006	0.15988303	0.00111643	-0.0010718	3.28601142	-0.0001946
3	Stabilator Roll	12.0772546	-0.0038548	0.0003586	-0.3474831	0.54481303	0.4988234	0.00035612	-0.0092592	1.92448613	0.01729682
4	Transmission Pitch	2.47914213	0.0037266	-0.0111794	0.00797378	0.07687148	0.30291982	0.00820197	-0.00682	3.28393516	0.01521342
5	Transmission Pitch/2nd Vertical Bending	0.63476344	0.00762224	-0.0041504	0.35234678	0.18927886	0.17608633	0.00329675	-0.0203792	0.07403971	0.0127302
6	Transmission Roll/Stabilator Yaw	0.68983416	-0.009386	-0.001733	0.00064987	0.08469975	-0.0023808	0.00165941	-0.0049782	0.19156038	0.00216039
7	Stabilator Roll/ Transmission Roll	0.27887324	-0.0379159	-0.047912	-0.0340253	0.03510717	0.90140986	0.09607282	-0.1228891	1.98031214	0.21744919
8	Transmission Roll/ Stabilator Roll	2.34758232	0.00458194	-0.0103763	0.04494609	0.0872923	0.19219859	0.01531415	-0.0182667	0.31428523	-0.0066959
9	2nd Vertical Bending/ Transmission Vertical	2.01786223	0.02858707	-0.000721	-0.0075381	0.58512922	1.13848987	0.02828845	-0.1042318	0.22983302	0.06118687
10	2nd Vertical Bending/ Transmission Pitch	0.67423208	0.01145617	-0.0100778	0.0480151	0.28826522	0.17244951	-0.0019931	-0.0155713	0.21522859	0.04674509
11	Cockpit/ Cabin Roll	10.6079338	-0.0083124	0.01375051	0.11270727	0.13853236	0.22627285	-0.0982431	-0.0240602	1.23351451	0.09498826
12	3rd Vertical Bending/ Cockpit/Cabin Torsion	2.23705322	0.05137047	-0.2412578	0.72651723	-0.1425883	0.08618884	-0.035877	-0.0181671	1.01294936	-0.0027373
13	3rd Vertical Bending	0.55732098	-0.0110787	-0.0009356	0.25705751	0.05216382	0.25709932	-0.0183136	-0.002008	2.47005306	-0.3331404
14	Cockpit/ Cabin Roll/ 3rd Vertical Bending	0.78564993	0.09772531	-0.089441	0.07249112	0.03203315	0.13946335	0.04088135	0.05230674	0.19209955	0.03827378
15	Transmission Pitch/ Cockpit/ Cabin Roll /3rd Vertical Bending	3.49413059	0.02706651	0.02491024	-0.0292009	0.01464855	0.01376938	0.00100845	-0.001403	0.04634485	-0.012534
16	Cockpit Vertical/ Stabilator Bending	1.36685094	0.01686934	-0.0149154	0.08395479	0.00909903	0.0097914	0.00311908	-0.0038554	0.03556641	-0.0116492
17	Cockpit Vertical I	1.13777585	0.18893582	-0.1054432	0.03010323	0.1133361	0.01346487	0.02178099	-0.0069015	0.11021771	0.04273674
18	4th Vertical Bending	2.78040453	0.01858643	0.14322796	-0.1427706	0.09190332	0.00492564	-0.0010945	0.0156183	0.16402972	-0.0007564
19	Transmission Pitch/ 4th Vertical Bending	1.47893003	-0.1412402	-0.2183621	0.44180969	-0.2629812	0.4964511	0.04027568	-0.2387403	0.53247252	0.1126621
20	Cabin Torsion	0.66779558	0.14231259	-0.2151105	0.8877612	-0.6492535	0.24689202	-0.1012872	-0.1012247	2.34959215	-0.5109265
21	Transmission Pitch/ Cabin Torsion	4.34802122	-0.1940905	-0.0229569	0.13985	0.65100452	0.24321347	-0.033702	-0.0127637	0.32763172	-0.0348451
22	Stabilator Vertical Bending/ Transmission Pitch	0.13626989	0.10607885	-0.1088907	0.1179844	-0.131542	0.0293942	0.03701118	0.03156913	0.671633	-0.1543346
23	Stabilator Vertical Bending	0.07726954	-0.0895111	-0.0238012	-0.0374322	0.09912009	-0.1200833	0.07940268	0.10310417	-0.0598173	0.22025954
24	Forward Cabin Bending	0.27134237	0.20741898	-0.1112004	0.06093459	-3.536E-05	-0.0959436	0.20262026	-0.0299571	0.01268612	0.52193749
25	Transmission Yaw/ 2nd Lateral Bending	1.25836248	0.08654357	-0.0118037	0.82865363	-1.096574	0.7368032	-0.243873	0.04064785	0.65722117	-0.0693738
26	Forward Cabin Torsion	0.26786402	0.0457654	0.193755	-0.1990082	-0.1150516	0.20962316	0.07834007	-0.1056597	0.27393195	-0.1133305
27	5th Vertical Bending	1.45709882	-0.7944103	1.45112727	0.98489595	-1.5596104	0.27310568	-0.0482782	-0.0869037	0.8158783	-0.3306575

Table IX

Percent Change between
Initial Starting Reference Config. & Built-Up Structure Config.
(Structural Modeling of Added Components Only)

Cumulative Build-Up of Flight Component Structure
MTRAP Flight Test Configuration

Mode #	Mode Description	Percent Change (%)
1	1st Vertical Bending	0.53888406
2	1st Lateral Bending	86.6212079
3	Stabilator Roll	15.0339933
4	Transmission Pitch	6.26490958
5	Transmission Pitch/2nd Vertical Bending	1.43281252
6	Transmission Roll/Stabilator Yaw	0.95401978
7	Stabilator Roll/ Transmission Roll	3.29544983
8	Transmission Roll/ Stabilator Roll	2.98673489
9	2nd Vertical Bending/ Transmission Vertical	4.02729636
10	2nd Vertical Bending/ Transmission Pitch	1.43587863
11	Cockpit/ Cabin Roll	12.4830718
12	3rd Vertical Bending/ Cockpit/Cabin Torsion	3.70770483
13	3rd Vertical Bending	3.24702846
14	Cockpit/ Cabin Roll/ 3rd Vertical Bending	1.36724568
15	Transmission Pitch/ Cockpit/ Cabin Roll /3rd Vertical Bending	3.58170859
16	Cockpit Vertical/ Stabilator Bending	1.49661694
17	Cockpit Vertical I	1.55111341
18	4th Vertical Bending	3.08228717
19	Transmission Pitch/ 4th Vertical Bending	2.25074744
20	Cabin Torsion	2.71527928
21	Transmission Pitch/ Cabin Torsion	5.46009792
22	Stabilator Vertical Bending/ Transmission Pitch	0.73511686
23	Stabilator Vertical Bending	0.24827285
24	Forward Cabin Bending	1.04292786
25	Transmission Yaw/ 2nd Lateral Bending	2.18765062
26	Forward Cabin Torsion	0.53609621
27	5th Vertical Bending	2.13930571

Table X

Cumulative Build-Up of Flight Component Mass
MTRAP Flight Test Configuration

Mode Shape Descriptions & Resonant Frequencies
(Weight & Structural Modeling of Added Components Only)

Mode #	Mode Description	Baseline Primary & Secondary Structure	+ Trimmable Ballast System	+ Instr. Test Boom	+ LASSIE Bar	+ Flight Engineer's Instr. Rack	+ Adapter Plate Assembly	+ Instrument. Panel	+ C.G. Rack	+ Pallet Rack	+ Over Fuel Cell Ballast (RHS & LHS)	+ Frequency Converter Baseplate
1	1st Vertical Bending	6.246643	6.246623	6.245571	6.245255	6.238937	6.238224	6.219175	6.219125	6.218782	6.198107	6.197905
2	1st Lateral Bending	9.354307	9.335275	9.334810	9.334056	9.327103	9.316888	9.313120	9.312887	9.312550	9.308288	9.301524
3	Stabilator Roll	11.88205	11.86936	11.86819	11.86407	11.83388	11.83115	11.76473	11.76506	11.76332	11.71597	11.70916
4	Transmission Pitch	12.17036	12.16272	12.16117	12.16059	12.14800	12.14217	12.12898	12.12739	12.12415	12.08569	12.08235
5	Transmission Pitch/2nd Vertical Bending	13.73909	12.96144	12.96143	12.96142	12.96130	12.96122	12.96117	12.96117	12.96114	12.96113	12.96110
6	Transmission Roll/Stabilator Yaw	13.92369	13.73263	13.72423	13.71954	13.70258	13.70251	13.70219	13.70054	13.69503	13.69331	13.69279
7	Stabilator Roll/ Transmission Roll	14.62605	13.92277	13.92051	13.92044	13.91465	13.91410	13.91030	13.91031	13.90947	13.90568	13.90542
8	Transmission Roll/ Stabilator Roll	15.14626	14.59607	14.59538	14.59431	14.59001	14.57543	14.53364	14.53343	14.52988	14.50115	14.49368
9	2nd Vertical Bending/ Transmission Vertical	16.97168	15.11952	15.11759	15.11615	15.09579	15.06909	15.06695	15.06571	15.06211	15.05409	15.05149
10	2nd Vertical Bending/ Transmission Pitch	19.67059	16.92284	16.91955	16.91916	16.92048	16.89827	16.85119	16.84882	16.84402	16.79185	16.78646
11	Cockpit/ Cabin Roll	21.23818	19.63903	19.63302	19.63241	19.59339	19.57571	19.53616	18.77962	18.77961	18.77960	18.77960
12	3rd Vertical Bending/ Cockpit/Cabin Torsion	21.40187	21.19007	21.17964	21.17730	21.12260	21.10033	21.07893	19.53809	19.53589	19.52714	19.50604
13	3rd Vertical Bending	22.02311	21.35126	21.35127	21.34641	21.27716	21.28236	21.18541	21.08221	21.06646	21.04823	21.04258
14	Cockpit/ Cabin Roll/ 3rd Vertical Bending	22.78160	22.00114	22.00082	22.00049	21.99015	21.98784	21.94175	21.19232	21.16392	21.13952	21.13731
15	Transmission Pitch/ Cockpit/ Cabin Roll /3rd Vertical Bending	22.96628	22.71936	22.71887	22.71706	22.69971	22.64972	22.63755	22.63453	21.93170	21.90035	21.89919
16	Cockpit Vertical/ Stabilator Bending	23.18161	22.92847	22.92768	22.92662	22.91617	22.89745	22.89229	22.89158	22.61974	22.60098	22.58687
17	Cockpit Vertical I	23.90517	23.17268	23.17066	23.16959	23.14267	23.14043	23.13880	23.13865	22.88796	22.88709	22.88349
18	4th Vertical Bending	25.54500	23.89669	23.89554	23.89492	23.88237	23.87882	23.87826	23.87761	23.13793	23.13654	23.13499
19	Transmission Pitch/ 4th Vertical Bending	25.94189	25.44457	25.44830	25.44587	25.40278	25.39355	25.19502	25.20072	23.87685	23.87124	23.86974
20	Cabin Torsion	26.13401	25.77518	25.76754	25.76687	25.67011	25.55514	25.53503	25.53287	25.13714	25.08164	25.07740
21	Transmission Pitch/ Cabin Torsion	27.18773	26.09234	26.09011	26.08770	26.06270	26.05084	26.00384	26.00574	25.50640	25.47453	25.44505
22	Stabilator Vertical Bending/ Transmission Pitch	28.46764	26.96616	26.96240	26.96230	26.60003	26.59426	26.59091	26.59430	25.99350	25.98503	25.984202
23	Stabilator Vertical Bending	29.78457	28.34462	28.34626	28.34245	26.85953	26.85080	26.86249	26.88146	26.57631	26.57412	26.57236
24	Forward Cabin Bending	30.06804	29.71166	29.71196	29.72297	27.22742	27.13887	27.12727	27.12236	26.81532	26.81120	26.80883
25	Transmission Yaw/ 2nd Lateral Bending	31.78256	30.04677	30.04453	30.04398	27.64794	27.64414	27.61421	27.62419	27.09985	27.07920	27.06275
26	Forward Cabin Torsion	32.15953	31.59760	31.59850	31.58075	28.34583	28.33909	28.30021	28.30124	27.59395	27.58302	27.58327
27	5th Vertical Bending	33.00950	32.02251	32.03967	32.01647	29.72712	29.69850	29.65341	29.65815	28.27207	28.24238	28.24199

Table XI

Cumulative Build-Up of Flight Component Mass
MTRAP Flight Test Configuration

Percent Change of Mode Frequency with Component Mass Build-Up
(Weight & Structural Modeling of Added Components Only)

Mode #	Mode Description	+ Trimmable Ballast System	+ Instr. Test Boom	+ LASSIE Bar	+ Flight Engineer's Instr. Rack	+ Adapter Plate Assembly	+ Instrument. Panel	+ C.G. Rack	+ Pallet Rack	+ Over Fuel Cell Ballast (RHS & LHS)	+ Frequency Converter Baseplate
1	1st Vertical Bending	-0.0003202	-0.0168411	-0.0050596	-0.1011648	-0.0114282	-0.3053593	-0.000804	-0.0055152	-0.3324606	-0.0032591
2	1st Lateral Bending	-0.2034571	-0.0049811	-0.0080773	-0.0744907	-0.1095195	-0.0404427	-0.0025018	-0.0036186	-0.0457662	-0.0726664
3	Stabilator Roll	-0.1067998	-0.0098573	-0.0347146	-0.2544658	-0.0230694	-0.5613994	0.00280499	-0.0147896	-0.4025224	-0.0581258
4	Transmission Pitch	-0.0627755	-0.0127439	-0.0047693	-0.1035312	-0.0479914	-0.1086297	-0.0131091	-0.0267164	-0.3172181	-0.027636
5	Transmission Pitch/2nd Vertical Bending	-5.6601274	-7.715E-05	-7.715E-05	-0.0009258	-0.0006172	-0.0003858	0	-0.0002315	-7.715E-05	-0.0002315
6	Transmission Roll/Stabilator Yaw	-1.3721937	-0.0611682	-0.0341731	-0.1236193	-0.0005109	-0.0023353	-0.00012042	-0.0004022	-0.0125593	-0.0037975
7	Stabilator Roll/ Transmission Roll	-4.8084069	-0.0162324	-0.0005029	-0.0415935	-0.0039527	-0.0273104	-7.18892E-7	-6.0387E-5	-0.0272476	-0.0018697
8	Transmission Roll/ Stabilator Roll	-3.6325139	-0.0047273	-0.0073311	-0.0294635	-0.0999314	-0.2867154	-0.0014449	-0.0244264	-0.1977305	-0.0515132
9	2nd Vertical Bending/ Transmission Vertical	-10.913239	-0.012765	-0.0095253	-0.00134690	-0.0017687	-0.0142013	-0.0082299	-0.0238953	-0.0532462	-0.0172711
10	2nd Vertical Bending/ Transmission Pitch	-13.968824	-0.0194412	-0.002305	0.00780181	-0.1312611	-0.2786084	-0.0140643	-0.0284886	-0.3097242	-0.0320989
11	Cockpit/ Cabin Roll	-7.5296	-0.0306023	-0.003107	-0.198753	-0.0902345	-0.2020361	-3.8725113	-5.325E-05	-5.325E-05	0
12	3rd Vertical Bending/ Cockpit/Cabin Torsion	-0.9896331	-0.0492212	-0.0110483	-0.2582954	-0.1054321	-0.1014202	-7.3098587	-0.0112601	-0.0447894	-0.1080547
13	3rd Vertical Bending	-3.0506591	4.6836E-05	-0.0227621	-0.3244105	0.02443935	-0.4555416	-0.4871277	-0.0747075	-0.0865357	-0.0268431
14	Cockpit/ Cabin Roll/ 3rd Vertical Bending	-3.4258349	-0.0014545	-0.0014999	-0.046999	-0.0105047	-0.2096159	-3.4155434	-0.1340108	-0.1152906	-0.0104544
15	Transmission Pitch/ Cockpit/ Cabin Roll /3rd Vertical Bending	-1.0751415	-0.0021568	-0.0079669	-0.0763743	-0.2202231	-0.0537313	-0.0133407	-3.105123	-0.1429438	-0.0052967
16	Cockpit Vertical/ Stabilator Bending	-1.0919863	-0.0034455	-0.0046232	-0.0455802	-0.081689	-0.0225353	-0.0031015	-1.1875109	-0.0829364	-0.0624309
17	Cockpit Vertical I	-3.0641489	-0.0087172	-0.0046179	-0.1161868	-0.0096791	-0.0070439	-0.0006483	-1.0834254	-0.0038011	-0.0157294
18	4th Vertical Bending	-6.4525739	-0.0048124	-0.0025946	-0.0525216	-0.0148645	-0.0023452	-0.0027221	-3.0977975	-0.0060075	-0.0066994
19	Transmission Pitch/ 4th Vertical Bending	-1.9170538	0.01465932	-0.0095488	-0.1693399	-0.0363346	-0.7818127	0.02262352	-5.2533023	-0.0234956	-0.0062837
20	Cabin Torsion	-1.3730384	-0.0296409	-0.0026002	-0.375521	-0.447875	-0.0786926	-0.008459	-1.5498845	-0.2207888	-0.0169048
21	Transmission Pitch/ Cabin Torsion	-4.0289866	-0.0085466	-0.0092372	-0.0958306	-0.0455056	-0.1804164	0.00730661	-1.9201146	-0.124949	-0.1157234
22	Stabilator Vertical Bending/ Transmission Pitch	-5.2743396	-0.0139434	-0.0003709	-1.3436168	-0.0216917	-0.0125967	0.01274872	-2.2591307	-0.0325851	-0.0031865
23	Stabilator Vertical Bending	-4.8345502	0.00578593	-0.0134409	-5.2321518	-0.0325024	0.04353688	0.07061892	-1.135169	-0.0082404	-0.006623
24	Forward Cabin Bending	-1.1852452	0.0010097	0.03705578	-8.3960318	-0.3252236	-0.0427431	-0.0180999	-1.1320549	-0.0153644	-0.0088396
25	Transmission Yaw/ 2nd Lateral Bending	-5.4614543	-0.007455	-0.0018306	-7.9751085	-0.0137442	-0.1082689	0.03614081	-1.898119	-0.0761997	-0.0607477
26	Forward Cabin Torsion	-1.7473203	0.00284832	-0.0561736	-10.243329	-0.0237777	-0.1371957	0.00363955	-2.4991484	-0.0396101	0.00090635
27	5th Vertical Bending	-2.990018	0.0535873	-0.0724102	-7.1505385	-0.0962757	-0.1518258	0.01598467	-4.6735214	-0.1050153	-0.0013809

Table XII

Percent Change between
Initial Starting Reference Config. & Built-Up Mass/Structure Config.
(Weight & Structural Modeling of Added Components Only)

Cumulative Build-Up of Flight Component Mass
MTRAP Flight Test Configuration

Mode #	Mode Description	Percent Change (%)
1	1st Vertical Bending	-0.7802271
2	1st Lateral Bending	-0.5642641
3	Stabilator Roll	-1.4550519
4	Transmission Pitch	-0.7231503
5	Transmission Pitch/2nd Vertical Bending	-5.6626021
6	Transmission Roll/Stabilator Yaw	-1.6583248
7	Stabilator Roll/ Transmission Roll	-4.9270309
8	Transmission Roll/ Stabilator Roll	-4.3085224
9	2nd Vertical Bending/ Transmission Vertical	-11.314083
10	2nd Vertical Bending/ Transmission Pitch	-14.662143
11	Cockpit/ Cabin Roll	-11.576227
12	3rd Vertical Bending/ Cockpit/Cabin Torsion	-8.8582446
13	3rd Vertical Bending	-4.4522776
14	Cockpit/ Cabin Roll/ 3rd Vertical Bending	-7.217623
15	Transmission Pitch/ Cockpit/ Cabin Roll /3rd Vertical Bending	-4.6463337
16	Cockpit Vertical/ Stabilator Bending	-2.5655681
17	Cockpit Vertical I	-4.2738872
18	4th Vertical Bending	-9.4343707
19	Transmission Pitch/ 4th Vertical Bending	-7.9876601
20	Cabin Torsion	-4.0430458
21	Transmission Pitch/ Cabin Torsion	-6.4098032
22	Stabilator Vertical Bending/ Transmission Pitch	-8.7237228
23	Stabilator Vertical Bending	-10.784812
24	Forward Cabin Bending	-10.839449
25	Transmission Yaw/ 2nd Lateral Bending	-14.850314
26	Forward Cabin Torsion	-14.229872
27	5th Vertical Bending	-14.442842

Table XIII

Element Type and Numbers of Elements
UH-60A Finite Element Model
(Primary & Secondary System: September 1990)

Element Type	# of Elements
CONROD	41
ELAS2	4
QUAD4	3,309
BAR	5,510
TRIA3	878
Total	**9,742**

Table XIV

Element Types and Number of Elements
UH-60A Finite Element Model (FEM I)
(Primary & Secondary Structure w/ Revisions: November 1992)

Element Type	# of Elements
ROD	14
CONROD	16
ELAS1	4
ELAS2	28
QUAD4	4,565
BAR	6,060
TRIA3	1,413
Total	**12,100**

This Page Intentionally Left Blank

Table XV

Element Types and Number of Elements
UH-60A Finite Element Model (FEM III)
(November 1992 Revised Model w/ MTRAP Flight Components)

Element Type	# of Elements
ROD	14
TUBE	53
CONROD	16
ELAS1	4
ELAS2	28
QUAD4	5,036
BAR	6,340
TRIA3	1,546
Total	**13,037**

Table XVI

Comparison of
Primary/Secondary Model (FEM I) with
Updated 'Best' Model (FEM III)

MTRAP Flight Configuration with Structural Flight Components and Mass Distribution

Mode #	Mode Description	Sep 90 Model wo/ Bungee (FEM I)	Sep 90 Model w/ Bungee (FEM I)	Percent Change (%)	Mode Description	Nov 92 Model wo/ Bungee (FEM III) "Best Model"	Nov 92 Model w/ Bungee (FEM III)	Percent Change (%)
1	1st Vertical Bending	6.107423	6.115006	0.12416039	1st Vertical Bending	6.322543	6.423392	1.59507021
2	1st Lateral Bending	9.349967	9.261598	-0.9451263	1st Lateral Bending	9.121788	9.119493	-0.0251595
3	Stabilator Roll	11.83551	11.37127	-3.9224334	Stabilator Roll	11.26758	11.45816	1.69140135
4	Transmission Pitch	12.25636	11.93673	-2.6078705	2nd Vertical Bending/Transmission Pitch	11.65715	11.66592	0.0752328
5	Transmission Pitch/2nd Vertical Bending	12.96258	12.95199	-0.0816967	Transmission Pitch /Stabilator Roll & Yaw	12.44405	12.45392	0.07931501
6	Transmission Roll/Stabilator Yaw	13.84717	13.07539	-5.5735576	Transmission Roll / Stabilator Yaw	12.77752	12.79469	0.13437662
7	Stabilator Roll/ Transmission Roll	13.97325	13.48782	-3.473995	Stabilator Roll / Transmission Roll	12.93762	12.93772	0.00077294
8	Transmission Roll/ Stabilator Roll	14.85491	13.90121	-6.4200995	Tailcone Lateral Bending/Transmission Roll/ Stabilator Roll & Yaw	13.25998	13.34020	0.60497829
9	2nd Vertical Bending/ Transmission Vertical	15.59394	14.98757	-3.8884977	2nd Vertical Bending/Transmission Vertical	14.53610	14.61375	0.5341873
10	2nd Vertical Bending/ Transmission Pitch	16.86673	15.34212	-9.0391558	Cockpit/Cabin Roll	14.65144	14.86315	1.44497742
11	Cockpit/ Cabin Roll	18.77963	18.77969	0.0003195	Cockpit/Cabin Torsion/3rd Vertical Bending	18.77941	18.77970	0.00154424
12	3rd Vertical Bending/ Cockpit/Cabin Torsion	19.75672	19.71037	-0.2346037	3rd Vertical Bending	19.55370	19.55770	0.02045649
13	3rd Vertical Bending	21.29389	21.17303	-0.5675807	Cockpit/ Cabin Roll/ 3rd Vertical Bending	20.93454	20.98990	0.26444336
14	Cockpit/ Cabin Roll/ 3rd Vertical Bending	21.54173	21.40453	-0.6369033	Transmission Pitch/ Cockpit/ Cabin Roll /3rd Vertical Bending	21.27896	21.48919	0.98797122
15	Transmission Pitch/ Cockpit/ Cabin Roll /3rd Vertical Bending	22.06924	21.55087	-2.3488348	Cockpit Vertical/ Stabilator Bending	21.48644	21.51475	0.13175752
16	Cockpit Vertical/ Stabilator Bending	22.80294	22.68626	-0.5116884	Cockpit Vertical I	22.59406	22.61289	0.08334049
17	Cockpit Vertical I	23.07297	22.95415	-0.5149749	4th Vertical Bending	22.99428	23.00655	0.0533611
18	4th Vertical Bending	23.17171	23.12177	-0.2155214	Transmission Pitch/ 4th Vertical Bending	23.06767	23.06877	0.00476858
19	Transmission Pitch/ 4th Vertical Bending	23.74067	23.71210	-0.120342	Cabin Torsion	23.61345	23.61543	0.00838505
20	Cabin Torsion	25.12059	25.03291	-0.3490364	Transmission Pitch/ Cabin Torsion	24.98433	24.99886	0.05815645
21	Transmission Pitch/ Cabin Torsion	25.47950	25.29341	-0.7303519	Stabilator Vertical Bending/ Transmission Pitch	25.31363	25.50732	0.7651609
22	Stabilator Vertical Bending/ Transmission Pitch	26.02042	25.93223	-0.3389261	Stabilator Vertical Bending	25.94569	25.95282	0.02748048
23	Stabilator Vertical Bending	26.58693	26.54038	-0.175086	Forward Cabin Bending	26.51327	26.51683	0.01342724
24	Forward Cabin Bending	26.81156	26.81980	0.03073301	Transmission Yaw/ 2nd Lateral Bending	26.79959	26.80039	0.00298512
25	Transmission Yaw/ 2nd Lateral Bending	27.11179	27.09543	-0.0603428	Forward Cabin Torsion	27.28508	27.30288	0.06523712
26	Forward Cabin Torsion	27.60130	27.58037	-0.0758298	5th Vertical Bending	27.39107	27.52168	0.47683424
27	5th Vertical Bending	28.39352	28.17291	-0.7769731	Cabin Compression/ Vertical Bending	27.62514	27.75306	0.46305648
28	Cabin Compression/ Vertical Bending	30.27037	29.58588	-2.2612542	Cockpit Vertical II	29.76653	29.76777	0.00416575
29	Cockpit Vertical II	30.85125	29.91700	-3.0282403	Cockpit Compression I	30.15243	30.18404	0.10483401

APPENDIX

Description of Optional Flight Components
MTRAP Flight Test Configuration

Tape Recorder Baseplate

In addition to the Formatter baseplate, the flight tape recorder also requires a separate mounting surface. The tape recorder baseplate is a one-piece 0.19 " aluminum sheet covering approximately 16" by 28" in area. The tape recorder plate installation is located on the right side of the ballast rack in front of the formatter baseplate between station lines 340.0 and 367.8 and buttlines 24.0 and 40.0. This assembly was also design and manufactured at NASA Ames.

Formatter Baseplate

Self-contained equipment may be individually installed onto the cabin floor through minor baseplates and mounts. The formatter baseplate in concert with other minor baseplate assemblies will contribute structural stiffness to the cabin floor in the same way that the ballast rack does. The formatter baseplate is a one-piece 0.19" thick aluminum sheet covering approximately an area 21" by 25". The plate installation is situated on the right aft side of the ballast rack between station lines 368.0 and 393.0 and buttlines 15.5 and 36.5. This component was designed and manufactured at NASA-Ames. The formatter equipment package and enclosure weighs 196.9 lbs (143 + 53.9 lbs).

Forward C.G. Plates (Forward Stub Wing Ballast)

Several flight experiments are to be conducted utilizing the aircraft in a forward center of gravity condition. This condition can achieved by the replacement of composite side panel fairings at the two forward stub wing assemblies (above the forward landing struts) with two large steel cover baseplates and multiple ballast plates (9.62" by 20.62" area, 0.75" thickness) including stub wing nose fairings. These assemblies are mounted on the stub wings at both the right and left sides of the cockpit/cabin transition section at station lines 234.3 through 247.05. Four lead ballast sheets, weighing 280 lbs were added to each side respectively to the aircraft to pronounce this forward center of gravity test condition. Lead ballast sheets used in this application are similar in composition and dimension to those used in the movable ballast cart in the trimmable ballast system. Laser cubes, used in tracking telemetry, are mounted on these additional plates. The forward ballast and associated installation hardware was designed and manufactured by Sikorsky Aircraft.

Nose Ballast

Under the Longitudinal Centroid of Gravity Expansion Program, additional mass may be included throughout the length of the rotorcraft fuselage. Up to 100 lbs may placed in the nose section at location (F.S. 174.591, B.L. 0.0, W.L. 215.0). The choice for the use of nose ballast is optional however and may be modified in terms of weight or excluded all together depending upon the flight test purpose. Under the general arrangement in the LCGEP, the Nose 'E' Ballast on respective shelf may weight between 100 lbs to as much as 310 lbs at station line 177.0 .

Subcomponents, Weights, & Comments of Flight Components Worksheet

MTRAP UH-60A Flight Test Configuration

Component	Sub-Component	Weight	Comments
INTERNAL STRUCTURAL COMPONENTS			
Trimmable Ballast System			Note: Total Cargo Ballast 4,550 lbs at C.G. STA 360 at NASA/AEFA
	Ballast Rack	Self Wt.=376 lbs	STA 333.20
	Observer Seat	Self Wt.=63.4 lbs	UH-60A Project Office
	Movable/Adjustable Ballast Box	Self Wt.=238 lbs	
	Guide Angle (2)	Negligible	
	Guide Rail (2)	Negligible	
	Observer Seat Track (2)	Negligible	
	Guide Shaft	Approximate Estimate = 15 lbs	
	Observer	Self Wt.=200 lbs	Customary passenger/flight operator weight assumption
	Lead Sheet Ballast	2900 lbs Max	
	Model J5 Screw Jack Assembly (on box)	Estimate 5 lbs	
	Gear Motor Assembly (on box)	Estimate 5 lbs	
	Upper Gusset	Neligible	
	Lower Gusset	Neligible	
	Support Assembly (optional)	Not included in Current Configuration	
Flight Engineer Instrumentation Rack (FWD RHS-NASA/AEFA)		Self Wt.=75 lbs*	Note: 75 lbs at NASA/AEFA
C.G. Rack		Calculated Estimate (35 lbs Self Wt. + 125 lbs Max Load) = 160 lbs	Note: Maximum Payload of component added to Self Wt.
	TMXM 1	Included in 125 lbs Max Load	Max Load 125 lbs per NASA stress analysis based on C.G. rack self wt = 25 lbs
	TM Signal Conditioner	Included in 125 lbs Max Load	Note: Also called C.G. Instrumentation Rack
	TMT Box	Included in 125 lbs Max Load	75% of Max Load used
	TCG Box	Included in 125 lbs Max Load	
	15V Power Supply	Included in 125 lbs Max Load	
	TCG Converter Box	Included in 125 lbs Max Load	
	Roll Accelerometer	Included in 125 lbs Max Load	
	Accelerometer Mount Synchronizer Box	Included in 125 lbs Max Load	
	Yaw Accelerometer	Included in 125 lbs Max Load	
	Gyroscope	Included in 125 lbs Max Load	

	Vertical Gyroscope	Included in 125 lbs Max Load	
	Axis 3 Rate Gyroscope	Included in 125 lbs Max Load	
Instrumentation Rack (Aft RHS - NASA/AEFA)		Self Wt. + Equipment=175 lbs	Note: Also 175 lbs at NASA/AEFA
Pallet Rack (AFT LHS)		Calculated Self Wt.=66 lbs Self Weight + 24 lbs Max Load = 90 lbs	Note: 100 lbs at NASA/AEFA* Different Rack/Set-Up
	Modified Shim Assembly	Included in 24 lbs Max Load	Note: Max Payload 24 lbs Max Single Tray Load (6 lbs)
	RCAL/TCG Box	Included in 24 lbs Max Load	Max payload of 24 Lbs added to Self Wt. of Pallet Rack
	Syn. Box (on top shelf)	Included in 24 lbs Max Load	Note: Pallet Rack also called 'ADAS Rack'
	Fuel Totalizers (3) (under top shelf)	Included in 24 lbs Max Load	100% of Max Load used since low estimate
	Power Supply (3) (under last shelf)	Included in 24 lbs Max Load	
Frequency Converter Baseplate		Calculated Self Wt = 7.5 lbs	
Tape Recorder 1 Baseplate		Not present in Flight Configuration	
Tape Recorder Baseplate		Not present in Flight Configuration	
Formatter Baseplate		Not present in Flight Configuration	
HALPS Multiplexer Enclosure Baseplate		Not present in Flight Configuration	
Static Frequency Converter		80 lbs	
Adapter Plate & Assembly		Self Wt = 44.1 lbs per NASA stress analysis	Calculated Estimate = 57 lbs Self Wt.
	Tape Recorder 1	50 lbs	Note: Also known as Power Source/Converter Mount
	Tape Recorder 2	50 lbs	
	Formatter	Self Wt.=143 lbs	
	HALPS Multiplexer Enclosure	Self Wt.=78.9 lbs	Note: Formatter & Multiplexer share mount
	Box Support Assembly (3)	Not present in Flight *Configuration	Enclosure estimate previously 53.9 lbs
	Tie Down Assembly (3)	Neligible	Note: Formatter & Multiplexer masses are lumped into single lumped mass.
Over Fuel Cell Ballast Assembly (2)		Self Wt.=260 lbs	STA 421.0
	Lead Ballast Plates (RHS)	750 lbs Max	
	Lead Ballast Plates (LHS)	750 lbs Max	
	Note: Max Gross Wt Appx 1760 lbs Each assembly contains 3 sets of 5 plates		
EXTERNAL STRUCTURAL COMPONENTS			
Instrumented Test Boom		Calculated Estimate = 19 lbs	22 lbs better
LASSIE Bar		Calculated Estimate = 6 lbs	10 lbs better
MASS ITEMS			

RDAS II		Self Wt.=133 lbs by UH-60A Project Office	Note: Dave Jordan estimates RDAS system to weigh 127 lbs 7/13/90 estimate of 90 lbs exists Also 80
Stub Wing Ballast			
	Lead Ballast & Support (RHS)	Not present in Flight Configuration	Note: 4 lead plates each side at C.G. 234.3 STA Max 280 lbs/side
	Lead Ballast & Support (LHS)	Not present in Flight Configuration	
Pilot		200 lbs*	Note: 240 lbs at NASA/AEFA
Co-Pilot		200 lbs*	Note: 220 lbs at NASA/AEFA
Flight Test Engineer		200 lbs*	
Full Fuel		2,448 lbs*	Note: 2,300 lbs at NASA/AEFA
Full Fuel + Tanks		2 tanks/1150 lbs ea.	LCGEP Estimate
Laser Cube Assembly			
	Laser Cubes (2)	Self Wt. = 8 lbs Ea.	Best Estimate
	Cube Mounts (2)	Included in Self Wt.	
Observer Station Seat		63.4 lbs	
Tape Recorder 1		50 lbs	
Tape Recorder 2		50 lbs	
Formatter		Self Wt.=143 lbs	
HALPS Multiplexer Enclosure		Self Wt.=78.9 lbs	
MTRAP Instrumented Main Rotor Blades		Included in Primary Model	Note: 50% Blade Flapping Mass included at Main Rotor Head 200 lbs/blade standard production or instrumented blades
Nose Ballast		0-100 lbs by Crew Chief Estimate.	Under LCGEP, ballast may be increased to 310 lbs
Gunner Windows (RHS & LHS)		Included in Secondary Model	
Cabin Doors (RHS & LHS)		Included in Secondary Model	

Build-Down of Extra Mass to Configuration for Cumulative Build-Up of Mass Study (BUCMS)
MTRAP Flight Test Configuration

Mode #	Mode Description	Full-Up Structural Configuration	-Flt Engr Instr Rack Mass	-Aft RHS Instr Panel	-Cargo Ballast
1	1st Vertical Bending	6.096318	6.102347	6.115000	6.246643
2	1st Lateral Bending	9.251403	9.256736	9.258144	9.354307
3	Stabilator Roll	11.44917	11.45724	11.49365	11.88205
4	Transmission Pitch	11.96494	11.97597	11.98021	12.17036
5	Transmission Pitch/2nd Vertical Bending	13.35577	13.35664	13.35853	13.73909
6	Transmission Roll/Stabilator Yaw	13.88671	13.88823	13.88976	13.92369
7	Stabilator Roll/ Transmission Roll	14.45312	14.44934	14.46006	14.62605
8	Transmission Roll/ Stabilator Roll	14.93354	14.94303	14.95117	15.14626
9	2nd Vertical Bending/ Transmission Vertical	15.55206	15.55546	15.55663	16.97168
10	2nd Vertical Bending/ Transmission Pitch	16.09477	16.09815	16.13959	19.67059
11	Cockpit/ Cabin Roll	19.45244	19.52459	19.54460	21.23818
12	3rd Vertical Bending/ Cockpit/Cabin Torsion	20.45733	20.46639	20.47840	21.40187
13	3rd Vertical Bending	20.85241	20.83837	20.92228	22.02311
14	Cockpit/ Cabin Roll/ 3rd Vertical Bending	22.08623	22.10312	22.11306	22.78160
15	Transmission Pitch/ Cockpit/ Cabin Roll /3rd Vertical Bending	22.81499	22.82952	22.83172	22.96628
16	Cockpit Vertical/ Stabilator Bending	23.08910	23.12728	23.13451	23.18161
17	Cockpit Vertical I	23.36225	23.38271	23.41683	23.90517
18	4th Vertical Bending	23.79668	23.81632	23.82469	25.54500
19	Transmission Pitch/ 4th Vertical Bending	24.24128	24.27744	24.29578	25.94189
20	Cabin Torsion	24.62076	24.65046	24.82432	26.13401
21	Transmission Pitch/ Cabin Torsion	25.84827	25.88219	25.97623	27.18773
22	Stabilator Vertical Bending/ Transmission Pitch	26.11708	26.11735	26.16414	28.46764
23	Stabilator Vertical Bending	26.79098	26.73185	26.81441	29.78457
24	Forward Cabin Bending	28.44996	28.39332	28.40096	30.06804
25	Transmission Yaw/ 2nd Lateral Bending	29.38551	29.39000	29.44183	31.78256
26	Forward Cabin Torsion	30.03727	30.04864	30.05103	32.15953
27	5th Vertical Bending	30.84510	30.86430	31.02151	33.00950

Percent Change of Mode Frequency
With Build-Down of Extra Mass to Configuration for Cumulative Build-Up of Mass Study (BUCMS)

MTRAP Flight Test Configuration

Mode #	Mode Description	-Flt Engr Instr Rack Mass	-Aft RHS Instr Panel	-Cargo Ballast
1	1st Vertical Bending	0.09889576	0.20734645	2.15278823
2	1st Lateral Bending	0.05764531	0.01521055	1.03868551
3	Stabilator Roll	0.07048546	0.31779032	3.37925724
4	Transmission Pitch	0.092186	0.03540423	1.58720089
5	Transmission Pitch/2nd Vertical Bending	0.00651404	0.01415027	2.84881645
6	Transmission Roll/Stabilator Yaw	0.01094572	0.01101652	0.24428068
7	Stabilator Roll/ Transmission Roll	-0.0261535	0.07419024	1.14792055
8	Transmission Roll/ Stabilator Roll	0.06354823	0.05447356	1.30484771
9	2nd Vertical Bending/ Transmission Vertical	0.02186206	0.00752147	9.09612172
10	2nd Vertical Bending/ Transmission Pitch	0.02100061	0.25742088	21.8778792
11	Cockpit/ Cabin Roll	0.37090463	0.10248615	8.66520676
12	3rd Vertical Bending/ Cockpit/Cabin Torsion	0.0442873	0.05868158	4.50948316
13	3rd Vertical Bending	-0.0673303	0.40267065	5.26152025
14	Cockpit/ Cabin Roll/ 3rd Vertical Bending	0.07647299	0.04497103	3.02328126
15	Transmission Pitch/ Cockpit/ Cabin Roll /3rd Vertical Bending	0.0636862	0.00963665	0.58935551
16	Cockpit Vertical/ Stabilator Bending	0.16535941	0.03126178	0.20359195
17	Cockpit Vertical I	0.08757718	0.14591978	2.08542318
18	4th Vertical Bending	0.08253252	0.03514397	7.22070256
19	Transmission Pitch/ 4th Vertical Bending	0.14916704	0.07554339	6.77529184
20	Cabin Torsion	0.12062991	0.70530124	5.27583434
21	Transmission Pitch/ Cabin Torsion	0.13122735	0.36333865	4.66387925
22	Stabilator Vertical Bending/ Transmission Pitch	0.00103381	0.17915294	8.80403484
23	Stabilator Vertical Bending	-0.2207086	0.30884507	11.0767308
24	Forward Cabin Bending	-0.1990864	0.02690774	5.86980158
25	Transmission Yaw/ 2nd Lateral Bending	0.01527964	0.1763525	7.95035499
26	Forward Cabin Torsion	0.03785297	0.00795377	7.01639844
27	5th Vertical Bending	0.06224652	0.50935871	6.40842435

Initial Modal Frequency Spread of UH-60A Finite Element Model FEM III Without MTRAP Flight Components and Weight Distribution

(Gross Weight = 13,220.7 lbs w/ 9,000 lbs at Cargo Hook)

Mode #	Mode Description	Mode Frequency (Hz)
	RB	0.002355508
	RB	0.00231521
	RB	0.0009323696
	RB	0.001399063
	RB	0.001566778
	RB	0.001093756
1	1st Lateral Bending	5.070051
2	1st Vertical Bending	6.294762
3	Stabilator Roll	9.567776
4	2nd Vertical Bending/Transmission Pitch	9.802797
5	Transmission Pitch /Stabilator Roll & Yaw	12.42569
6	Transmission Roll / Stabilator Yaw	12.68499
7	Stabilator Roll / Transmission Roll	12.89486
8	Tailcone Lateral Bending/Transmission Roll/ Stabilator Roll & Yaw	13.88850
9	2nd Vertical Bending/Transmission Vertical	14.14049
10	Cockpit/Cabin Roll	15.90280
11	Cockpit/Cabin Torsion/3rd Vertical Bending	17.58992
12	3rd Vertical Bending	19.33992
13	Cockpit/ Cabin Roll/ 3rd Vertical Bending	20.45883
14	Transmission Pitch/ Cockpit/ Cabin Roll /3rd Vertical Bending	21.43938
15	Cockpit Vertical/ Stabilator Bending	22.45831
16	Cockpit Vertical I	22.71815
17	4th Vertical Bending	23.00682
18	Transmission Pitch/ 4th Vertical Bending	23.35931
19	Cabin Torsion	23.44646
20	Transmission Pitch/ Cabin Torsion	23.82937
21	Stabilator Vertical Bending/ Transmission Pitch	25.77211
22	Stabilator Vertical Bending	26.15101
23	Forward Cabin Bending	26.87042
24	Transmission Yaw/ 2nd Lateral Bending	27.72230
25	Forward Cabin Torsion	29.89976
26	5th Vertical Bending	30.63633
27	Cabin Compression/ Vertical Bending	31.21655
28	Cockpit Vertical II	31.88605
29	Cockpit Compression I	32.15541

Initial Modal Frequency Spread of UH-60A Finite Element Model FEM III Without MTRAP Flight Components and Weight Distribution

(Gross Weight = 13,220.7 lbs wo/ 9,000 lbs at Cargo Hook)

Mode #	Mode Description	Mode Frequency (Hz)
	RB	0.001396
	RB	0.001410
	RB	0.001532
	RB	0.001749
	RB	0.002369
	RB	0.002388
1	1st Lateral Bending	5.073329
2	1st Vertical Bending	6.453679
3	Stabilator Roll	9.857296
4	2nd Vertical Bending/Transmission Pitch	12.40500
5	Transmission Pitch /Stabilator Roll & Yaw	12.89724
6	Transmission Roll / Stabilator Yaw	13.11315
7	Stabilator Roll / Transmission Roll	13.92263
8	Tailcone Lateral Bending/Transmission Roll/ Stabilator Roll & Yaw	14.31117
9	2nd Vertical Bending/Transmission Vertical	16.26623
10	Cockpit/Cabin Roll	17.60811
11	Cockpit/Cabin Torsion/3rd Vertical Bending	20.48149
12	3rd Vertical Bending	20.84509
13	Cockpit/ Cabin Roll/ 3rd Vertical Bending	21.83280
14	Transmission Pitch/ Cockpit/ Cabin Roll /3rd Vertical Bending	22.69803
15	Cockpit Vertical/ Stabilator Bending	22.99302
16	Cockpit Vertical I	23.00739
17	4th Vertical Bending	23.31153
18	Transmission Pitch/ 4th Vertical Bending	25.14907
19	Cabin Torsion	25.56007
20	Transmission Pitch/ Cabin Torsion	26.13902
21	Stabilator Vertical Bending/ Transmission Pitch	27.45024
22	Stabilator Vertical Bending	27.58374
23	Forward Cabin Bending	29.85217
24	Transmission Yaw/ 2nd Lateral Bending	30.55613
25	Forward Cabin Torsion	31.59493
26	5th Vertical Bending	31.97023
27	Cabin Compression/ Vertical Bending	32.37553
28	Cockpit Vertical II	32.82457
29	Cockpit Compression I	33.00284